_ ON _ _ >

BY V. F. SYROMYATNIKOV

11 DECEMBER 1979 (FOUO) 1 OF 2

JPRS L/8805

11 December 1979

Translation

Automation as a Diagnostic Tool on Maritime Ships

By

V. F. Syromyatnikov

FBIS FOREIGN BROADCAST INFORMATION SERVICE

FOR OFFICIAL USE ONLY

APPROVED FOR RELEASE: 2007/02/08: CIA-RDP82-00850R000200030017-8

NOTE

JPRS publications contain information primarily from foreign newspapers, periodicals and books, but also from news agency transmissions and broadcasts. Materials from foreign-language sources are translated; those from English-language sources are transcribed or reprinted, with the original phrasing and other characteristics retained.

Headlines, editorial reports, and material enclosed in brackets [] are supplied by JPRS. Processing indicators such as [Text] or [Excerpt] in the first line of each item, or following the last line of a brief, indicate how the original information was processed. Where no processing indicator is given, the information was summarized or extracted.

Unfamiliar names rendered phonetically or transliterated are enclosed in parentheses. Words or names preceded by a question mark and enclosed in parentheses were not clear in the original but have been supplied as appropriate in context. Other unattributed parenthetical notes within the body of an item originate with the source. Times within items are as given by source.

The contents of this publication in no way represent the policies, views or attitudes of the U.S. Government.

For further information on report content call (703) 351-2938 (economic); 3468 (political, sociological, military); 2726 (life sciences); 2725 (physical sciences).

APPROVED FOR RELEASE: 2007/02/08: CIA-RDP82-00850R000200030017-8

JPRS L/8805

11 December 1979

AUTOMATION AS A DIAGNOSTIC TOOL ON MARITIME SHIPS

Leningrad AVTOMATIKA KAK SREDSTVO DIAGNOSTIKA NA MORSKIKH SUDAKH in Russian 1979 signed to press 17 Jan 79 pp 13-61, 74-77, 97-117, 163-168, 176-181, 220-226, 273-280, 309-310, UDC 681.51:629.12.03

Excerpts from Chapters 1-3, 5-6 and Bibliography from book by V. F. Syromyatnikov, Izdatel'stvo "Sudostroyeniye" 312 pages, 3000 copies

CONTENTS PAGE

CONTENTS (Continued)

PUBLICATION DATA

English title	:	AUTOMATION AS A DIAGNOSTIC TOOL ON MARITIME SHIPS
Russian title	:	AVTOMATIKA KAK SREDSTVO DIAGNOSTIKA NA MORSKIKH SUDAKH
Author (s)	:	V. F. Syromyatnikov
Editor (s)	:	
Publishing House	:	Sudostroyeniye
Place of Publication	:	Leningrad
Date of Publication	:	1979
Signed to press	:	17 Jan 79
Copies	:	3000
COPYRIGHT	:	Izdatel'stvo "Sudostroyeniye", 1979

UDC 681.51:629.12.03

CHAPTER 1. A MARINE STEAM-TURBINE PLANT AS AN OBJECT OF TECHNICAL DIAGNOSTICS

[Text] 1. Peculiarities of an Experimental Study of the Dynamics of a Steam-Turbine Plant in Operation

The construction of mathematical models of the processes that occur in objects being controlled is a first step in the study of a steam-turbine plant (PTU). These models, unlike the models that are known, should be suitable for statistical analysis of functions of automated marine systems.

It should be noted that not one of the models that are appropriate for the mission of such an analysis can encompass all the relationships and interactions of the physical process being examined. It is assumed below that the overall structure of the differential equation that reflects the model is established from a theoretical analysis of the basic phenomena, and its quantitative characteristics are determined from a comparison of the solutions of the theoretical equations with the experimental data.

In the experimental study of the dynamic characteristics of objects being regulated, both the deterministic and statistical methods that are described in the literature are used. The frequency method, the method of a transient or impulse function and the method of analyzing the passage of a random signal through a section being studied are the methods most widely disseminated. A particular method can be chosen correctly only where the object's overall characteristics and the conditions of its operation are considered. It is known that every system or section operates in the presence of disturbances, which are divided into useful

disturbances and into interference, which are random functions of time. Therefore, the measured value of a parameter at an object's output also contains, aside from systematic error, random deviations from the value that is being determined by the given effect.

The dispersion D of a parameter at the output of a dynamic system with the transfer function $W(j\omega)$, which is subjected to a random effect with the spectral density $S(\omega)$, is equal to

$$D = \frac{2}{\pi} \int_0^\infty |W(j\omega)|^2 S(\omega)\, d\omega. \qquad (1)$$

Expression 1 indicates that the dispersion that arises under the random signal's effect is determined by the degree of coincidence of the frequency spectrum of this signal with the frequencies of the characteristic oscillations of the object's control loop, which form an effective pass band.

The above-mentioned methods of analyzing the dynamic properties of objects being regulated are not equivalent in precision of results, which are determined by the dispersion of the output signal. Thus, experimental determination of the amplitudinal and phase-frequency characteristics is desirable only in an area with rather strong damping; it is not very applicable where there is considerable random noise. Where the noise is strong, it is most desirable of all that test disturbances in the form of an impulse function that has less spectral density than a jump function be used. Figures 1-3 show the amplitude and phase characteristics of a closed system for regulating an intermediate steam superheater of the stationary unit of a steam generator--a turbine of 100 Mw capacity [48]. Each of the characteristics has been plotted according to the data of measurements made under operating conditions, and the extent of the distance of the curves from each other in the charts at various frequencies characterizes the dispersion of the final result. In analyzing these data, it is not difficult to establish that for inertial power plants, the method of transient functions, under which there is minimal error in the area of low frequencies, which are more important for objects of the type being examined (figure 2), is preferred. The virtue of this method is the simplicity of the experiment, with minimal dislocations of the installation's operating regime.

Analysis of the passage of a periodic test signal by means of correlational functions (figure 3) enables acceptable results, even at a higher noise level. However, this method can be used only where the overall structure of the dynamic system of the object being studied is known and there is special apparatus for measuring, filtering and the statistical processing of current information.

The boundaries of permissible simplification of the models are determined by an evaluation of their precision. Therefore, the dispersions of the main parameters that were computed from a comparison with the experiment's results are cited for all the models being examined in this chapter.

Operations for the optimal approximation and establishment of the dispersions have been simplified considerably by using the procedures set forth below.

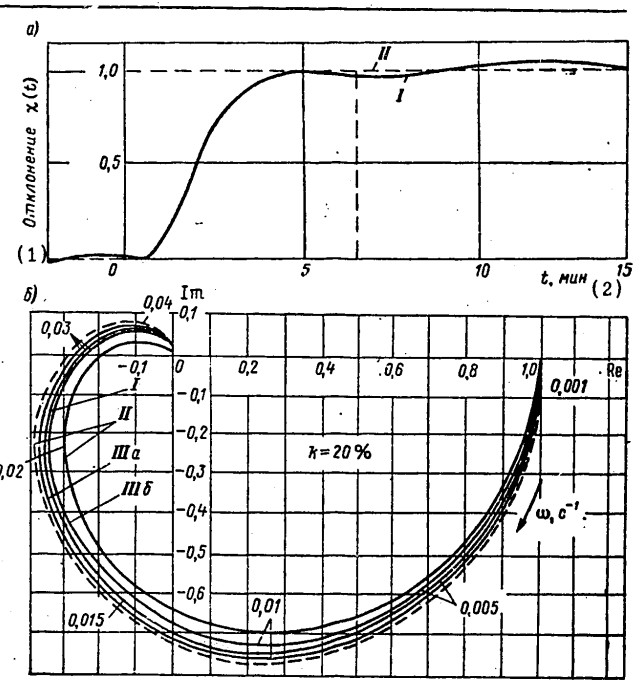

Figure 1. Dynamic Characteristics of a System for Regulating an Intermediate Steam Superheater That Are Obtained by the Transient Function Method for 16 Realizations [48]

Key:
- а. Transient functions.
- б. Amplitude and phase characteristics of the closed system.
- k. Random noise-effect factor, equal to the ratio of noise signal power to input signal power.
- I. Standard curve for the determinated process.
- II. Boundary curves for the aggregate of realizations.
- IIIа and IIIб. Curves plotted according to the averaged transient functions.
- 1. Deviation.
- 2. Time, minutes.

The experimental data is processed with an assumption of the normal law of distribution. As is known, this assumption leads to the conclusion that the arithmetical average is the greatest approximation to the true magnitude of the value being measured and that the sum of the squares is minimal when the deviations are taken from this average. An evaluation of the error that ensues from the assumption made is carried out in accordance with the coefficient of variation.

The precision of the mathematical models of the object's dynamics is determined mainly from a comparison of the appropriate integral curves with the experimental transient function. The method of transient functions in

studying the dynamics of the elements of a power plant installation during a normal operational trip by the ship is the most acceptable one.

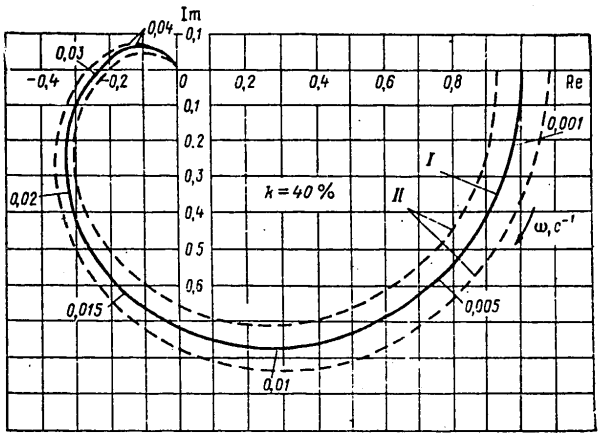

Figure 2. Amplitude and Phase-Frequency Characteristics of a System for Regulating an Intermediate Steam Superheater of a Steam Generator, Obtained by the Frequency Method.

Notation the same as for figure 1.

In analyzing the processes that take place in a marine heat-and-power plant, mathematical modeling is necessary in two basic areas.

The first embraces the processes that occur in various components of the plant and that characterize the technical and economic effectiveness of operation, and also the links with neighboring components and external conditions. A desirable minimum of factors that influence operating indicators considerably is established precisely on the basis of an analysis of models of the various units.

The second includes the mathematical characteristics of the operating conditions that are typical for a powerplant of a maritime carrying ship. The basic operating regime of such a plant is considered to be an unchanging power regime (close to the nominal value) for the main engine. However, observations indicate that a full-speed regime at sea is accompanied by constant regular or random disturbances that arise as a result of the ship's motions, changes in the external loading of the main engine and in environmental conditions, fluctuation in the expenditure of energy on auxiliary needs as a consequence of change in the number of customers and their loads, and so on. Thus, the dynamic regime of the heat-and-power plant installation as a whole that occurs under the influence of small but essentially continuous changes in internal and external operating conditions is the steady-load regime for the main engine. This circumstance influences appreciably the indices of the quality of operation of the ship's power-plant equipment, since, on the one hand, it increases the dispersion of the main parameters, and, on the other, it intensifies the mutual effect of the plant's control circuits.

The method of analyzing the dynamics in accordance with the exerimentally established transient function of the object being studied permits in most

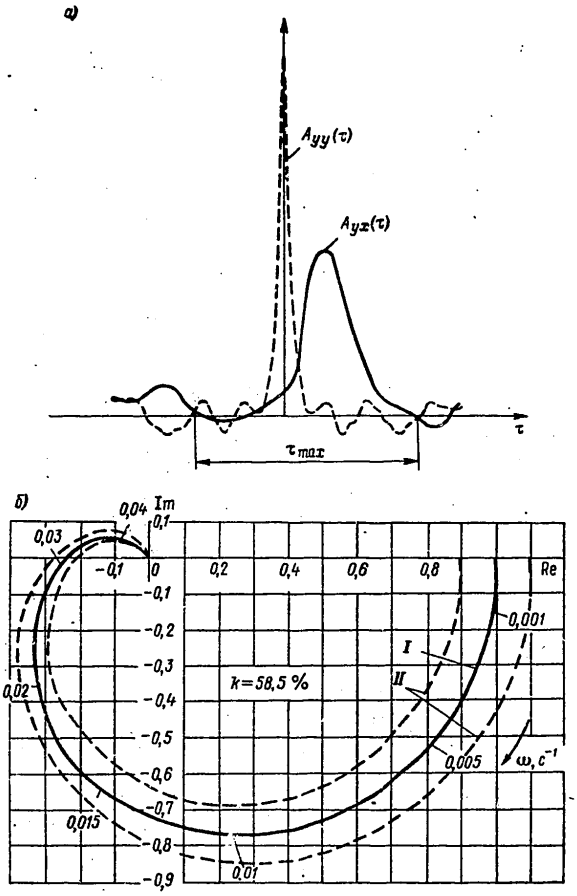

Figure 3. Dynamic Characteristics of a System for Regulating an Intermediate Steam Superheater Obtained by Analyzing the Passage of a Random Signal:

а. Autocorrelational $A_{yy}(\tau)$ and mutual-correlational $A_{yx}(\tau)$ of the signal's function.

б. Gain and phase-frequency characteristics.

Notation is the same as for figure 1.

cases an approximation of such a function by the solutions of a system of linear differential equations with time-lag arguments. Graph-analysis methods of approximation are widely known. Based upon the characteristics of exponential functions, they presuppose determination of the location of a point of discontinuity on the experimental curve, the construction of tangents or asymptotes, visual or graphic determination of time lags, and so on. The difficulties that arise in this case are connected both with the condition of the power plant of the experiment (under operating conditions it is not always possible to permit sufficiently large deviations of a parameter for the purpose of establishing, for example, the location of a point of discontinuity; data about the initial portion of a transient response, which is subject to the largest errors, proves to be less authentic), and with graph-plotting methods, under which subjective errors are inevitable. Meanwhile the approximating data, as a rule, reflects only formally the essence of the phenomenon studied. Therefore, it is especially important to seek the magnitude of approximating values that are equally acceptable for the whole area of the experiment. It is no less important to be assured that the result obtained for the chosen form of approximation is the most authentic, as well as to establish the amount of the error permitted in carrying out the operations.

The method set forth below was developed by the author; use of this method has made possible analytical computation of parameters of the approximating function that are optimal for the whole set of experimental data being examined.

The essence of the method consists in the use of transformations that linearize the components of the solutions of the approximating equations. In accordance with experimental data that have been standardized in specially chosen coordinates, it proves possible to apply in general form the method of least squares and thereby to establish in unique (or optimal) form the values of the inertial coefficients, the time lag, and the precision of the approximation being conducted.

The choice of an approximating equation is determined by the type of experimental transient function. If the speed of deviation of parameter y at the acceleration section is reduced (or at least does not increase) and the experimental data is of the form presented in figure 4, then the approximating should be done by means of the equation

$$T_1 y'(t-z) + y(t-z) = \lambda(t), \tag{2}$$

where $\lambda(t) = \begin{cases} 0, \text{ where } t < 0 \\ \text{a constant where } t \geqslant 0 \end{cases}$ is the input effect.

Under the initial conditions, the solution of equation (2) can be presented in the form

$$y_* = \frac{t}{T_1} + z_*, \tag{3}$$

where

$$\left.\begin{aligned} y_* &= -2{,}3\lg\left(1-\frac{y}{\lambda}\right), \\ z_* &= \frac{z}{T_1}. \end{aligned}\right\} \tag{4}$$

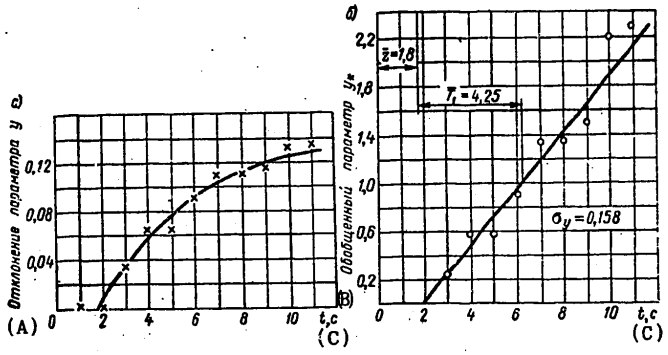

Figure 4. Transient Function of a Single-Capacity Object with a Time Lag.

a. Baseline (experimental) dependence.
б. The same dependence in linearizing coordinates.

The graph lines are the integral curves of equation (1) where T_1 = 4.25 seconds and z = 1.8 seconds.

A. Deviation of parameter y.
B. Generalized parameter y_*.
C. Time, seconds.

In coordinates (y_*, t) the solution (3) is a straight line with a slope equal to the inverse value of the inertial coefficient T_1; the intercept on the abscissa axis is the time z of the time lag. If the first k's of the experimental points (from 0 to k - 1) lie on the abscissa axis, then the least root mean square error of the approximating curve relative to the entire aggregate of the experimental data that are assumed to be uniformly precise will be reached where the values $\bar{T}_1$ and $\bar{z}$, which have been computed according to these expressions, are

$$\bar{T}_1 = \frac{(n-k)\sum_{i=k}^{n} t_i^2 - \left(\sum_{i=k}^{n} t_i\right)^2}{(n-k)\sum_{i=k}^{n} t_i y_{*i} - \sum_{i=k}^{n} t_i \sum_{i=k}^{n} y_{*i}}, \tag{5}$$

$$\bar{z} = z_* \bar{T}_1 = \frac{\sum_{i=k}^{n} t_i \sum_{i=k}^{n} t_i y_{*i} - \sum_{i=k}^{n} t_i^2 \sum_{i=k}^{n} y_{*i}}{(n-k)\sum_{i=k}^{n} t_i y_{*i} - \sum_{i=k}^{n} t_i \sum_{i=k}^{n} y_{*i}}. \tag{6}$$

Where the time lag is negligible

$$T_1 = \frac{\sum_{i=1}^{n} t_i^2}{\sum_{i=1}^{n} t_i y_{*i}}. \tag{7}$$

The experimental data can be presented in generalized coordinates, if dimensionless time τ is introduced:

$$\tau = \frac{t}{T_1}. \tag{8}$$

Figure 5 shows, in coordinates (y_*, τ), experimental data obtained during tests of first-order objects that are different in inertness, which illustrate the convenience and clarity of the use of generalized coordinates in which the integral curves of transient functions of any first-order objects are reflected in one straight line [22].

With approximation, the coefficients of self-regulation a_c and of the object's loading a_H (which expresses the ratio of the loading level at which the experiment is being conducted to its base value) can be computed.

In this case equation (2) will have the form

$$T_1 y'(t-z) + a_c a_H y(t-z) = \lambda_0, \tag{9}$$

and the first of equations (4)

$$y_* = -\frac{2,3}{a_c a_H} \lg\left(1 - \frac{a_c a_H}{\lambda_0} y\right). \tag{10}$$

We use the method of approximation of the transient function of a single-capacity object that has been set forth also in the case where the disturbing effect has the form of an arbitrary continuous, increasing function that takes the constant value $\lambda(t) = \lambda_0 =$ a constant after a certain portion t_0 of a monotonic increase (figure 6). If this portion is not great in comparison with the period of acceleration and, where $t > t_0$, there is sufficient experimental data (practically, if the portion 0 - t does not exceed 10-15 percent of the time constant T_1), the transient response can be viewed as a single-capacity object, beginning from the moment $t = t_0$ under the initial conditions $t = t_0 = 0$:

$$\left.\begin{aligned} \lambda(t) &= \lambda_0, \\ y(t) &= y_0. \end{aligned}\right\} \tag{11}$$

In this case, instead of (4) or (10), we will have

$$y_* = -2,3 \lg \frac{1 - \frac{y}{\lambda_0}}{1 - \frac{y_0}{\lambda_0}},$$

or

$$y_* = -2{,}3 \lg \frac{1 - \frac{a_c a_н}{\lambda_0} y}{1 - \frac{a_c a_н}{\lambda_0} y_0}. \qquad (12)$$

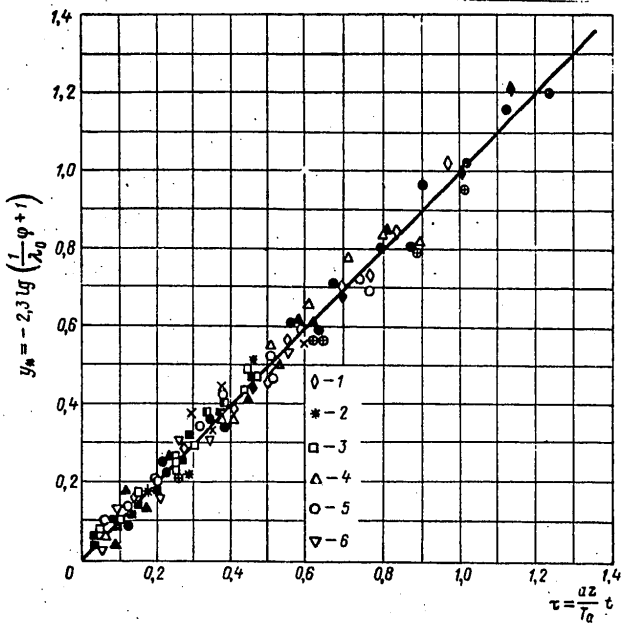

Figure 5. Processes of Change in Steam Pressure in Generalized Coordinates (y_*, τ), That Were Recorded for Steam Generators of Various Types and Inertnesses and for Various Disturbances (the correlation coefficient is 0.995).

1. The steamship "Sovetskaya Gavan'."
2. The steamship "Yenisey."
3. The steamship 3C-50
4. A factory electric-power plant.
5. A marine steam generator.
6. The turbine ship "Sofiya".

The coefficient T_1 of the object's inertness will be determined in accordance with the (n - k) values of the function of the acceleration characteristic (figure 6) where $t \geqslant t_0$, by means of (7).

If the experimental measurements are not of uniform precision and various weights have been ascribed to the points, for example, weight ω_1 for point 1 and weight ω_i for the point i (in this case the ω_i of the measurements which on the average yield y_i correspond to the value x_i), then we will have for these weighted observations, respectively, instead of (5) and (6),

$$T_1 = \frac{\sum_{i=k}^{n} w_i \sum_{i=k}^{n} w_i t_i^2 - \left(\sum_{i=k}^{n} w_i t_i\right)^2}{\sum_{i=k}^{n} w_i \sum_{i=k}^{n} w_i t_i y_{*i} - \sum_{i=k}^{n} w_i t_i \sum_{i=k}^{n} w_i y_{*i}}, \qquad (13)$$

$$z=\frac{\sum_{i=k}^{n} w_i t_i \sum_{i=k}^{n} w_i t_i y_{*i}-\sum_{i=k}^{n} w_i t_i^2 \sum_{i=k}^{n} w_i y_{*i}}{\sum_{i=k}^{n} w_i \sum_{i=k}^{n} w_i t_i y_{*i}-\sum_{i=k}^{n} w_i t_i \sum_{i=k}^{n} w_i y_{*i}}. \quad (14)$$

Similarly, instead of (7), we will have

$$T_1=\frac{\sum_{i=1}^{n} w_i t_i^2}{\sum_{i=1}^{n} w_i t_i y_{*i}}. \quad (15)$$

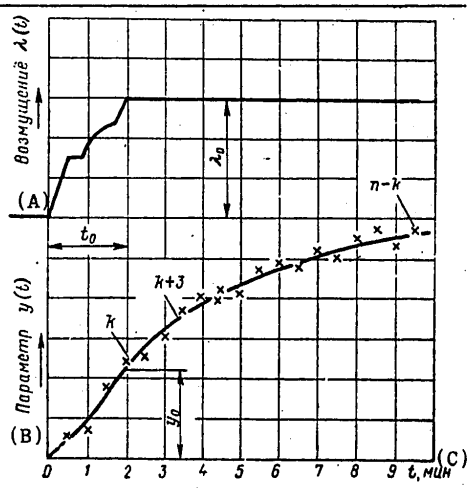

Figure 6. For Determination of the Approximation Coefficient of an Equation for a Single-Capacity Element, Where the Form of the Disturbance Is Unlike a Single Jump.

Key:
A. Disturbance.
B. Parameter.
C. Minutes

The error of the approximation performed is evaluted by the root mean square deviation of the experimental values of y_{*i} from the ordinate of equation (3), computed in accordance with the correlation

$$\sigma_{y_*}=\sqrt{\frac{\sum_{i=1}^{n}\left[w_i\left(y_{*i}-z_*-\frac{t_i}{T_1}\right)^2\right]}{n-1}}. \quad (16)$$

Precision in determining the values of T_1 and z is characterized by the root mean square deviations σ_{T_1} and σ_z and they are established in

accordance with the corresponding characteristics of the value y_{*i} by the method usual for indirect measurements. In the given case, using (13), we obtain the following expressions:

$$\sigma_{\overline{T}_1} = \frac{\partial T_1}{\partial y_*}\sigma_y = \overline{T}_1\sigma_{y_*}\frac{(n-k-1)\sum_{i=k}^{n} t_i}{\sum_{i=k}^{n} w_i \sum_{i=k}^{n} w_i t_i y_{*i} - \sum_{i=k}^{n} w_i t_i \sum_{i=k}^{n} w_i y_{*i}}, \tag{17}$$

$$\sigma_z = \frac{\bar{z}}{\overline{T}_1}\sigma_{\overline{T}_1}. \tag{18}$$

For the case of absence of time lag, in accordance with (15) we get

$$\sigma_{\overline{T}_1} = T_1\frac{\sum_{i=1}^{n} w_i t_i}{\sum_{i=1}^{n} w_i t_i y_{*i}}\sigma_{y_*}. \tag{19}$$

Thus the method set forth enables determination, on the basis of the experimental data, of both the value of the mathematical expectations of the constants of the dynamic processes and their scattering characteristics at the minimum root mean square error.

Let us turn to the method of approximation set forth for the case of more complicated dynamic systems.

If the analyzed portion of a control circuit can be represented as a series connection of an elementary element of the first order and a more complicated element, the transient function is approximated by the solution of a differential equation of the second order with a time lag. In so doing, first the coefficients of the equation of the chosen element of the first order are established as a result of a special experiment. For example, for a steam generator (PG), first the inertness of a unit volume--the steam-and-water volume--is established in accordance with the transient function that is obtained as a result of a disturbance in steam consumption, and then the transient function that is obtained at the output of the steam-and-water volume during the disturbance on the part of the firebox is approximated.

By means of a second-order equation with a time lag the transient functions of an extremely large number of real objects can be approximated. The transfer function of an approximating equation in this case has the form

$$K_2(s) = \frac{\lambda e^{-sz}}{(1-sT_1)(1-sT_2)}, \tag{20}$$

where T_2 is the coefficient of inertness of the second element.

Where z = 0 the transient function $\Phi(\tau)$ that corresponds to (20) is described by the equation

$$\left.\begin{aligned}\Phi(\tau) &= 1 - \frac{w_2 e^{-\tau} + e^{w_2 \tau}}{w_2 + 1},\\ w_2 &= -\frac{T_1}{T_2}.\end{aligned}\right\} \tag{21}$$

Equation (21) is reduced to the form

$$v = \frac{e^q - 1}{q}, \tag{22}$$

where

$$\left.\begin{aligned}q &= \tau(w_2 + 1),\\ v &= \frac{1}{\tau}[(1 - \Phi)e^{\tau} - 1].\end{aligned}\right\} \tag{23}$$

The values of the second of the functions (23) can be determined for each of the selected points (Φ_i, τ_i) in accordance with the experimental data, after which equation (22) is solved relative to the function q (on a computer, or graphically, using tables of exponential functions). As a result, a number of values $q_i = q_i(v_i)$ are obtained that correspond to the coordinates of the experimental points of the transient function. The first of the equations (23) in the plane [(τ - q), t] is a straight line, which enables the most authentic value of the average inertness coefficient $\overline{T}_2$ to be determined:

$$\overline{T}_2 = \frac{\sum_{i=1}^{n} t_i^2}{\sum_{i=1}^{n} (\tau_i - q_i) t_i}. \tag{24}$$

Where there is a time lag by virtue of linearity of the process in the plane [(τ - q), t], the constants $\overline{T}_2$ and $\overline{z}$ should be determined in accordance with expressions (5) and (6), or (13) and (14), after inserting therein

$$y_{ai} = \tau_i - q_i. \tag{25}$$

The error that is allowed in determining values for $\overline{T}_2$ and $\overline{z}$ is found in accordance with (17) and (18).

Figure 7 compares the experimental data and the approximating equation (a straight line) that is obtained when determining the coefficient T_2 of inertness of the steam generator firebox in accordance with (22)-(24). The

data obtained in the experiments, which vary in magnitude and sign of the disturbance, are denoted by different dots [22].

The correctness of the chosen form of the approximating function can be characterized by a correlation coefficient. For the data shown in figure 7, this coefficient is 0.912.

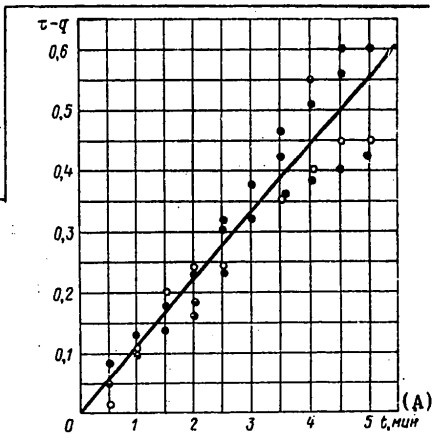

Figure 7. Results of the Processing of Experimental Data for Establishing the Coefficient of Inertness in a Two-Capacity Object (a marine steam generator with mechanical firebox).

Key:
A. Time, minutes.

The General Case of Two Inertial Nondirectional Elements of the First Order. A system of equations (without taking time lag into account) in this case has the form

$$\left.\begin{aligned} T_1 \frac{dy_1}{dt} &= a_{11}y_1 + a_{12}y_2 + b_{11}\lambda, \\ T_2 \frac{dy_2}{dt} &= a_{21}y_1 + a_{22}y_2 + b_{21}\lambda, \end{aligned}\right\} \qquad (26)$$

where a_{ik} are the coefficients that determine inertness and self-correction; and b_{ik} is the influence of the external disturbance.

Where the zero initial conditions are (t = 0): $y_1(0) = y_2(0) = 0$ and the disturbances are forms of a unit function:

$$\lambda = \begin{cases} 0 & \text{where } t < 0, \text{ and} \\ \text{a constant} & \text{where } t \geqslant 0 \end{cases}$$

and the partial solution $y_{1\infty}$ of the system (26) expresses the value of the parameter for the new regime that is established:

$$y_{1\infty} = \frac{b_{21}a_{12} - b_{11}a_{22}}{a_{11}a_{22} - a_{12}a_{21}}\lambda. \qquad (27)$$

The standardized experimental function should be determined as the ratio $y_1 : y_{1\infty}$ or $y_2 : y_{2\infty}$.

The general solution of system (26), for example, relative to the function $y_1(t)$, under the stipulated initial conditions, has the form

$$\frac{y_1}{y_{1\infty}} = 1 - \frac{w_2 - d}{w_2 - w_1} e^{w_1 t} + \frac{w_1 - d}{w_2 - w_1} e^{w_1 t}, \tag{28}$$

where $d = \frac{b_{11}}{t_1 y_{1\infty}} \lambda$ and ω_1 and ω_2 are the roots of the performance equation and can be reduced by simple transformations to the form of equation (22), in which the following should be inserted

$$v = \frac{\left(1 - \frac{y_1}{y_{1\infty}}\right) e^{-w_1 t} - 1}{w_2 - d},$$
$$q = (w_2 - w_1) t. \tag{29}$$

One of the roots of the performance equation that corresponds to system (26), namely ω_1, is determined in accordance with the data of the special experiment (as described above) or in accordance with the design and operating characteristics of the element being examined. The mathematical expectation of the value of the second root ω_2 is established in accordance with the aggregate of the experimental data that are obtained for the system as a whole that is being studied. Thus,

--Where the time-lag section on the experimental curve of acceleration is absent

$$w_* = \overline{(w_2 - w_1)} = \frac{\sum_{i=1}^{n} q_i t_i}{\sum_{i=1}^{n} t_i^2}; \text{ and} \tag{30}$$

--Where the time-lag section is present

$$w_* = w_2 - w_1 = \frac{(n-k)\sum_{i=k}^{n} q_i t_i - \sum_{i=k}^{n} t_i \sum_{i=k}^{n} q_i}{(n-k)\sum_{i=k}^{n} t_i^2 - \left(\sum_{i=k}^{n} t_i\right)^2}, \tag{31}$$

$$z = \frac{\sum_{i=k}^{n} t_i^2 \sum_{i=k}^{n} q_i - \sum_{i=k}^{n} t_i \sum_{i=k}^{n} t_i q_i}{(n-k)\sum_{i=k}^{n} t_i q_i - \sum_{i=k}^{n} t_i \sum_{i=k}^{n} q_i}. \tag{32}$$

The coefficients a_{ik} and b_{ik} are established in accordance with the statistical characteristics of the object being studied. As was explained above,

the value q_{ik} of a function that contains the unknown root ω_2 is determined in accordance with the corresponding value of the function v_i, which is computed on the basis of the experimental data.

The root mean square deviation for the aggregate of the experimental values of q_i is determined in accordance with the expression

$$\sigma_q = \sqrt{\frac{\sum_{i=k}^{n} (q_i - \bar{q}_i)^2}{n-k-1}},$$

where

$$\bar{q}_i = \bar{w}_* t_i + z,$$

after which, in accordance with (17)

$$\sigma_{w_*} = \frac{(n-k-1)\sum_{i=k}^{n} t_i}{\left[(n-k)\sum_{i=k}^{n} t_i^2 - \left(\sum_{i=k}^{n} t_i\right)^2\right]^2}. \qquad (33)$$

Precision in determining the value of T_2 is evaluated by means of the algebraic dependence among the coefficients of the performance equation of system (26), the expressions of which include the value T_2 and its roots ω_1 and ω_2 (for example, according to Vieta's theorem, based upon correlation (17).

Often proving to be of use is the introduction of dimensionless time in accordance with the correlation

$$\tau = -\omega_1 t.$$

The sequence of transformations and separate operations cited is made more precise, depending upon the concrete conditions of the task (as is done, for example, in approximating the linear portion of the equation of the steam superheater's dynamics that is carried out in section 3).

2. The Marine Steam Generator

A block diagram of a steam-turbine installation for a high-tonnage tanker is shown in figure 8.

The characteristics of the PG's scheme are the presence of an intermediate gas-steam preheater, in which the temperature of the steam prior to entering the low-pressure turbine casing is brought up to the original temperature, and organization of the combustion process at fuel and air ratios that are close to stoichiometric. High efficiency values for the steam generator are provided also by the well-developed heat-recovery surfaces of the steam generator.

The main turbine is joined to the propeller shaft by a semiplanetary gear transmission that provides high efficiency with minimal reduction gear size. In order to raise the efficiency of the plant's main cycle, five regenerative steam bleedings from the turbine are called for. As a result, feedwater is preheated by steam that has been partially spent in the turbine to a temperature that is 0.8-0.85 the temperature of the water in the boiler. The bleeds are usually numbered according to the direction of the condensate flow from the main condenser. Steam from the second bleed is sent to the deaerator--an apparatus that combines the functions of a mixing regenerative feedwater preheater and an extractor of the gases dissolved therein.

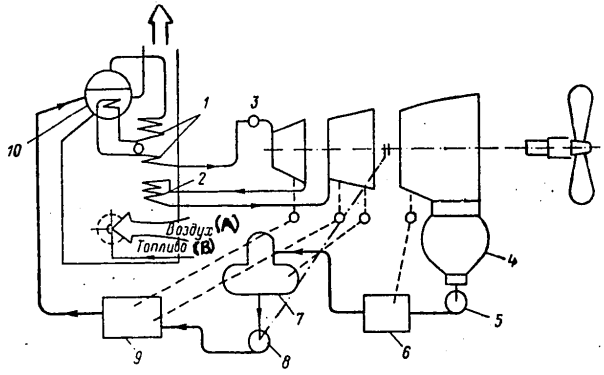

Figure 8. Diagram of a Marine Steam-Turbine Plant.

Key:
1. Main steam superheater.
2. Intermediate steam superheater.
3. Turbine manipulation valve.
4. Main condenser.
5. Condensation pump.
6. Groups of regenerative low-pressure preheaters.
7. Deaerators.
8. Feed pump.
9. Group of regenerative high-pressure preheaters.
10. Steam superheater cooler.
A. Air.
B. Fuel.

A feature of the installation also is the drive of the main feed pump and the electric generator off the main turbine. In this case, it is essential to improve the operating economy of the installation as a whole, since self-contained drives for the units would consume considerably more energy.

With regard to dynamics, regimes where there are intense changes in loading (or manipulation) are much more complicated. Let us note that the diagram of the installation is somewhat simplified for manipulations, namely:

--Steam bleeds from the main turbine are disengaged and all the feedwater preheaters except for the deaerator (which in this case is fed by cooled and reduced steam from the PG) are disengaged from operation;

--The temperature of the feedwater at the feed pump intake and prior to entry into the PG is preserved unchanged and is equal to the

temperature at the deaerator outlet; this thus stabilizes operation of the condensate-and-feed system; and

--The feed pump and the generator are switched over to operation off self-contained drives.

Maneuvering regimes make up an extremely small (2-5 percent) portion of the operating time of modern maritime carrying ships. The basic operating regime of such a ship is movement at main-engine power, which is close to nominal. Mathematical models of the plant's units should provide sufficient precision within a narrow band of loading, in a region of the plant's most characteristic operating regime that corresponds to full-speed.

In the overall diagram of the steam-turbine the steam generator proper occupies a special place, since changes of its operating regime lead to deviations of the most important parameters of the plant--steam pressure and temperature, water level in the PG drums, and chemical composition of the exhaust gases (which determines the economy of operation, the degree of smokiness, the suitability for use in the inert-gases system on tankers, and the explosion hazard).

The phenomena of heat exchange, motions of the two-phase medium, accumulations of heat and matter, and so on interact in a steam generator. In the general case these phenomena can be described by nonlinear equations and equations in partial derivatives. Linearization of the equations that characterize PG operation presents a certain simplification that is necessary for subsequent analysis of the processes inside the boiler. A study of the system of high-order linear equations that is obtained with such linearization do not present difficulties on electronic models and, at the same time, enable adequate matching with the experimental data to be provided for.

The basic features of the method used in the present derivation are reduced to the following:

1. The PG's heater surfaces are viewed as separate capacities. The heat transfer from the gases to the walls and from the walls to the atmosphere (steam or liquids) is determined by means of empirical formulas for turbulent flow for average operating conditions.

2. The condition of the working medium is established in accordance with tables for steam by linearization in the neighborhood of the point of the regime.

3. The compressibility of the flow of air between the air-feed control element and the firebox is taken into account. The inertness of the air channel turns out to be substantially greater than that of the control circuit and even of certain parts of the PG's steam and water volume.

4. The dynamics of the gas preheater for air and also, in particular examples of the analysis, the dynamics of the water economizer, are excluded from the examination.

A design scheme of a steam generator is shown in figure 9.

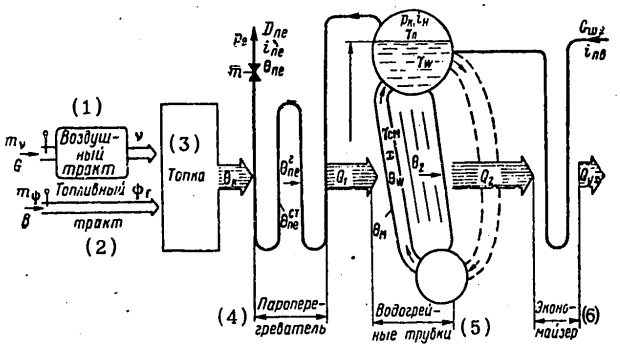

Figure 9. For the Derivation of Equations of the Dynamics of a Steam Generator.

Key:
1. Air channel.
2. Fuel channel.
3. Firebox.
4. Steam superheater.
5. Water-heating tubes.
6. Economizer

The Characteristics of Processes That Occur in the Firebox and the Air-and-Gas Channel of a Steam Generator. The organization of fuel combustion in the firebox has a definite effect upon PG operating economy and on the successful solution of problems of protecting the environment from pollution. The fuel is atomized in the nozzles into the smallest particles commensurate with the sizes of its molecules and is thoroughly mized with air. The atomization and mixing are accomplished in firebox installations and are functions of the constructional characteristics thereof and upon the parameters of the agent being mixed; this process is not regulated automatically. Only the amount of fuel and air, which is determined by firebox-installation characteristics and should be maintained with very high precision, is regulated. Firebox installations have now been created that execute complete and smokefree fuel combustion where the fuel and air ratios exceed the stoichiometric by about 2-3 percent. The sole indicator that determines fuel-combustion quality unambiguously is the chemical composition of the combustion products. However, existing instruments for gas analysis are marked by substantial inertness and time lag, as a result of which it is impossible to organize automatic regulation of the ratio between the amounts of fuel and air fed into the firebox in accordance with gas-analysis data.* Therefore, all existing systems for fuel combustion, both in marine and stationary power installations have been built as open-circuit systems, that is, as circuits without main feedback, in which input signals for feeding fuel and air into the firebox are formulated without a consideration of how the combustion process is actually occurring. Under these circumstances, successful solution of the problem of optimal regulation consists in stabilizing all input parameters: temperature (viscosity of the fuel, air temperature, quality of fuel atomization in the nozzles,

*The Westinghouse firm (USA) recently arranged for the industrial manufacture of gas analyzers based on a zirconium ceramic with a measurer inertness of only 0.2 second and a total instrument inertness of about 2 seconds [42]. Automatic regulation of fuel combustion in steam generators in accordance with combustion products composition can be organized on the basis of such instruments.

and so on, as well as in regulating the ratios of the amounts of fuel and air that arrive in the firebox.

The necessary feedback (diagnostic) is accomplished by the operator, who observes the progress of fuel combustion (in particular, in accordance with instruments for gas analysis) and, where necessary, corrects the input variables.

From the dynamic point of view the channels for feeding air and fuel into the firebox are characterized somewhat differently. The consumption of fuel that is delivered to the nozzle changes as a result of movement of the device that regulates fuel feed, with a speed of propagation of the pressure wave in the fluid, that is, in relation to the speeds of other processes that occur in the PG it is instantaneous. Large volumes for air ducts and the air preheater (gas or steam) are placed between the air-feed regulating device (which usually is located on the suction side of the blower) and the firebox. An inertness is created, as a consequence of which the change in air feed at the firebox intake always lags behind changes in fuel feed, if the signal for these changes are sent to both of them simultaneously. But even a brief deficit of air can and does cause impermissible smoke, so increased air consumption often has to be established in order to compensate for a possible shortage thereof during the manipulation to increase the loading.

A calculation for PG air-channel inertness was introduced for the first time in the works of TsNIIMF [Central Scientific-Research Institute of the Maritime Fleet] [22]. The procedure for studying the dynamics of the ratio between the amounts of air and fuel fed into the firebox is given there.

Combustion of the mazut that is atomized by the nozzles in the firebox space occurs in hundredths of a second, so fuel combustion, in light of the problems examined here, can be considered noninertial.

The amount of heat $Q_к$ that is sensed by the PG's heating surfaces is determined by the known expression

$$Q_к = BQ_p^н\eta_к,$$

which in increments takes the form

$$\frac{\Delta Q_к}{Q_{к0}} = \psi + \rho_т + \frac{\Delta\eta_к}{\eta_{к0}}. \qquad (34)$$

The quality of the fuel combustion is determined by means of the last addend on the right side of the expression obtained and is characterized by coefficient of concentration of air α at which combustion occurs. The functional dependence $\frac{\Delta\eta_k}{\eta_{k0}} = f_\eta(\chi)$ is governed by the type of firebox installation, the grade of fuel, PG configuration characteristics, firebox tightness, and so on. If the function $\Delta\eta_k/\eta_{k0}$ is computed for optimal

efficiency values, it will be negative and its maximum value will be equal to zero (figure 10). The experimental data are shown by the points on the graph in figure 10; the continuous line is an approximation of the equation

$$\frac{\Delta\eta_k}{\eta_{k0}} = 0{,}118\chi^3 - 0{,}0807\chi^2 - 0{,}008575\chi, \tag{35}$$

which is carried out where $-0.8 < \chi < 0.6$ with the error $\sigma_\chi = 0.00685$.

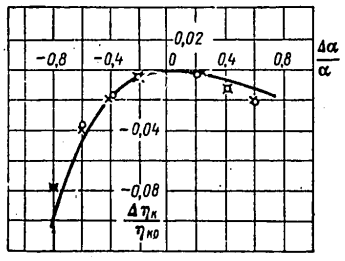

Figure 10. Relative Change of KPD [Efficiency] in a Steam Generator $\Delta\eta_k/\eta_{k0}$ as a Function of the Deviation in Air Concentration $\chi = \frac{\Delta\alpha}{\alpha_{opt}}$ from the Optimum.

The left branch of the curve corresponds to a reduction in coefficient of the concentration of air below the optimal value and it descends more steeply than the right branch, since, where the deviations are equal in absolute value, a reduction in air concentration is accompanied by the appearance of incomplete chemical combustion of the fuel.

The formula for computing the coefficient of air concentration is

$$\alpha = \frac{G_в}{L_0 Q_p^н B},$$

where L_0 = the amount of air theoretically necessary for realization of a unit of the heat of combustion and is written in increments thusly

$$\frac{\Delta\alpha}{\alpha_{opt}} = \chi = \nu - \psi - \rho_т. \tag{36}$$

Consolidating expressions (34) and (36) and giving consideration to the fact that $\frac{\Delta\eta_k}{\eta_{k0}} = f_\eta(\chi)$, one can write

$$\frac{\Delta Q_к}{Q_{к0}} = \psi + \rho_т + f_\eta(\nu - \rho_в - \psi). \tag{37}$$

Equation (37) expresses change in heat sensing of the PG in established and in transient regimes. The last addend on the right side (37) considers the effect of the changed efficiency on the dynamics of the processes that are determined by the energy balance.

As will be shown below, in many cases calculations of changes in efficiency that air-concentration deviations cause in the dynamics of such parameters

as, for example, steam pressure, prove to be insignificant and can be disregarded. Of much greater importance is the fact that expression (36), along with function (35), enables the coefficient of air concentration to be viewed as a regulatable parameter that is introduced into the system of equations of an automated PG through correlation (37). This enables analysis and synthesis of schemes for regulating fuel combustion from the point of view of establishing conditions for minimal deviations in air concentration--conditions that are most important for modern steam generators that operate with minimal air-concentration coefficients (α = 1.02-1.05).

Among the arguments of the function $f_\eta(\chi)$, deviation in fuel feed can, by virtue of the incompressibility of mazut, be considered an algebraic function of pressure of the fuel before it enters the nozzles, and change in fuel-combustion heat can be considered an external disturbance (aboard ship this is insignificant, for the grade of fuel can be changed appreciably only when bunkering). Change in the air inflow, which is shown in formulas (36) and (37) by the function ν, appears to be the most important influence on completeness of combustion of a prepared fuel.

Observations indicate that the air channel of a PG can be viewed as a concentrated volume, and change of air feed into the firebox is described by an equation of the form

$$T_T\nu' + \nu = \mu_\nu + \frac{1}{2} y_B, \tag{38}$$

in which the function μ_ν expresses the effect of moving the air-regulating device, and the function y_B is the effect of change in the productivity of the blower itself.

The coefficient T_T of inertness of the PG's air tract depends upon the ratio of the volume of the air line and the precombustion space to the blower's productivity.

The results of three tests for determining T_T for a steam generator of the turbine ship "Trud" are shown in figure 11.

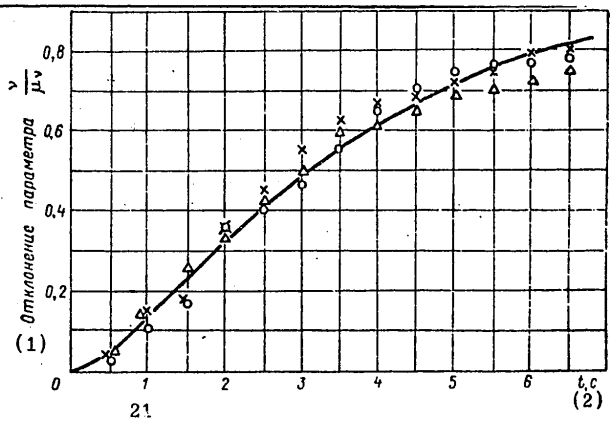

Figure 11. Relative Change ν/μ_ν in Pressure at the Fuel-Air Ratio Regulator Output as the Result of a Single Disturbance in Delivery of Air into the Steam-Generator Firebox (for Determining the Air Channel's Coefficient of Inertness).

Key:
1. Deviation of the parameter.
2. Time, seconds.

In accordance with what was said above, these results should be viewed as the solution of a system of differential equations that is made up of the equation (38) where $y_B = 0$ and of equations of the dynamics of the pneumatic regulator of the fuel-air ratio:

$$\left.\begin{aligned} T_r\nu' + \nu = \mu_\nu, \\ T_p\zeta' + \zeta = \nu \end{aligned}\right\} \tag{39}$$

with the initial conditions

where $t = 0$

$$\left.\begin{aligned} \nu(0) = \zeta(0) = 0; \\ \mu_\nu = \begin{cases} 0 \text{ where } t < 0, \\ \text{a constant where } t \geqslant 0. \end{cases} \end{aligned}\right\} \tag{40}$$

The following have been designated here: ζ is the relative change of output of the fuel-air ratio regulator; and T_p is the coefficient of this regulator's inertness.

The value of T_p has been adopted as 0.8 second, in accordance with the data for the previously cited bench tests.

The characteristics shown in table 1 have been established from a comparison of the solution of system (39) with experimental data based upon formulas (22)-(24).

Table 1

Characteristics of Inertness of the Air Channel of the Steam Generators of the Turbine Ship "Trud"

Parameters	Series of tests (for notation see figure 11)		
	o	×	Δ
Single disturbance μ_ν	+0.07	+0.12	-0.098
Coefficient of inertness of air channel T_T, seconds	3.261	3.168	3.574
Average value of $\overline{T}_T$, seconds	-	3.33	-
Root mean square deviation σ_ν of the entire aggregate of points (see figure 11) from the average where $T_T = 3.33$, seconds	-	0.039	-
Range R of the value T_T, seconds	-	0.406	-

By means of Student's tables of distribution and tables of selected ranges, the boundaries of the confidence interval for values of T_T have been established

$$\pm t^{c}_{n-1,\ p}\frac{\sigma}{\sqrt{n}}.$$

In accordance with Student's tables for probability, $\bar{p} = 0.95$ and $n = 3 t^{c}_{n-1,\ p} = 4.303$.

In order to determine the average square deviation $\bar{\sigma}$ the theorem of selected ranges is used; according to the tables for these ranges, it has been determined that where $n = 3$, $d_R = 0.1693$. Then

$$\bar{\sigma} = \frac{R_{\text{н}}}{d_R} = \frac{0{,}406}{1{,}693} = 0{,}24 \text{ с.}$$

Next, we make an evaluation of the boundaries of the confidence interval: $\pm 4.303\ 0.24/1.73 = \pm 0.55$ seconds.

Finally

$$\bar{T}'_{\text{т}} = \bar{T}_{\text{т}} \pm 0{,}55 = 3{,}33 \pm 0{,}55 \text{ с.} \tag{41}$$

The second term y_B in the right side of equation (38) expresses the effect of change of productivity of the PG's blower, and it is found by solving a differential equation of the form

$$T_{\text{в}}\bar{y}'_{\text{в}} + \bar{y}_{\text{в}} = \bar{\lambda}_{\text{в}}, \tag{42}$$

where T_B is the coefficient of inertness of the electric-drive blower; and λ_B is a function that expresses the disturbance at the blower intake.

The characteristics of random disturbances that are included in the functions λ_B and y_B and are caused by factors that do not yield to calculation (for example, by change of frequency of the current in the ship's power grid) are examined in Chapter III. It is convenient to define the blower's inertness by the results of research of the dynamics of change in the head at the blower's delivery that is caused by switching the speed of its asynchronous electric drive.

The results of tests of the blower installed on "Varshava" and "Sofiya" type tankers are cited in table 2; part of them are illustrated by the data of figure 12. We determine by formula (7), in accordance with the discrete values of the ordinates of curves 2 and 4 that are taken at 1-second intervals directly from oscillograms of transient processes, that the most probable value of the time constant in equation (42) for an EKV-2 ventilator is $T_B = 4.4$ seconds.

The Steam Generator's Steam and Water Volume. The movement of the steam-and-water mix in steam generators with natural circulation is caused by the difference in density of the water in the downcomer bundle of tubes and the density of the steam-and-water mix in the riser tubes. The motive forces are equalized by pressure losses.

Pressure losses in the downcomer bundle have been studied well; they usually are presented as a function of the mass velocity of the flow and consist of losses to friction, local drags, and acceleration of the flow, and to hydrostatic losses.

Table 2

Results of Bench Tests of the EKV-2 Electric-Drive Blower

Indicators	Operating regimes	Shutter position in degrees, п.к.в.		
		0	60	90
Pressure, Pascals	1st speed.....	1,720	1,720	1,720
	2d speed.....	3,250	3,000	2,800
	3d speed.....	7,000	4,700	4,500
Total duration of the transient process during switchings, seconds	Switchings:			
	from 1st to 2d speed.....	4	4	4
	from 2d to 3d speed.....	7	10	7
	from 3d to 2d speed.....	5	10	9
	from 2d to 1st speed.....	12	10	9
Relative change λ_B of pressure during switching of speed (H_{nom} = 7,750 Pascals)	Switchings:			
	from 1st to 2d speed, or from 2d to 1st speed	0.216	0.174	0.153
	from 2d to 3d speed, or from 3d to 2d speed	0.542	0.243	0.18

A two-phase mix of steam and water flows in the riser tubes, a fact which substantially complicates formulation of equations of the balance of pressures. Thus, the friction coefficient becomes a function of the steam-and-water ratio, and losses to acceleration rise sharply with increase in volume.

A design diagram of the steam-and-water volume of a PG is shown in Figure 13.

Useful pressure is defined as the difference between the motive pressure and the hydraulic resistance of the loop.

Returning to the diagram in Figure 13 and examining the downcomer and riser bundles of the loop separately, one can write for the downcomer tubes:

$$p_w - p_{D1} = \sum \Delta p, \quad \text{and} \tag{43}$$

where the full value of the hydraulic resistances of the pipe bundle has been written on the right side

$$\sum \Delta p = \Delta p_{тр} + \sum \Delta p_м + \\ + \Delta p_{уск} + \Delta p_{геод}.$$

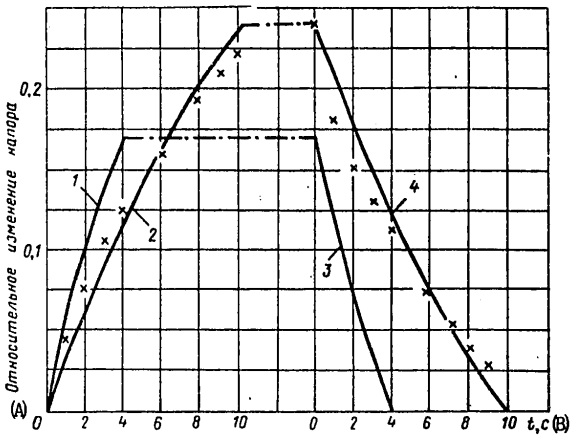

Figure 12. Oscillograms of the Process of Relative Change of Head of the EKV-2 Blower During Switchings of Its Electric Drive

1. From 1st to 2d speed
2. From 2d to 3d speed
3. From 2d to 1st speed
4. From 3d to 2d speed

The position of the air-regulating shutter is 60 degrees. The points are approximations of curves 2 and 4 with solutions of equation (42), where $\lambda_B = \pm 0.248$ and $T_B = 4.4$ seconds.

A. Relative change of head. B. Time, seconds.

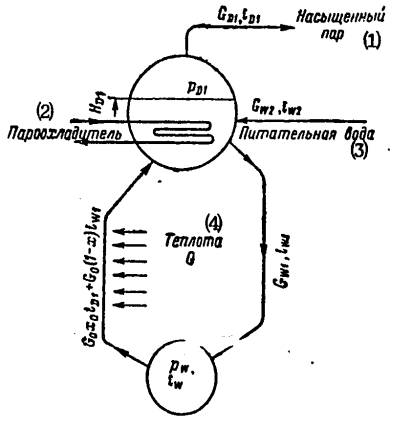

Figure 13. Diagram of a Design of the Steam-and-Water Volume of a Steam Generator.

Key:
1. Saturated steam.
2. Steam cooler.
3. Feedwater.
4. Heat.

Here Δp_{TP} are losses of pressure to friction; $\Sigma \Delta p_M$ is the sum of the losses to local resistances; $p_{уск}$ are losses to flow acceleration; and $p_{геод}$ is the fluid's potential energy.

The design was made in accordance with the mass velocity: $\omega = G_\omega / f_{оп}$.

Losses to friction for movement of a homogeneous medium (water or steam) are determined according to the formula

$$\Delta p_{тр} = \zeta_{т.о} L_{труб} \frac{G_{\omega 1}^2}{2 f_{оп}^2 \rho_\omega}, \qquad (44)$$

where $\zeta_{T.\,0}$ is the adjusted coefficient of friction [15]:

$$\zeta_{\text{т.о}} = \frac{\zeta}{d_э} = \frac{1}{4d_э\,(\lg 3{,}7d/k)^2}\ \text{м}^{-1}. \tag{45}$$

The absolute roughness of steel pipes is usually taken as k = 0.08 mm.

Losses to local drags for a homogeneous moving medium are determined according to the well-known formula

$$\sum \Delta p_м = \frac{G_{w1}^2}{2f_{on}^2\rho_{w1}} \sum \zeta_i, \tag{46}$$

where $\Sigma\zeta_i$ is the sum of the coefficients of local drags.

For the downcomer bundle

$$\Delta p_{\text{геод}} = -g\rho_{w1}H_o,$$

where H_0 is the average height of the downcomer bundle.

Losses to acceleration of flow

$$\Delta p_{\text{уск}} = \frac{H_o}{f_{on}} \cdot \frac{dG_{w1}}{dt}. \tag{47}$$

Thus, instead of (43), one can write

$$p_w - p_{D1} = \frac{G_{w1}^2}{2f^2{}_{on}\rho_{w1}}\left(1 + \sum_{i=1}^{n}\zeta_{oi} + \zeta_{\text{т.о}}L_{\text{тр}}\right) - g\rho_{w1}H_o + \frac{H_o}{f_{on}} \cdot \frac{dG_{w1}}{dt}. \tag{48}$$

In the case of the riser bundle the terms of the right side (43) turn out to be functions of a number of additional factors: local pressure losses at the input from the lower drum into the riser bundle are determined by water consumption $G_{\omega 1}$, while other losses, which depend upon velocity, are determined by the consumption G_0 of the steam-and-water mix. For the riser bundle, the pressure between the lower and upper drums is represented by the following equation

$$p_{D1} - p_w = \zeta_{\text{т}}^{(\text{вх})}\frac{G_{w1}^2}{2f_{\text{п}}^2\rho_{w1}} + \frac{G_o^2}{2f_{\text{п}}^2\rho_o}\left(1 + \zeta_{\text{т. п}}L_{\text{тр}} + \sum_{i=1}^{n-1}\zeta_{\text{п}i}\right) + g\rho_o H_o + \frac{H_o}{f_{\text{п}}} \cdot \frac{dG_o}{dt}. \tag{49}$$

The coefficient of friction where a steam-and-water mix is moving is determined from the correlation [17]

$$\zeta_{т.п} = \psi\zeta_{т}\frac{\pi}{n}\left[1+\bar{x}\left(\frac{\rho'}{\rho''}-1\right)\right], \tag{50}$$

where x is the average mass steam content of the flow (the degree of dryness):

$$\bar{x} = \frac{i_k - i'}{2r}, \tag{51}$$

ρ' and ρ'' are the separate densities of the water and steam for a given pressure and temperature of saturation.

The coefficients of local resistances $\zeta_{пi}$ for the steam-and-water mix can be computed in accordance with the appropriate coefficients ζ_{oi} for water in the following form

$$\zeta_{пi} = \zeta_{oi}\left[1+\bar{x}\left(\frac{\rho'}{\rho''}-1\right)\right]. \tag{52}$$

We move over to a determination of the density of the steam-and-water mix in the riser bundle.

It follows from assumptions about the constancy of the thermal loading along the riser bundle that the degree of steam content x of the mix is changed linearly. However, the steam's speed is higher than the water's speed, as a result of which the number of steam bubbles that characterizes the ratio of ε = the steam volume/mix volume is changed nonlinearly.

Rising speed is proportional to the proportion of steam in the mix and inversely proportional to its mass; for the steam this is determined by the ratio $x/\varepsilon\rho''$, and for water by

$$\frac{1-\bar{x}}{(1-\varepsilon)\rho'}. \tag{53}$$

If the concept of steam slip-past S_k = steam speed/water speed > 1 is introduced, then the preceding expressions are joined in the following form:

$$\frac{\bar{x}}{\varepsilon\rho''} = S_k\frac{1-\bar{x}}{(1-\varepsilon)\rho'}. \tag{54}$$

Thus, an excess of steam speed over water speed characterizes slip-past S_k. The following dependence of slip-past on the volumetric dryness of the mix, the density of its components and relative speed has been established empirically [44]:

$$S_k = \frac{1-\varepsilon}{1/C_0-\varepsilon}\left(1+\frac{C}{C_0}\sqrt{\frac{\rho'-\rho_D}{\rho' Fr^2}}\right), \tag{55}$$

where $Fr^2 = \dfrac{G_\omega^2}{g\rho'^2 A_r D_r}$ is the square of the Froude number; and C and C_0 are constants.

The density of the steam-and-water mass

$$\rho = \rho' - \varepsilon(\rho' - \rho''). \tag{56}$$

The average density in the riser bundle is determined by integration according to the length of the path of the mix:

$$\rho_{a1} = \frac{1}{L_{r1}} \int_0^{L_{r1}} \rho\, dl = \rho' - \frac{\rho' - \rho''}{C_0 - b} + \\ + \frac{(\rho' - \rho'')\, b}{x_0 (C_0 - b)^2} \ln \left[\frac{(C_0 - b)\, x_0 + b}{b} \right], \tag{57}$$

where

$$b = \frac{\rho''}{\rho'} \left(C_0 + C \sqrt{\frac{\rho' - \rho''}{\rho' \mathrm{Fr}^2}} \right). \tag{58}$$

On the other hand, change of the density of the steam-and-water mix in the riser bundle by the volume $V_{\text{п}}$ is characterized by the correlation

$$\frac{d\rho''}{dt} = \frac{G_{w1} - G_{D1}}{V_{\text{п}}}. \tag{59}$$

Change in water level and steam pressure in the upper drum is governed by the amount of heat Q_{riser} that has been absorbed by the riser bundle of the PG's pipes.* This heat takes shape from the following components: the radiant heat $Q_{\text{л}}$ in the firebox space

$$Q_{\text{л}} = k_{\text{л}} \left[\left(\frac{\theta_{\text{л}} + 273}{100} \right)^4 - \left(\frac{\theta_{\text{м}} + 273}{100} \right) \right]^4 \tag{60}$$

(the proportional difference of the fourth power of the equivalent temperature of radiation $\theta_{\text{л}}$ and the temperature θ_{M} of the metal of the tubes of the riser bundle) and the heat Q_{k} of convective heat transfer.

As is known, the heat that is transferred to the two-phase flow is approximately proportional to the third power of the difference in temperature between the metal of the wall and the flow:

$$Q_{\text{к}} = k_{\text{к}} (\theta_{\text{м}} - \theta_0)^3; \tag{61}$$

it equals the heat returned by the flue gases that flow over the bundle

$$Q_{\text{к}} = k_{\text{г}} G_{\text{г}}^{0,6} (\theta_{\text{г}0} - \theta_{\text{м}}). \tag{62}$$

The mass balance of the water in the PG's drum

$$G_0 (1 - x_0) + G_{w2} + D_{\text{кон}} - G_{w1} = \frac{dW_6}{dt}. \tag{63}$$

The heat balance of the water in the drum:

$$G_0 (1 - \bar{x}_0) i_w + Q_{\text{ох}} + G_{w2} i_{w2} + D_{\text{кон}} i_{\text{кон}} - G_{w1} i_{w1} = \frac{d}{dt} (W_6 i_{w1}), \tag{64}$$

*As is known, the downcomers in modern ship PG's are not warmed.

where $Q_{ox} = D_{ox}\ [i_{пе} - (i_{нас} - \Delta i)]$ is the heat returned to the water by the steam cooler.

The level of water in the steam-generator drum and the steam volume are functions of the weight of the water in the drum:

$$H_б = \frac{W_б - W_{б0}}{C_б},$$

where $C_б$ is a coefficient that is determined by the drum's geometry:

$$V_{п.б} = V_б - \frac{W_б}{\rho'}, \tag{65}$$

$$\frac{dV_{п.б}}{dt} = \frac{C_{б2}}{C_{б1}} \frac{dW_б}{dt}. \tag{66}$$

The mass balance of the steam volume

$$G_0 x - D_{кон} - D_{D1} = \frac{d}{dt}(V_{п.б}\rho_{D1}). \tag{67}$$

The heat balance of the lower drum

$$G_{в1}(i_{в1} - i_в) = V_{п.б} \frac{di_в}{dt}. \tag{68}$$

The feedwater temperature is determined by the equation of heat transfer in the economizer.

Experimental Study of the Dynamics of the Steam Pressure in a Steam Generator. Experimental data and numerous theoretical studies testify that changes in steam pressure caused by a disturbance in the energy balance of the PG's steam-and-water volume can be described with adequate precision by a differential equation of the first order:

$$T_a \frac{d\varphi_1}{dt} = \frac{\Delta Q_к}{Q_{к0}} - \lambda_D, \tag{69}$$

in which T_a is the coefficient of inertness of the PG for the steam pressure.

The first term on the right side is determined by equation (37), and the second expresses change in steam consumption.

The coefficient T_a is determined by the ratio of the heat that has been accumulated by the steam-and-water volume and the metal of the evaporator surfaces to the flow of heat per second at the PG output.

In the transient process, a deviation of steam pressure from the established value causes an additional change in steam consumption, which coincides in sign with the pressure deviation. This self-regulation can be established from the formula for polytropic outflow

$$D = \zeta f \sqrt{2g \frac{m}{m-1}} \sqrt{\frac{p_0}{v_0}} \sqrt{\left(\frac{p_1}{p_0}\right)^{\frac{2}{m}} - \left(\frac{p_1}{p_0}\right)^{\frac{m+1}{m}}}, \tag{70}$$

where ζ is the outflow coefficient, m is the indicator of polytropy of the flow, and v_0 is the initial specific volume of the steam.

Taking into consideration the fact that $p_0 v_0^m$ is a constant, we obtain the expression for the increment in steam consumption:

$$\Delta D = \left[\frac{\partial D}{\partial \zeta}\Delta\zeta + \frac{\partial D}{\partial f}\Delta f + \frac{\partial D}{\partial\left(\frac{p_1}{p_0}\right)}\Delta\left(\frac{p_1}{p_0}\right) + \Phi_*(D)\right] + \frac{\partial D}{\partial p_1}\Delta p_1. \qquad (71)$$

Here $\Phi_*(D)$ is the sum of the members of the Taylor series obtained from (70), in which the increment of the argument enters into powers higher than the first.

We designate the sum of the members of the last expression that was enclosed in brackets as ΔD_0; this sum is determined by the valve characteristics and it expresses changes in steam consumption that result from moving the valve when the steam pressure is unchanged.

The term $\frac{\partial D_1}{\partial p_1}\Delta p_1$ governs the self-regulation referred to above. It can be established from (70)

$$\frac{1}{D_0}\frac{\partial D}{\partial p_K} = \frac{m+1}{2m}\frac{\Delta p_1}{p_{10}}, \qquad (72)$$

which enables (71) to be written in the form

$$\Delta D = D_0 + D_{10}\frac{m+1}{2m}\frac{\Delta p_1}{p_{10}}.$$

The coefficient of self-regulation a_c can be expressed as:

$$a_c = \frac{\Delta\lambda}{\varphi_1} = \frac{m+1}{2m}. \qquad (73)$$

For dry saturated steam m = 1.135, since a_c = 0.94.*

Let us compare the result obtained with the experimental data.

Figure 14 presents data about steam-pressure changes in the ship's steam generator that arise as a result of various disturbances. Let us reduce these data to dimensionless coordinates

$$\Delta\lambda = \frac{D - D_{10}}{D_{10}}, \quad \varphi = \frac{p_1 - p_{10}}{p_{10}},$$

*Taking into consideration the assumptions that were made when deriving correlation (73), this latter should be viewed as an evaluation of the self-regulation coefficient in the equation of the PG's dynamics with regard to steam pressure.

the ratio of which determines the value of the coefficient a_c.

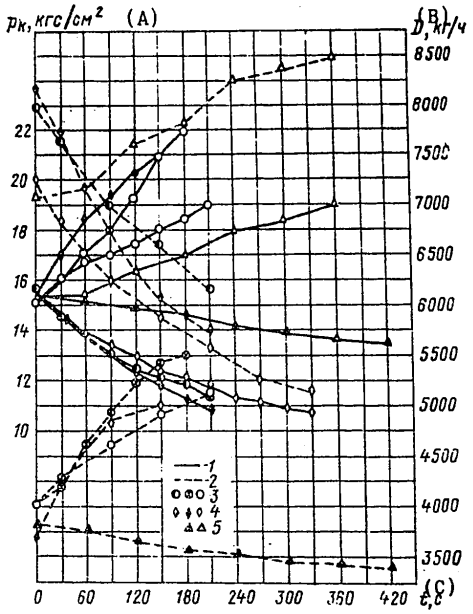

Figure 14. Change of Pressure and Deviations in Steam Consumption as a Result of Various Disturbances When There Is No Change in Degree of Opening of the Check Valve (according to steam-generator bench-test data).

Key:
1. Change in steam pressure.
2. Change in steam consumption.
3. Disturbance in fuel feed.
4. Disturbance in steam consumption.
5. Disturbance in feedwater feed.

A. Kg-force/cm².
B. Kg/hr.
C. Time, seconds.

The function $\Delta\lambda = \lambda(\phi_1)$, which was constructed according to the data of figure 14, is shown in figure 15 and can be expressed by the linear equation

$$\Delta\lambda = \bar{a}_c\Phi_1. \tag{74}$$

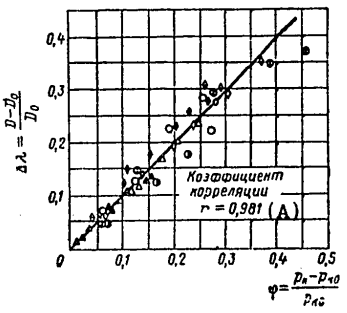

Figure 15. The Relation Between Dimensionless Changes in Steam Pressure and Consumption, Which Determines the Coefficient a_c in Formula (73). Plotted in accordance with the data of Figure 14; the notation is the same.

Key:
A. Coefficient of correlation r = 0.981.

The value of a_c, which is determined by approximation in accordance with the method of least squares for the whole aggregate of values of $\Delta\lambda$ and ϕ_1 that were presented in figure 15, proved to be equal to

$$\bar{a}_c = \frac{\sum_{i=1}^{n=51} \varphi_{1i}\,\Delta\lambda_i}{\sum_{i=1}^{n=51} \varphi_{1i}^2} = \frac{1{,}441}{1{,}452} = 0{,}9924.$$

The straight line that corresponds to the value $\bar{a}_c$ that is obtained, is shown in figure 15 by a continuous line.

The experimental value of the self-regulation coefficient a_c that was obtained corresponds well with the value calculated in accordance with formula (73). The full change λ_D of steam consumption in the transient process is expressed by the formula

$$\lambda_D(t) = \lambda_0^{\prime}(t) + a_c\varphi_1, \tag{75}$$

in which $\lambda_0(t)$ is a function that characterizes changes in steam consumption that are caused by movement of the steam-regulating valve with unchanged pressure of the steam in the steam generator.

Taking into account (37) and (75), equation (69) of the dynamics of steam pressure takes the form

$$T_a\varphi_1' + a_c\varphi_1 = -\lambda_0(t) + \psi + \rho_* + \eta(\nu - \psi - \rho_в). \tag{76}$$

In accordance with the recommendations set forth in the preceding section of the book, generalized coordinates for the transient process were used in determining the statistical characteristics (mathematical expectation, dispersion, and confidence interval) and the values of the coefficient of inertness in accordance with the data of several experiments, which are distinguished by the value and sign of the disturbance.

Figure 16 shows experimental data obtained under operating conditions about steam-pressure deviations in KVG-34 steam generators. The changes that are related to the various realizations are designated by various symbols in the figure.

In connection with equation (76), during the processing of these data, dimensionless time τ and the generalized deviation $\varphi_{1об}$ of the parameters were introduced in accordance with the correlations:

$$\tau = \frac{a_c}{T_a}\,t,$$

$$\varphi_{1\,об} = -\frac{2{,}3}{a_c}\lg\left(1 + \frac{a_c}{\lambda_в}\varphi_1\right)$$

(for disturbance with respect to steam); and

$$\varphi_{1\,об} = -\frac{2{,}3}{a_c}\lg\left(1 + \frac{a_c}{\psi}\varphi_1\right)$$

(for a disturbance with respect to fuel).

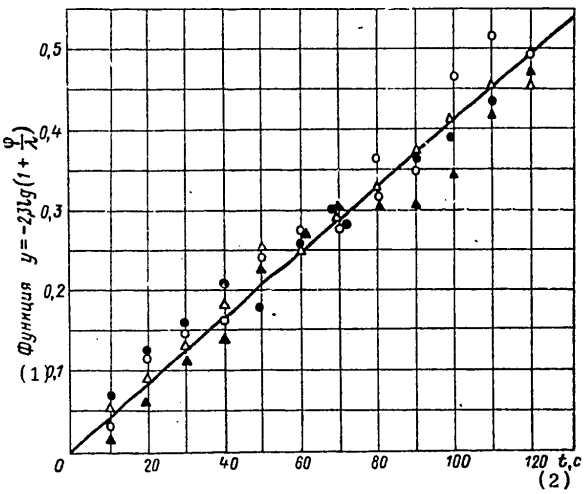

Figure 16. Transient Functions for Steam Pressure for KVG-34 Steam Generators During Disturbance in Fuel Consumption λ_D (light-colored points) and in the Firebox (black points), Which Are Presented in Generalized Coordinates.

The straight line is an approximation where the value of the coefficient of inertness T_a = 239.5 seconds.

Key:
1. Function. 2. Time, seconds.

The functions ρ_T and fn are equal to zero under the conditions for conducting the experiment.

Values for the coefficient T_a in (76) and also for the root mean square error σ_y were determined by means of expressions (7) and (16) for each of the realizations, which contain current time values and the corresponding ordinates of the transient function for 13 pairs. Then the error σ_T was determined for each of the realizations in accordance with (17).

The mathematical expectation for the value of T_a and the scattering characteristics were established in accordance with the generally accepted rules. The results of this processing are shown in table 3.

A Dynamic Model of a Steam Superheater. It is known that Soviet and foreign scientists have conducted much research of the dynamics of boilers for steam superheaters [18, 20, 26, 40 and 44]. A substantial part of this research is based upon an analysis of experimental data.

Existing mathematical models of steam superheaters can be divided into two groups:

--Models with extended parameters that consider temperatures changes of the tube wall and the steam parameters in the axial direction; because of this, differential equations in partial derivatives enter into the system

of equations for the dynamics of the steam temperature at the output of steam superheaters; and

--Models with concentrated parameters that were constructed on the basis of simplifying assumptions that the steam's thermodynamic properties are unchanged throughout the whole volume of the steam superheater.

Table 3

Results of Determination of Inertness of a KVG-34 Steam Generator According to Steam Pressure

Indicators	Samples (see figure 16)			
	o	•	Δ	▲
Coefficients of inertness T_a, seconds	224	236	245	253
Root mean square deviation σ_y	$2.9 \cdot 10^{-2}$	$2.8 \cdot 10^{-2}$	$1.29 \cdot 10^{-2}$	$2.7 \cdot 10^{-2}$
Root mean square deviation σ_T for T_a for the samples, seconds	17.5	18.7	9.5	21.2
Average value of the coefficient of inertness $\overline{T}_a$, seconds	239.5			
Root mean square error $\sigma_{\overline{T}}$ for the average value of $\overline{T}_a$, seconds	$\sigma_{\overline{T}} = \left[\frac{1}{4}\sum_1^4 (T - \overline{T}_a)^2\right]^{\frac{1}{2}} = 8{,}6$			
Root mean square deviation $\sigma'_{\overline{T}}$, seconds	$\sigma'_{\overline{T}} = \frac{1}{4C_2}\sum_1^4 \sigma_T = 21^*$			

*Here $C_2 = 0.7979$ is the table value of the ratio $\overline{\sigma}/\sigma'$ for the amount of the sample of the four elements.

A comparison of the results of the calculations made with these models with full-scale measurements data inevitably displays certain discrepancies, the causes for which still remain unclear. Moreover, it was established by [26] and [44] that in the case of transient regimes, models with concentrated parameters give a completely acceptable approximation for changes in steam temperature that are caused by disturbances in steam consumption, heat loading, or the injection of cooling water, while, in the case of disturbances in change in steam temperature at the input into the steam superheater, these models led to erroneous results and it proves necessary to use models with distributed parameters.

Because of the fact that, for modern marine steam superheaters with automatic thermal-combustion regulation, the temperature of the saturated steam deviates by no more than 3-4 degrees C, even with deep changes in loading; this work does not examine disturbances in steam temperature at the input into the steam superheater. This makes it possible to present a dynamic model of a steam superheater as a model of a concentrated volume

with a time delay; the model's parameters are made more precise by a comparison with the static and dynamic characteristics established during full-scale studies.

The form of equations that describe a steam superheater's dynamics should, in accordance with the conditions described above, be adapted to a maximum extent to introduce various data of experimental observations into the coefficients of these equations. Meeting these conditions is a mathematical model whose construction is based upon the following basic assumptions:

The coefficient of heat emission from the wall of the steam superheater's tubes is, in accordance with a known empirical correlation [15], proportional to steam consumption to the 0.8-th power;

The coefficient of heat emission from the gases to the walls of the steam superheater is determined by the amount of the gases (or fuel consumption) to the 0.6-th power; and

The temperatures are taken as the average value of the input and output temperatures.

The equation of mass balance of a flow of steam through a steam superheater in increments has the form (see figure 9):

$$V_{\text{пе}}\frac{d\gamma}{dt} = \Delta D_{\text{и}} - \Delta D_{\text{пе}}. \tag{77}$$

The equation of thermal balance for that same flow is

$$\frac{d}{dt}(V_{\text{пе}}\gamma_{\text{пе}}i_{\text{пе}}) = D_{\text{и}}i_{\text{и}} - D_{\text{пе}}i_{\text{пе}} + Q_{\text{п}}^{\text{ст}}.$$

The steam pressure in automated steam superheaters is changed slightly, which permits the enthalpy of the superheated steam to be viewed as a function of one parameter--the temperature of superheating: $i_{\text{пе}} = i_{\text{пе}}(\theta_{\text{пе}})$. Taking this simplification into account and moving over to increments of the functions in the latter equation, we get

$$V_{\text{пе}}i_{\text{пе}}\frac{d\gamma_{\text{пе}}}{dt} + V_{\text{пе}}\gamma_{\text{пе}}\frac{\partial i_{\text{пе}}}{\partial\theta_{\text{пе}}}\frac{d\theta_{\text{пе}}}{dt} =$$

$$= i_{\text{и}_0}\Delta D - i_{\text{пе}_0}\Delta D + \Delta Q_{\text{п}}^{\text{ст}} - D_{\text{пе}_0}\frac{\partial i_{\text{пе}}}{\partial\theta_{\text{пе}}}\Delta\theta_{\text{пе}},$$

which, taking (77) into account, yields

$$V_{\text{пе}}\gamma_{\text{пер}}\frac{\partial i_{\text{пе}}}{\partial\theta_{\text{пе}}}\frac{d\theta_{\text{пе}}}{dt} + D_{\text{пе}_0}\frac{\partial i_{\text{пе}}}{\partial\theta_{\text{пе}}}\Delta\theta_{\text{пе}} = \Delta Q_{\text{п}}^{\text{ст}} -$$

$$- (i_{\text{пе}_0} - i_{\text{и}_0})\Delta D. \tag{78}$$

In these transformations of the equation of thermal balance the assumption is made

$$\Delta D_{\text{и}} = \Delta D_{\text{пе}},$$

which is tantamount to a disregard of the heat that is accumulated in that amount of steam by which the steam content of the steam superheater was changed during the period of the transient response. Calculations indicate that the error here is in tenths of a percent.

The amount of heat that is transmitted from the tube's wall to the steam, with regard to both statics and dynamics, can be computed according to the empirical function

$$Q_{\text{п}}^{\text{ст}} = K_{\text{пе}}^{\text{п}} D_{\text{пе}}^{0,8} (\theta_{\text{пе}}^{\text{ст}} - \theta_{\text{пе}}),$$

which in increments has the form

$$\Delta Q_{\text{п}}^{\text{ст}} = \frac{0,8 K_{\text{пе}}^{\text{п}}}{D_{\text{пе}_0}^{0,2}} (\bar{\theta}_{\text{пе}_0}^{\text{ст}} - \theta_{\text{пе}_0}) \Delta D_{\text{пе}} + \\ + K_{\text{пе}}^{\text{п}} D_{\text{пе}_0}^{0,8} \Delta\theta_{\text{пе}}^{\text{ст}} - K_{\text{пе}}^{\text{п}} D_{\text{пе}_0}^{0,8} \Delta\theta_{\text{пе}}. \qquad (79)$$

Here $K_{\text{пе}}^{\text{п}}$ is the coefficient of heat emission that is computed according to test data or statics computations data.

After setting the expression for $\Delta Q_{\text{п}}^{\text{ст}}$ that was obtained for equation (79) into (78), we proceed to the first equation of the steam superheater's dynamics:

$$V_{\text{пе}} \gamma_{\text{пе}_0} \frac{\partial i_{\text{пе}}}{\partial \theta_{\text{пе}}} \frac{d\theta_{\text{пе}}}{dt} + \left[D_{\text{пе}_0} \frac{\partial i_{\text{пе}}}{\partial \theta_{\text{пе}}} + K_{\text{пе}}^{\text{п}} D_{\text{пе}_0}^{0,8} \right] \Delta\theta_{\text{пе}} = \\ = - \left[(i_{\text{пе}_0} - i_{\text{в}_0}) - \frac{0,8 K_{\text{пе}}^{\text{п}}}{D_{\text{пе}_0}^{0,2}} (\theta_{\text{пе}_0}^{\text{ст}} - \theta_{\text{пе}_0}) \right] \Delta D_{\text{пе}} + \\ + K_{\text{пе}}^{\text{п}} D_{\text{пе}_0}^{0,8} \Delta\theta_{\text{пе}}^{\text{ст}}. \qquad (80)$$

Equation (80) establishes the dependence of the temperature of the superheated steam on its consumption and on the temperature of the steam superheater's wall. The process of accumulation of heat by the metal of the heating surface of the steam superheater has, in increments, the form

$$c_{\text{м}} G_{\text{пе}} \frac{d\theta_{\text{пе}}^{\text{ст}}}{dt} = \Delta Q_{\text{пе}}^{\text{г}} - \Delta Q_{\text{п}}^{\text{ст}}. \qquad (81)$$

Here $c_{\text{м}}$ is the specific thermal capacity of the tube's metal.

The heat flow from the gases to the wall of the steam superheater can be determined by the equation

$$Q_{\text{пе}}^{\text{г}} = K_{\text{пе}}^{\text{г}} B_0^{0,6} (\theta_{\text{пе}_0}^{\text{г}} - \theta_{\text{пе}_0}^{\text{ст}}).$$

In this equation the heat-emission coefficient $K^{г}_{пе}$ should be determined in accordance with test results or with data on thermal analysis of the steam generator.*

Moving over to increments of functions, we get from the latter equation

$$\Delta Q^{г}_{пе} = \frac{0{,}6K^{г}_{пе}}{B_0^{0,4}}(\theta^{г}_{пе_0} - \theta^{ст}_{пе_0})\Delta B + K^{г}_{пе}B_0^{0,6}\Delta\theta^{г}_{пе} - K^{г}_{пе}B_0^{0,6}\Delta\theta^{ст}_{пе}. \quad (82)$$

The average temperature of the gas flow $\theta^{г}_{пе}$ in the steam superheater is determined by the loading for fuel, therefore

$$\Delta\theta^{г}_{пе} = \frac{\partial\theta^{г}_{пе}}{\partial B}\Delta B.$$

Taking into account this correlation we get from (82) an equation that expresses change in the amount of heat transmitted from the gases to the steam superheater's wall

$$\Delta Q^{г}_{пе} = K^{г}_{пе}\left[\frac{0{,}6}{B_0^{0,4}}(\theta^{г}_{пе_0} - \theta^{ст}_{пе_0}) + B_0^{0,6}\frac{\partial\theta_{пе}}{\partial B}\right]\Delta B - K^{г}_{пе}B_0^{0,6}\Delta\theta^{ст}_{пе}. \quad (83)$$

Substituting (79) and (83) into (81), we get the second equation of the dynamics of the steam superheater, which describes the change in temperature of the walls of its tubes:

$$c_м G_{пе}\frac{d\theta^{ст}_{пе}}{dt} + [K^{г}_{пе}B_0^{0,6} + K^{п}_{пе}D_{пе_0}^{0,8}]\Delta\theta^{ст}_{пе} = K^{г}_{пе}\left[\frac{0{,}6}{B_0^{0,4}}(\theta^{г}_{пе_0} - \theta^{ст}_{пе_0}) + B_0^{0,6}\frac{\partial\theta^{г}_{пе}}{\partial B}\right]\Delta B - \frac{0{,}8K^{п}_{пе}}{D^{0,2}_{пе_0}}(\theta^{ст}_{пе_0} - \theta_{пе_0})\Delta D_{пе} + K^{п}_{пе}D_{пе_0}^{0,8}\Delta\theta_{пе}. \quad (84)$$

Equations (80) and (84) form a system of equations of the dynamics of the steam superheater.

In order to reduce the coefficients in these equations to dimensionless form, we divide them term by term into the value of the thermal flow through the steam superheater in the established regime:

$$D_{пе_0}(i_{пе_0} - i_{н_0}) = K^{п}_{пе}D_{пе_0}^{0,8}(\theta^{ст}_{пе_0} - \theta_{пе_0}) = K^{г}_{пе}B_0^{0,6}(\theta^{г}_{пе_0} - \theta^{ст}_{пе_0}).$$

*Where necessary, the effect of measuring the coefficient of air concentration on heat transfer in the steam superheater can also be considered here. For this it is sufficient to take advantage of the dependence of the coefficient of the heat emission $K^{г}_{пе}$ on air concentration α, after which the term appears in (82) in the form:

$$B_0^{0,6}(\theta^{г}_{пе} - \theta^{ст}_{пе})\frac{\partial K^{г}_{пе}}{\partial\alpha}\Delta\alpha.$$

As a result, we obtain

$$\left.\begin{aligned} T_{11}\frac{d\varphi_2}{dt}+a_{11}\varphi_2 &= -b_{11}\lambda_D + b_{12}\varphi_3,\\ T_{21}=\frac{d\varphi_3}{dt}+a_{21}\varphi_3 &= -b_{21}\lambda_D + b_{22}\psi + b_{23}\varphi_2,\end{aligned}\right\} \tag{85}$$

where it is specified

$$\left.\begin{aligned} T_{11} &= \frac{V_{\text{пе}}\gamma_{\text{пе}_0}\frac{\partial i_{\text{пе}}}{\partial\theta_{\text{пе}}}\theta_{\text{пе}}}{D_{\text{пе}_0}(i_{\text{пе}_0}-i_{\text{н}_0})};\quad a_{11}=\frac{\theta^{*}_{\text{пе}_0}}{\theta^{\text{ст}}_{\text{пе}_0}-\theta_{\text{пе}_0}};\\ b_{11} &= 0{,}2;\ b_{12}=\frac{\theta^{\text{ст}}_{\text{пе}_0}}{\theta^{\text{ст}}_{\text{пе}_0}-\theta_{\text{пе}_0}};\\ T_{21} &= \frac{c_{\text{м}}G_{\text{пе}}\theta^{\text{ст}}_{\text{пе}}}{D_{\text{пе}}(i_{\text{пе}0}-i_{\text{н}0})};\\ a_{21} &= \frac{\theta^{\text{ст}}_{\text{пе}_0}}{\theta^{\text{г}}_{\text{пе}_0}-\theta^{\text{ст}}_{\text{пе}_0}}+\frac{\theta^{\text{ст}}_{\text{пе}_0}}{\theta^{\text{ст}}_{\text{пе}_0}-\theta_{\text{пе}_0}};\\ b_{21} &= 0{,}8;\\ b_{23} &= \frac{\theta_{\text{пе}_0}}{\theta^{\text{ст}}_{\text{пе}_0}-\theta_{\text{пе}_0}}=a_{11};\ b_{22}=0{,}6+\frac{B_0\frac{\partial\theta^{\text{г}}_{\text{пе}}}{\partial B}}{\theta^{\text{г}}_{\text{пе}_0}-\theta^{\text{ст}}_{\text{пе}_0}}.\end{aligned}\right\} \tag{86}$$

The form of equations (85) corresponds to physical representations about the effect of the main factors on the dynamics of the steam superheating process. The coefficients of (86) of these equations have a clear physical meaning.

The parameters of the mathematical model of a specific steam superheater are established from a comparison of the general solutions of the (80) and (84) system with the approximate experimental data. These operations are carried out with reference to the characteristics of KVG-34 steam generators.

Appendix 1 shows the calculated data and coefficients for KVG-34 steam generators. Let us turn to an analysis of the experimental data.

Figure 17 shows the static characteristics of a steam superheater that were obtained during full-scale tests of the PG of the tanker "Sofiya." These data should correspond to the solution of equations of the steam superheater's status that are obtained from (85) by setting the derivatives in time as equal to 0; the solution of this has the form

*The coefficient where $\Delta\theta_{\text{пе}}$ in (80) is taken as $K^{\text{п}}_{\text{пе}}D_0^{0.8}$, since

$$D_0\frac{\partial i_{\text{пе}}}{\partial\theta_{\text{пе}}} \ll K^{\text{п}}_{\text{пе}}D_0^{0.8}.$$

$$\varphi_2 = -\frac{b_{11}a_{21} - b_{12}b_{21}}{a_{11}a_{21} - b_{12}b_{23}}\lambda_D + \frac{b_{12}b_{22}}{a_{11}a_{21} - b_{12}b_{23}}\psi. \qquad (87)$$

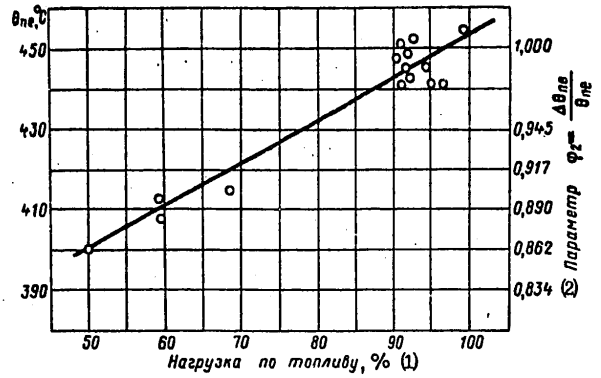

Figure 17. Static Characteristics of the KVG-34 Steam Generator.

Key:
1. Fuel loading, percent.
2. Parameter.

Where the numerical values of the coefficients a_{ik} and b_{ik} accord with Appendix 1, the equation of static chacteristics is expressed by the straight line $\phi = 0.905\lambda_D + 1.33\psi$.

In the area of the steam generator's nominal loading, there is a certain band within which changes in steam consumption are not accompanied by changes in the unit's efficiency and, consequently, the equality $\lambda_D = \psi$ is correct; from the last expression it follows that the slope of the static characterics in this band is $(\phi_{20} : \lambda_D)_{\text{theoretical}} = 0.425$.

The average slope of the experimental characteristics according to figure 17 is $(\phi_{20} : \lambda_D)_{\text{actual}} = 0.310$.

Revision of the slope of the theoretical characteristics should be performed through the second term on the right side of equation (87), which contains the derivative $\frac{\partial \theta_{ne}^{f}}{\partial B}$, since the error in determining its numerical value in comparison with other coefficients is, obviously, maximal.

Having thus made the static model of the steam superheater more accurate, let us undertake to determine the coefficients of system (85), which characterizes its inertial properties. This operation is performed by computation of the coefficients in the approximating equations in accordance with the experimental data based upon the prerequisites for minimal error of approximation.

The results of the experiments that were set up on the ship's steam generator under operating conditions for the purpose of constructing a dynamic model of a steam superheater are shown in figure 18. The tests were

conducted on a steam generator with a system included for regulating fuel combustion, whose relatively high speed in analyzing such an inertial process as change in steam temperature, enables the changes in heat release in the firebox that coincide with loading changes with respect to steam to be considered in the approximating solutions of the (85) system, that is, to set $\lambda_D = \psi$.

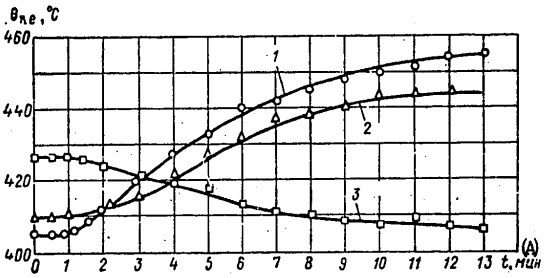

Figure 18. Transient Functions for Steam Temperature at the Output from a Steam Superheater Where There Is a Change of Steam Generator Loading with Respect to Steam in the Form of a Single Impulse.

Disturbances in the tests:
1. $\lambda_D = 0.50$;
2. $\lambda_D = 0.274$; and
3. $\lambda_D = 0.204$.

A. Time, minutes.

The differential equations of approximating system (85) contain members that express the mutual effect of both volumes. Therefore, in making an analysis of their solutions, which is associated with an approximation of experimental conditions, it is suitable to use arguments and expressions that correspond to the general case set forth above in the procedure for the experimental study of the objects.

The values of the roots of the performance equation that corresponds to the (85) system, given the values of the coefficients for the examined steam superheater that are cited in Appendix 1, are equal to

$$\left.\begin{aligned} w_1 &= -1{,}0578; \\ w_2 &= -0{,}0024. \end{aligned}\right\} \qquad (88)$$

The first of these roots is determined mainly by the inertness coefficient T_{11} of the steam volume, the second by the coefficient T_{21}, which expresses the thermal inertness of the heating surface's metal. In view of the considerable difference in the values of these roots, the component of the general solution (28) that corresponds to the first root ω_1 attenuates much more rapidly than the component that corresponds to the second; thus, where the value of t = 10 seconds, this first term in the example examined

does not exceed $5 \cdot 10^{-5}$. Therefore, the simultaneous determination of both roots in accordance with experimental data is associated with errors, the magnitudes of which cannot be established. In order to avoid similar indeterminancy, the experimental transient function should be approximated by a solution in the form of (28), setting $e^{\omega_1 t} = 0$ into it; in this case the solution will have the form

$$\frac{\varphi_2}{\varphi_{2\infty}} = 1 + \frac{w_2 - \frac{b_{11}}{T_{11}\varphi_{2\infty}}\lambda_D}{w_1 - w_2} e^{w_2 t}. \tag{89}$$

The value of the root ω_1 in (89) is taken as equal to the computed value for (88). The mathematical expectation of the second root ω_2 is determined as a result of an approximation of the experimental data of function (89); in so doing, the dispersion σ_ω^2 characterizes the precision of the approximation.

If substitutions of types (10) and (29) are introduced into (89), and assuming

$$\left.\begin{aligned} y_w &= 2{,}3 \lg \frac{1 - \varphi_2/\varphi_{2\infty}}{\frac{b_{11}}{T_{11}\varphi_{2\infty}}\lambda_D - w_1}; \\ z &= \overline{w}_2 t - z_w, \end{aligned}\right\} \tag{90}$$

then function (89) will be reduced to the form

$$y_w = \overline{w} t - z_w. \tag{91}$$

The maximum dispersion in computing ω_2 in accordance with experimental pairs of values $(y_{\omega i}, t_i)$ will be provided if the following expressions are used:

$$\left.\begin{aligned} \overline{w}_2 &= \frac{n\sum_{i=1}^{n} y_{wi}t_i - \sum_{i=1}^{n} t_i \sum_{i=1}^{n} y_{wi}}{n\sum_{i=1}^{n} t_i^2 - \left(\sum_{i=1}^{n} t_i\right)^2}, \\ z_w &= \frac{\sum_{i=1}^{n} t_i \sum_{i=1}^{n} y_{wi}t_i - \sum_{i=1}^{n} t_i^2 \sum_{i=1}^{n} y_{wi}}{n\sum_{i=1}^{n} t_i^2 - \left(\sum_{i=1}^{n} t_i\right)^2}. \end{aligned}\right\} \tag{92}$$

The root mean square deviation relative to the function y_ω is determined by the usual expression of the form (16), the dispersion σ^2_ω of the value of the root ω_2 being determined in accordance with (92):

$$\sigma^2_{w_2} = \frac{\partial w_2}{\partial y_\omega}\sigma^2_{y_\omega}.$$

The expression for the time constant T_{21} is established on the basis of the ratio between the roots and the coefficients of the performance equation which corresponds to system (85); in this case this expression has the form

$$T_{21} = -\frac{a_{21}}{w_1 + w_2 - a_{11}/T_{11}}, \tag{93}$$

and its dispersion is determined by the usual method by means of (93) and the previously computed value of $\sigma_{\omega 2}$.

Expressions of the (14) or (32) type are used where there is a time lag section.

Thus, also in this case, the coefficients in the equation of the dynamics are found on the basis of experimental data by the only possible method, given the least root mean square error, and where the precision of the approximation that is made is known.

The results of processing of the experimental data cited in figure 18 by the method set forth above are shown in table 4.

Table 4

Values of the Inertness Coefficients of the Steam Superheaters of Turbine Ship "Sofiya," Determined in Accordance with Experimental Data]

Indices	Test groups (see Fig 18)		
	1	2	3
Coefficient of inertness of the tube metal T_{21}, seconds	415	487	438
Coefficient of inertness of steam volume T_{11}, seconds	21.3	21.3	21.3
Average value of coefficient $\overline{T}_{21}$, seconds		447	
Root mean square deviation $\sigma_{T_{21}}$	21	32	43
Root mean square deviation of error of the average value $\sigma_{\overline{T}_{21}}$, seconds	$\sqrt{\frac{1}{3}\sum_1^3 (T_{21} - \overline{T}_{21})^2} = 30{,}3$		
Time lag τ, seconds	50	70	60
Root mean square deviation $\sigma_{T_{21}}$	$\frac{1}{3C_2}\sum_1^3 \sigma_{T_{21}} = 44{,}3$ *		

*Here $C_2 = 0.7236$ is the table value of the ratio σ/σ'.

3. The Main Turbogear Unit

Dynamics of Propeller-Shaft Rotating Frequency. In accordance with the research task being performed, a mathematical model of GTZA [main turbogear unit] dynamics should correspond to the condition of the main operating regime. In such a model the paramount role is played by the system's response characteristics, there being disturbances on the part of the regulating organ (the steam valve) and the external load--the moment of resistance of the screw. The first determines the response of the power plant, while the second marks the characteristics of the element that directly filters continuous disturbances--deviations of the loading on the part of the propeller shaft that acts on all the dynamic elements of the ship's installation that are connected with the GTZA.

Numerous theoretical studies made by various researchers as well as the data of our full-scale observations indicate that, under the conditions mentioned, it is possible to use a linear model of a ship's GTZA that is described by the equation

$$T_n = \frac{d\varphi_n}{dt} + \varphi_n = k_m\psi - \lambda_m, \qquad (94)$$

in which ϕ_n expresses the relative deviation of propeller-shaft rotating frequency and k_m characterizes the regulating action.

The numerical value of the coefficient of inertness T_n is determined here in accordance with the data of full-scale tests, under which the process of change of propeller-shaft rotating frequency as a result of a reduction in the input of steam into the turbine by a high-speed shutoff valve was oscillographed.

The initial conditions for which the solution of the approximating equation (94) was obtained has the form
where t = 0

$$\phi_n = \lambda_n = 0;$$

$$K_m\psi = \begin{cases} 0 \text{ where } t < 0, \text{ and} \\ \text{a constant where } t \geqslant 0. \end{cases}$$

The magnitude of the disturbance was established in relation to the nominal propeller-shaft rotating frequency regime of a laden ship.

Figure 19 shows an oscillogram of the transient response of change of the main parameters that characterize GTZA operation in dynamics. The form of the function that expresses change of shaft rotating frequency confirms the admissibility of presenting the dynamics of the object being studied as a single concentrated volume. Therefore, the results of the measurements were processed in accordance with expressions (7) and (16). Experimental transient functions in generalized coordinates of the forms of (8) and (10) are shown in figure 20, the results of processing the data obtained during the tests of the turbine ship "Sofiya" in table 5.

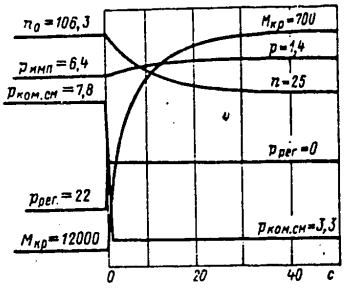

Figure 19. Change in Main Parameters of GTZA [main turbogear unit] Operation During Manipulation of the PPKh-SMPKh.

$P_{имп}$, $P_{kom.cm.}$, P_{per} are pressures: of oil for the impeller, oil to the servo motor, and steam for regulating the regulating stage of the turbine.

M_{kp} is the torque on the shaft.

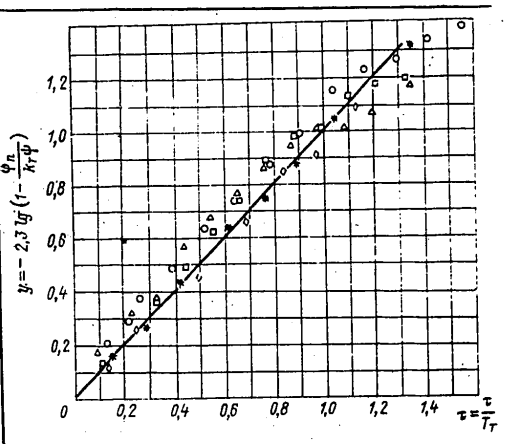

Figure 20. Transient Functions for Change of Rotating Frequency of the Propeller Shaft, Caused by Disturbance in the Turbine's Steam Consumption.

The Status of a Turbine's Flow Section. The most general indicator of a turbine's operating quality is its internal efficiency, which is a function essentially of the perfection of its manufacture and the condition of the blading section. Blading profiles change with time, leading to an increase in losses of steam energy and a reduction in efficiency (figure 21).

The internal efficiency of a turbine can be computed in accordance with measurements data by a method developed by TsNIIMF. For purposes of this computation, steam enthalpy values at the starting point of the line of expansion and at the bleed points must be available. The enthalpy of the steam at the end of the line of expansion (for the last stage of a low-pressure turbine) is determined from the heat balance and the effective power at the flange of the reduction gear; it is assumed here that the mechanical efficiency of the turbine and the reduction gear are known [24].

For the three-stage TS-3 turbine with intermediate steam superheater it is possible to use a monitoring of the blading section, also developed by TsNIIMF, which consists of the following (per notation in figure 22).

From Flugel's formula for a group of stages that operate with a speed less than critical, it follows that

$$\frac{D}{D_1} = \frac{D}{D_0} : \frac{D_1}{D_0} = \sqrt{\frac{p_{11}^2 - p_{21}^2}{p_{10}^2 - p_{20}^2}} \sqrt{\frac{T_{10}}{T_{11}}},$$

Table 5

Results of Approximating the Transient Response of Change of Propeller-Shaft Rotating Frequency of the Main Turbogear Unit with an Equation of the Form of (94)

Indicators	Realizations (see Fig 23)		
	□	Δ	o
Disturbance in steam consumption $k_T\psi$.....	-0.925	-0.975	-0.919
Coefficient of inertness T, seconds.....	9.07	9.2	7.7
Root mean square deviation σ_T of the value T, seconds.....	0.31	0.79	0.56
Average value of the coefficient of inertness $\overline{T}$, seconds		8.57	
Root mean square error $\sigma_{\overline{T}}$ of the average value of $\overline{T}$, seconds.....		0.70	
Weighted root mean square deviation $\overline{\sigma}$, seconds		0.64	
Root mean square σ_1.....		$\sigma_1 = \frac{\overline{\sigma}}{C_2} = \frac{0,64}{0,7236} = 0,89$	

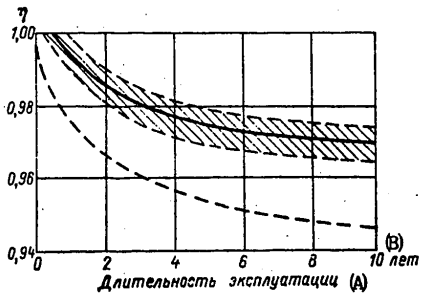

Figure 21. Relative Reduction of Internal Efficiency $\Delta\eta/\eta_0$ of a Steam Turbine with the Passage of Time.

Key:
- + → Normal changes
- - - Changes in efficiency of machine with poorly machined blades.

The zone of probable deviations is hatched.

A. Duration of operation.
B. Years.

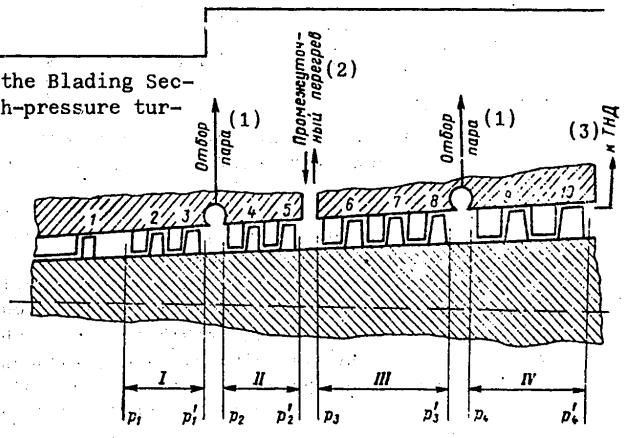

Figure 22. Diagram of the Blading Section of a TS-3 TVD [high-pressure turbine] Unit with Indication of Points and Sections Monitored (I-IV).

Key:
1. Steam bleed.
2. Intermediate superheating.
3. To TND [low-pressure turbine].

or, if the change in absolute temperature T_{1i} is disregarded:

$$\frac{D}{D_1} = \sqrt{\frac{p_{1i}^2 - p_{2i}^2}{p_{10}^2 - p_{20}^2}}.$$

The expression for absolute consumption can be obtained by introducing efflux coefficients μ_i. For the i-th group of stages

$$D_i = \mu_i \sqrt{p_{1i} - p_{2i}}.$$

Where the condition of the blading section is being monitored, the efflux coefficient, which is computed in accordance with measured values of pressure and steam consumption through the given i-th group of stages, can be used:

$$\mu_i = \frac{D_i}{\sqrt{p_{1i}^2 - p_{2i}^2}}, \tag{95}$$

and the ratio (overfall) of pressures for the group of stages being examined:

$$\beta_i = \frac{p_{2i}}{p_{1i}}, \tag{96}$$

$$\left.\begin{aligned} D_i^2 &= \mu_i^2 p_{1i}^2 \left[1 - \left(\frac{p_{2i}^2}{p_{1i}^2}\right)\right], \\ \beta_i^2 &= 1 - \left(\frac{D_i}{\mu_i p_{1i}}\right)^2. \end{aligned}\right\} \tag{97}$$

The results of computations under formulas (95) and (96), based on the designers' calculations data for the various turbine operating regimes, are shown in table 6. This data embraces groups I-IV of the high-pressure turbine (TVD) stages (see figure 22) and also groups V-VI of the TND stages. Certain of these results have been depicted graphically (figure 23).

Thus the coefficients μ_i and β_i depend only slightly upon the loading with respect to steam, thanks to which they can be used to monitor measurements of blading profile during operation. An advantage of this monitoring method is the fact that the required measurements are completed by the monitoring of the pressures.

The data cited relate to turbine operation without bleeds. The inclusion of steam bleeds and change in the amount of steam bled distorts to a certain extent the picture obtained. Therefore, where a turbine operates with the bleeds engaged, the described method is in need of additional checking.

As the designers' data shown in figure 24 indicates, steam pressure for the TVD control stage (ahead of the first group of nonregulated stages)

Table 6

Data of Calculations for the Blading Section of a Steam Turbine

(1)	(2)	(3) Группы ступеней проточной части турбины																					
		(4) ТВД (по рис. 23)										ТНД (5)											
		I			II			III			IV			V			VI					
	Расход пара, кг/с	Частота вращения ротора турбины, об/мин																					
		30	50	65	30	50	65	30	50	65	30	50	65	30	50	65	30	50	65	30	50	65	
p_4	5	0,573	0,573	0,573	1,118	1,118	1,118	2,510	2,510	2,510	9,69	9,69	9,69	22,9	22,9	22,9	535	535	535	535	535	535	535
	10	0,573	0,573	0,568	1,129	1,129	1,083	2,500	2,500	2,490	9,53	9,53	9,18	22,3	22,3	21,3	536	536	536	536	536	469	536
	15	0,575	0,575	0,575	1,124	1,124	1,124	2,665	2,665	2,665	9,58	9,58	9,58	20,85	20,85	20,85	536	536	536	536	536	536	536
	(6) Среднеарифметические значения	0,5730			1,118			2,570			9,57			21,9			527						
	(7) Среднеквадратичные отклонения	0,00216			0,01384			0,062			0,1576			0,973			8,09						
p_1	5	0,696	0,696	0,696	0,674	0,674	0,674	0,527	0,527	0,527	0,570	0,570	0,570	0,208	0,208	0,208	0,225	0,225	0,225	0,225	0,225	0,225	0,225
	10	0,694	0,694	0,698	0,674	0,674	0,667	0,524	0,524	0,532	0,566	0,566	0,556	0,207	0,207	0,212	0,114	0,114	0,114	0,114	0,114	0,1064	0,1064
	15	0,694	0,694	0,694	0,670	0,670	0,670	0,526	0,526	0,526	0,555	0,555	0,555	0,203	0,203	0,203	0,077	0,077	0,077	0,077	0,077	0,077	0,077
	(6) Среднеарифметические значения	0,695			0,677			0,526			0,560			0,207			0,138						
	(7) Среднеквадратичные отклонения	0,001 45			0,006 06			0,002 43			0,007 28			0,003 17			0,06						

1. Groups of turbine blading section stages.
2. Coefficients.
3. Steam consumption, kg/second.
4. TBD [high-pressure turbine] (in accordance with figure 23).
5. TND [low-pressure turbine].
6. Root mean square values.
7. Root mean square deviations.

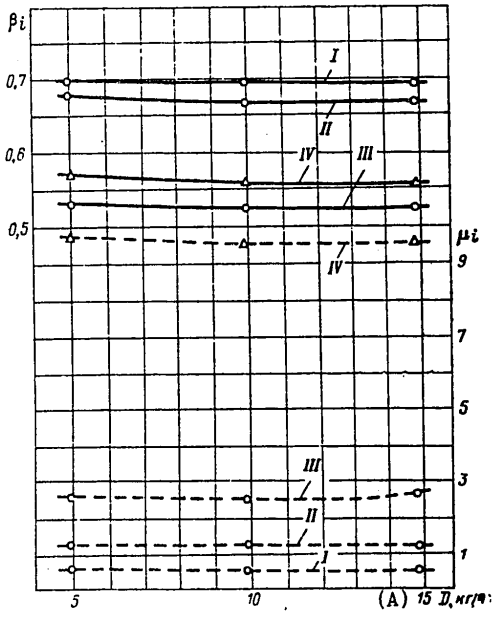

Figure 23. Coefficients of Resistance μ_i (- - -) and Pressure Ratios β_i (———) by Groups of Stages I-IV (see figure 22) as a Function of Steam Consumption D (n_B = 30 rpm).

Key:
A. Consumption, kg/hr.

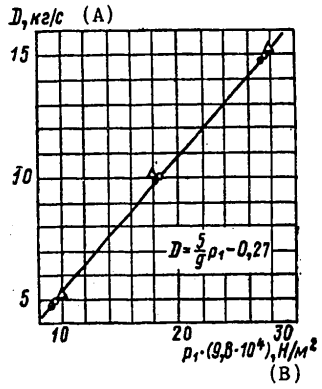

Figure 24. Steam Consumption for a Turbine with Disengaged Bleeds as a Function of Steam Pressure p_1 Following the Control Stage.

Key:

Triangle--n_B = 30 rpm.

Circle-----n_B = 50 rpm.

Dot-------n_B = 85 rpm.

A. Consumption, kg/seconds.
B. $p_1\cdot(9.8\cdot10^4)$, Newtons/m².

defines turbine steam consumption with high precision. The indicated feature permits the use of pressure sensors instead of consumption sensors.

CHAPTER 2. THE MARINE DIESEL POWER PLANT AS A SUBJECT FOR ENGINEERING DIAGNOSTICS.

6. The Structure and Characteristics of Diesel Power Plant Operating Regimes

Ships with a diesel as the main engine now comprise the basic nucleus of the domestic maritime fleet. The striving to reduce specific fuel consumption and to increase power per unit of engine weight governs the two main features of modern diesel power plants: intensive utilization of the heat,

and a high degree of engine supercharging. The machinery is a system of units whose operation is closely interconnected with operation of the main engine. An analysis of the dynamics of the installation is possible only by taking these mutual relationships into account.

Figure 33 shows a block diagram of a modern diesel installation.

Figure 33. Diagram of a Diesel Propulsion Plant.

Key:
1. Heat-recovery steam generator.
2. Gas turbine.
3. Air receiver.
4. Exhaust gas receiver.
5. Exhaust valve.
6. Piston.
7. Injector.
8. Fuel pump.
9, 11. Fuel filters.
10. Fuel preheater.
12. Engine crankshaft.
13. Water-to-water cooler.
14. Water and oil cooler.
15. Air cooler.
16. Compressor.
17. Air cleaner.

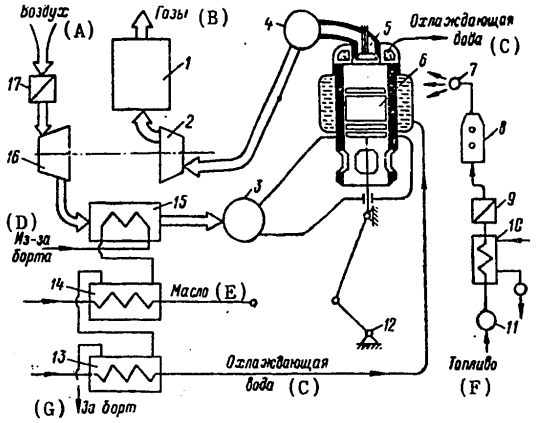

A. Air.
B. Gases.
C. Cooling water.
D. From over the side.
E. Oil
F. Fuel.
G. Overboard.

Air enters the main engine cylinders from a receiver, into which it has been injected by a compressor with drive off a gas turbine. In order to increase the mass charge after the compressor, the air is cooled in a surface cooler that pumps outside water. In so doing, vapor from the water that is contained in atmospheric air is condensed; in the tropics this condensation is especially abundant. The gas turbine of the compressor is brought into action by the energy of gases that are accumulated in the gas receiver. After the gas turbine, the spent gases are cooled in a heat-recovery steam generator, which generates steam for shipwide needs and for a steam-turbine electric generator, usually of sufficient capacity to provide for all the ship's needs while under way.

The fresh-water loop that cools the main engine sometimes includes a waste-heat recovery vacuum distiller (not shown in the diagram).

As the diagram being examined shows, the dynamics of scavenging and the air charge for the cylinder are characterized by the mutual action of four volumes of energy and flow: the engine proper, its air and gas receivers, and the turbosupercharging unit. The main engine parameters, aside

from power and crankshaft rotating frequency, also include air and fuel consumption, mechanical efficiency, the scavenging coefficient, and, for the supercharging unit, the pressure and temperature of the gases and the air at the intake and output of the turbine and compressor, as well as the efficiency of the turbine and the compressor.

The processes that comprise the diesel's operation are linked by definite relationships with the loading, with external conditions, and with each other. These are thermodynamic, hydrodynamic, aerodynamic, kinematic, static and general physico-chemical relationships which, for the task examined here of diagnosing the technical condition with adequate precision, can be described mathematically by means of relatively simple or simplified empirical functions. The relationships that ensue therefrom among the various values, within whose limits the studied phenomena occur, can be determined from the design data of the engine and from its operating characteristics.

The operating regimes of a ship's propulsion diesel are determined from a combined examination of the characteristics of the engine and the screw. Figure 34 shows the dimensionless characteristics of an engine with turbosupercharging; lines of constant values of torque M_{kp} (or the average effective cylinder pressure p_e that is proportional to this torque) are shown here. The maximum moment that the engine develops corresponds to the point C. The curve BC is the engine's external characteristic; when operating under this characteristic, as the engine rotating frequency decreases, the regimes of its operation approach the limits of the area of compressor surge. To avoid the danger of surging, engine operating regimes should be set to the right of the EC curve, which is characteristic of the VFSh [fixed-pitch screw], on which the maximum torque is realized at point C. The characteristic curve of the VFSh that passes through the point N_{max} of maximal power is used for prolonged operation.

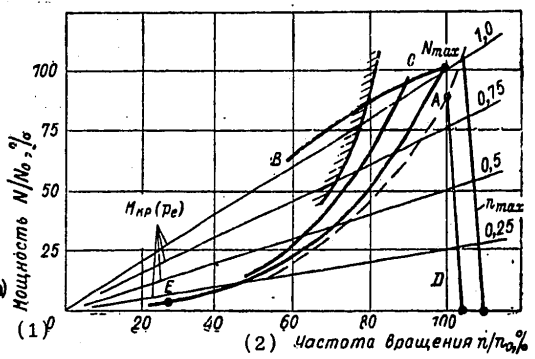

Figure 34. The Dimensionless Characteristic Curve of a Marine Propulsion Diesel with Turbosupercharging, During Operation with VShF [fixed-pitch screw] or VRSh [adjustable-pitch screw].

Key:
BC. External characteristic of the diesel.
EC. Characteristic curve (VFSh)
EN_{max}. Line for prolonged operation with VFSh.
DN_{max}. Line for prolonged operation with VRSh.
Point A. Operation under stormy conditions.
1. Power, N/N_0 percent.
2. Rotating frequency, n/n_o percent.

In the case of engine operation with an adjustable pitch screw (VRSh), the rotating frequency of its shaft is constant, and the limits line of the operating regimes is the curve DN_{max}.

CHAPTER 3. STATISTICAL ANALYSIS OF THE OPERATING CONDITION OF A MARINE POWER PLANT.

11. Peculiarities of a Study of the Probability Characteristics Curves of the Plant's Operating Regimes.

For a seagoing carrying ship the main operating regime is prolonged sailing at nominal main-engine power. It is customary to evaluate the operating indices for marine power plant operation at static regimes that define uniquely an aggregate of determinate values for certain parameters. Such an approach is convenient and completely justified in establishing the technical and economic effectiveness of carrying ships. It is different with the characteristics of the operating regimes when solving problems of providing higher precision of control or the prerequisites for reliability during prolonged operation of the equipment. In this case, consideration should be given both to quantitative expressions and to consistency in the appearance of minor and short-term disturbances of these regimes.

Observations indicate that the movement of a ship at constant power developed by the main engine is accompanied by continuous change of all powerplant parameters. The data shown in figure 43 can serve as an illustration that will enable the average sizes of such changes to be judged. These changes are provoked by numerous causes, which are engendered by sailing conditions and the characteristics of concrete regimes for operating the ship's powerplant. The normal operating regime for such an installation, which has been tentatively adopted as the steady-state, is actually a continuous alternation of dynamic processes that die down and are resumed under the influence of various sorts of small disturbances that do not yield to prognostication and are random with respect to the ship.

Three basic groups of causes that give birth to such disturbances can be pointed out. They are, primarily, conditions imposed by the characteristics of the ship and the voyage; these include the power of the main engine, the speed of the ship, its steerability, its draft, tuning of the automatic steering, and so on. The second group is occasioned by the conditions of the power plant's assemblies, the closeness of concrete operating regimes to the rated regimes, and the technical servicing operations that are conducted at sea. These are the condition of the hull and screw (fouling), the degree of wear of mechanisms and change in the effectiveness of their operation, the presence or absence of damage, clogging of the steam generators' air-blast cleaners, flushing of the turbosupercharger, choking of the evaporators, and so on. Finally, the third consists of external conditions: the sea state, air and water temperatures, the wind, currents, and so on.

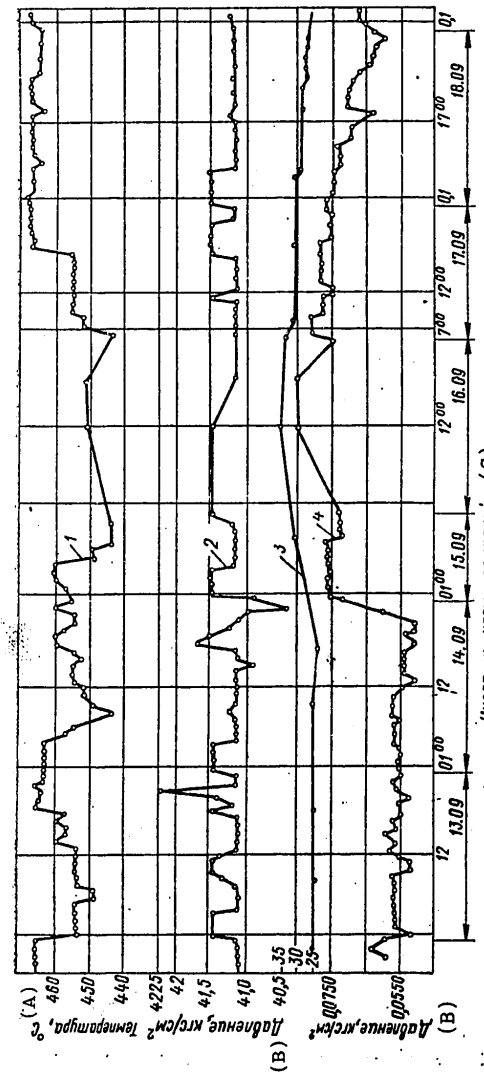

Figure 43.

Change of Some Power-Plant Parameters on the Tanker "Mir" During a Week, with Unchanged Main Engine Power

Operating Area: Indian Ocean-Red Sea.

Key:
1. Steam temperature ahead of the nozzles $t^{0}_{n.c.}$;
2. Steam pressure in the nozzle box $p_{n.c.}$;
3. Temperature of outside water.
4. Vacuum in the main condenser.

A. Temperature
B. Pressure, kg-force/cm^2.
C. Dates and hours of the tests.

The disturbances that the enumerated random factors introduce to the established operating regime of a marine power plant are much more profound than are generally considered. Figure 44 shows the shaft-rotating frequency curves of a main diesel with a power of about 17,000 kw, with direct drive to a fixed-pitch screw, and the curves of torque on a propeller shaft at a rotating frequency of about 114 rpm (for a cargo with a deadweight of 110,000 tons), which were obtained during several voyages. Measurements were conducted hourly.

Average propeller shaft rotating frequency changes somewhat, depending upon the ship's draft and on additional resistance to movement by the sea and the wind. Periodically the rotating frequency and the torque are lowered considerably for a period of about 1 hour (these situations have been noted in figure 44 by the letter A); during these periods the diesel's gas turbosuperchargers were flushed.

The main engine's rotating frequency and the power on the propeller shaft also are reduced under stormy conditions (portions of B of the oscillogram). Figure 44 shows the various variants (a to г) of such a reduction.

Figure 44б's oscillogram shows the case where the rotating frequency has been reduced and the torque has been kept at the previous level; this is caused by a strong increase in drag resistance to the ship's way. In figure 44, в is a reduction in rotating frequency accompanied by an increase in torque, so the engine's power is kept unchanged. Finally, the oscillogram in figure 44г indicates that during a strong storm both rotating frequency and total power must be reduced. Cases B and г are characteristic for a ship at less than full draft.

The effect of external conditions on the operating characteristics of a propulsion diesel with fixed-pitch screw is traced in more detail in the data of operational measurements that are made synchronously (figure 45). During a strong storm, exit of the screw from the water causes compressor surge. As the sea state worsens, the heat stress of the engine increases considerably, as is evident in the changes in exhaust-gas temperatures $\theta_{г_1}$. Such measurements are one of the most important factors that give rise to low-cycle fatigue, which is the result of thermal stress and is especially dangerous for combustion chamber walls. Therefore, under stormy conditions, engine power is reduced, shifting its characteristic curve to point A of the diagram in figure 34, or automatic regulation of the cyclic fuel feed as a function of supercharging pressure is provided for.

From the point of view of an analysis of the processes occuring in the power plant, random disturbances that accompany the operating regimes can be divided into the external and the internal. The first are connected with operating conditions; they can act on the object directly, the same as an internal loading (for example, random oscillations in propeller-shaft rotating frequency caused by changes in drag on the screw), or they can enter the control system through the sensor (as in loops for leveling control when the ship is rolling). Internal random disturbances are not

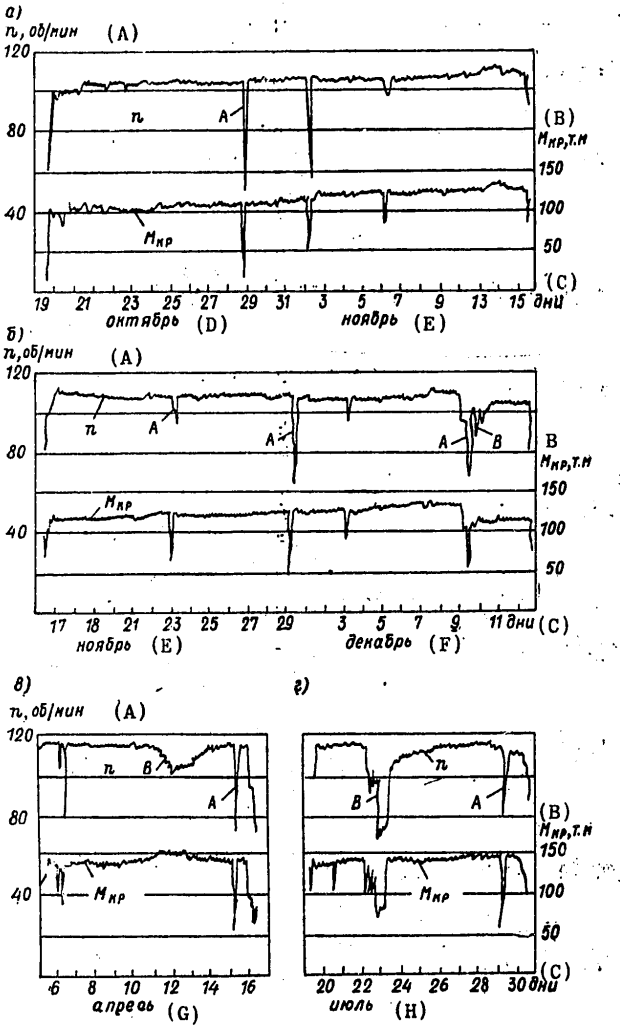

Key:
A. Number of revolutions per minute.
B. Torque, tons-meters.
C. Days.
D. October.
E. November.
F. December.
G. April.
H. July.

Figure 44. Change of Rotating Frequency and Torque on the Propeller Shaft of a 110,000-Tons' Deadweight Ore Carrier with a Diesel Power Plant in Operation

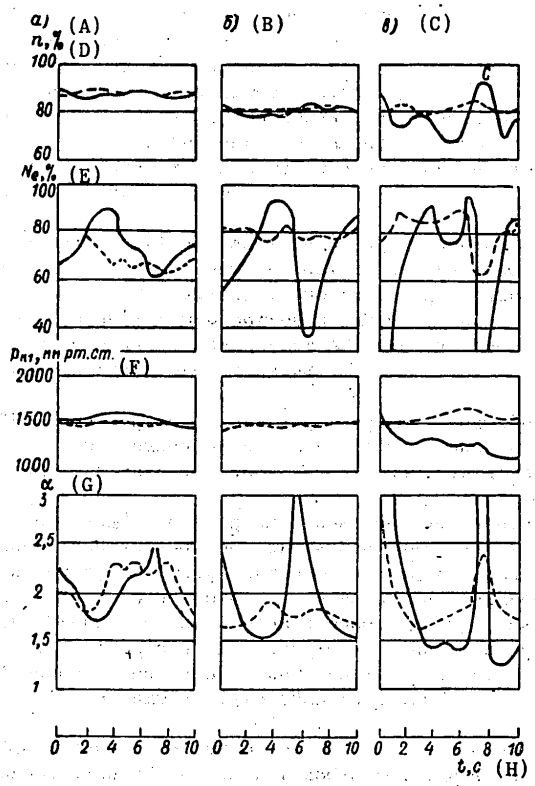

Figure 45. Change in Basic Parameters of the Main Engine of a Cargo Ship Sailing into the Wind:

A. Wind force 8, t_A = 427 degrees C.
B. Wind force 10, t_A = 493 degrees C.
C. Wind force 11-12, t_A = 512 degrees C.

Continuous lines correspond to conditions at which the propeller screw leaves the water (point C).

D. Number of rpms.
E. Engine power.
F. Pressure, mm of mercury.
G. Air concentration. factor.
H. Time, seconds.

monitored, but they exert a direct effect on the process's indices, such as atmospheric conditions, scouring of the fuel injectors, or deviations in resistance of the heat-exchange surfaces.

Random disturbances are inevitable and it is impossible to completely eliminate their influence on the indices of the process. Thus the accuracy of control and monitoring systems is determined not only by their design but also by operating conditions. The effect of random noise, which is insignificant within the limits of the simplest insulated control loops, increases with the degree of design complexity of the system being controlled, the appearance of mutually connected objects and processes, and a rise in the demands for precision in regulating and monitoring. The tasks of studying the consistency of the appearance and quantitative characteristics of random processes that accompany normal operation of the power plant are:

--Minimization of dispersion of the parameters at the output of the dynamic systems;

--Organization of the collection of information about the parameters of generalized systems for the monitoring, diagnosis and prediction of the technical condition of the equipment, with the use of computer equipment;

--Establishment of ranges of deviation of generalized indices that characterize the flow of the process or the condition of the basic equipment; and

--Analysis of the mutual effects of the interfacing and dynamic relations of control loops.

The peculiarities of the main maritime power-plant operating regimes that are governed by random disturbances that are typical for operating conditions are analyzed in this chapter. To start with, dispersions of the main parameters that determine operating economy and reliability, as well as the probable deviations of comprehensive indicators that are important for generalized monitoring systems, are studied. Then the characteristics of random disturbances that are external in relation to the power plant's main objects and to systems for the automatic control thereof are examined. Studies are made of realizations obtained in the form of changes in observed parameters in time. Characteristics of the main types of random processes are expressed through mathematical expectations, dispersions and correlation functions. The approximation of correlation functions are carried out by means of one equation which has enabled certain important generalizations to be made.

It should be emphasized also that the probability characteristics of random processes can be determined only on the basis of experiment. A systematic study of such chacteristics was started with reference to the operating conditions of marine power installations of transport ships of the domestic fleet, based upon full-scale observations that were conducted for a long time by TsNIIMF on tankers of the Black Sea and Novorossiysk shipping companies [22].

Because of the novelty of the information set forth in this chapter, a brief description of the observational procedures is given below.

Full-scale research of statistical characteristics is performed during a normal operational voyage at established under-way regimes. They consist in the recording of a definite set of parameters and quantities that characterize the work of an assembly or part of an installation without manual intervention in adjustment of the automatic equipment or the correction of regimes.

The parameters registered are subdivided into three groups. The first group determines the external conditions of the voyage, the second the level of the loading on the main engine and the stability of the observed regime, and the third the magnitudes proper of the parameters of the process being examined. Figure 46 illustrates the sailing conditions that are characteristic for the fall period in temperate and tropical latitudes, and figure 47 shows the recurrence of the main operating regimes during the voyage.

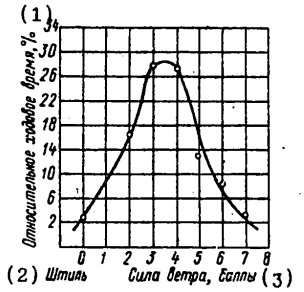

Figure 46. Sea State During the Testing Period of the Turbine Ship "Sofiya" (October-December 1964).

Key:
1. Relative steaming time.
2. Calm.
3. Wind force, number.

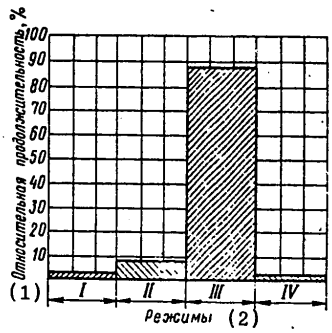

Figure 47. Distribution of the Period of Tests of the Turbine Ship "Sofiya" with Regard to Main Operating Regimes.

Key:
I. Partial speed.
II. At anchor.
III. Full speed.
IV. Maneuvers.

Total duration of the trip was 849 hours.

1. Relative duration.
2. Regimes.

Taking into consideration the duration and frequency of recordings necessary for obtaining sufficiently representative data about realizations of the random process, automatic recording instruments should be considered the basic type of measuring apparatus. It is extremely important that such instruments provide simultaneity of measurements of the various parameters in accordance with which consolidated indices (coefficients of heat transfer, efficiency, specific speed and so on) or mutually correlated functions will be computed later.

A peculiarity in conducting the measurements that are described below was, in particular, that the periodicity of the main harmonics of the random processes, the phenomena of which were to be registered, was not known. Consequently, neither was optimum frequency of the sensor interrogation known; this information was to be obtained for the first time. Therefore, at first preliminary rough observations of the random processes of change in the main parameters were made and the prerequisites for optimal organization of the collection of primary information were chosen on that basis.

Given discrete connecting of the sensors, the interval between the switchings for measuring the various parameters should, in accordance with

V. A. Kotel'nikov's theorem, be $\Delta t \leqslant \pi/\omega_{max}$, where ω_{max} is the frequency of the highest of the main components [14].

From the data cited below, the parameters of slowly occurring processes (temperature, chemical composition of boiler exhaust gases, and vacuum in the condenser) were measured discretely. The processes that occur relatively rapidly--such as change of propeller-shaft rotating frequency, ship roll and change of position of automatically controlled regulating devices were recorded by special sensors with output on an oscillograph.

In order to obtain an adequate number of readings under comparable conditions, self-recording instruments of the multiple-point potentiometer type were left connected continuously for periods measured in days, and even weeks. In order to obtain high precision in measurements, three to five times per day the results that had been recorded on tapes in accordance with the indications of the monitoring and measuring instruments, which were connected in parallel to the automatic measurement sensors, were calibrated. Calibration consisted in the synchronous marking of the indications of the monitoring instrument in the log of observations and on the tape of the automatic recorder. Given this organization of measurements, the scale of deviations of the automatically recorded parameters can be determined for each of the periods between calibrations. The diagram in figure 48 gives a representation of the total number and mix of measurements of the parameters of the main cycle of the steam-turbine installation.

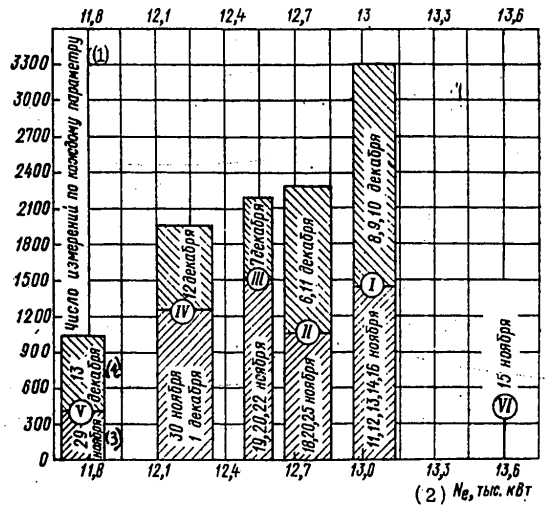

Figure 48. Power Range and Average Number of Measurements for Each Parameter Recorded on the Turbine Ship "Sofiya" During the Tests.

The tests were amalgamated into groups for comparative analysis of the ship's full-speed regimes. The numbers of the groups are the Roman numerals in the small circles (I-VI).

Key:
1. Number of measure-meants for each parameter.
2. Engine power, thousands of kw.
3. November.
4. December.

Simultaneous with the recording of process parameters for the calibration of the automatic recorders, observations of external conditions (water and air temperatures, sea state, wind and atmospheric pressure), loading of the main turbine and the ship's electric power plant, fuel consumption and other parameters that characterize the operating regime of the power plant that is being studied were reported in the record book. This enabled the data that was obtained at various times to be amalgamated during processing of the observational data, in accordance with the criterion for conformity of the external conditions and the loading.

The data cited in this work was amalgamated on the basis of two quantitative criteria that characterize the level of loading of the main engine and statistical compatibility. The first criterion adopted was that the power on the propeller shaft at any of the regimes that were combined into one group should not differ by more than 1 percent from the average magnitude of the power for the group being examined.

The compatibility of the data was established by means of Chauvin's criterion from a comparison of the differences of the values $\bar{x}_1$ and $\bar{x}_k$ (i and k are items of amalgamated groups) of the x values that were examined with a mean square deviation $\sigma_{i,k}$ of this difference:

$$\sigma_{i,k} = \sqrt{\sigma_i^2 + \sigma_k^2}. \qquad (150)$$

The boundary values have been established this way: if the computed values $\sigma_{i,k}$ indicate the probability that the difference $\bar{x}_i - \bar{x}_k$ will be less than 0.01, then the average value is considered to be incompatible and the corresponding i-th series of observations of the group is excluded. Since the probability 0.01 corresponds to the tabular value $h_x = 1.83$, the formulated criterion is expressed by the inequality

$$h_x = \frac{\bar{x}_i - \bar{x}_k}{\sqrt{2\sigma_{ik}}} < 1{,}83. \qquad (151)$$

The execution of this inequality is mandatory for each pair of the recorded data that is supposed to be amalgamated into the group.*

The ranges of average powers in the groups that are formed on the basis of the two criteria set forth and the volume of the measurements that are carried out on the static operating regimes of the tanker "Sofiya" are shown in the diagram in figure 48.

The values of the mathematical expectations and the root mean square deviations of the installation's operating parameters are calculated in

*When evaluating the authenticity of each observation in the aggregate of measurements being examined, sometimes the simpler, albeit less meaningful, Royt's [transliterated] criterion is used. Under this criterion, a measurement is excluded from an aggregate if its deviation from the average value exceeds the zone's limit by a width of $\pm 4\sigma$.

accordance with the aggregates that are amalgamated into groups similar to those shown in figure 48.

The characteristics of the random processes of change of parameters in the form of correlational functions of distribution are established in accordance with realizations chosen from series of observations conducted under the most typical conditions. The mutual-correlation functions are established in accordance with realizations obtained synchronously.

A large number of measurements of the very same parameter that were made under comparable conditions provide sufficiently high precision of the random value's probability characteristics.

Processing of the results of the observations that are analyzed below were conducted on an ETsVM [electronic digital computer]. In so doing, known formulas for the main characteristics were used in the form:

--for the mathematical expectation $\tilde{M}$ of the random value

$$\tilde{M}[X] = \frac{1}{n}\sum_{i=1}^{n} x_i; \tag{152}$$

--for dispersion

$$\tilde{\sigma}_X^2 = \frac{1}{n-1}\sum_{i=1}^{n}(x_i - \tilde{M})^2; \tag{153}$$

--for the k-th ordinate of a standardized autocorrelational function (with the displacement τ)

$$A_{kk}(\tau) = \frac{1}{\sigma_k^2 (n-k)}\sum_{i=1}^{n-k} y_k y_{i+1}; \quad \text{and} \tag{154}$$

--for the k-th ordinate of the standardized mutual-correlation function

$$A_{vy}(\tau) = \frac{1}{\sigma_y \sigma_v (n-k)}\sum_{i=1}^{n-k} y_k v_{i+1}. \tag{155}$$

When organizing full-scale observations, it should be kept in mind that the probability characteristics of the processes are determined not only by external or internal disturbances but also by the basic equipment's dynamic characteristics. This follows, for example, from the expression for the dispersion σ^2 of the signal at the output of the linear system

$$\sigma^2 = \frac{2}{\pi}\int_0^{\infty} |K(j\omega)|^2 S(\omega)\, d\omega, \tag{156}$$

where $|K(j\omega)|$ is the absolute value of the frequency characteristics of the dynamic system or section that passes a random signal with spectral density.

Therefore, strictly speaking, the results of the concrete research can be extended only to power plants that are closed with regard to dynamics. The boundaries of permissibility of such an extension should be made more precise as the results of experimental research are accumulated. Apparently there exist correlational ties between the characteristics of the random processes and the dynamic characteristics of automated marine objects. This allows hope that it will prove possible to rely upon generalizations of the stochastic characteristics of power-plant operating regimes and then the specific conditions of operation of a seagoing ship will be expressed in analytical form.

12. Analysis of the Operating Conditions of a Motorship's Power Plant*

As was indicated above, the characteristics of operation of a power plant change as a result of the effects of external and internal factors. The correlational links between current parameter deviations can be traced first, by external conditions and, second, by steady changes (or deteriorations) of these characteristics in time only on the basis of sufficiently lengthy and, what is especially important, simultaneous observations of the main indicators of the condition of the units and of the parameters of the processes that are linked with them.

Figure 49 shows the recordings of the main parameters of the diesel installation of an ore carrier with a deadweight of 110,000 tons that characterize a fairly lengthy period of operation. The authors of the observations being examined remark that, other conditions being equal, the difference in speed of the given ship between ballast voyages and running with a full load, are negligible, thanks to the bulbous shape of the ship's bow. However, in the period between the ship's drydocking, a trend toward a reduction in speed was noted that is explained by fouling of the ship's hull.

The propeller shaft rotating frequency is maintained fairly stably at an average level. The shaft's torque and, along with it, total power, change in accordance with weather conditions; it is not difficult to trace a certain increase in their average values during winter months.

The second group of parameters, which are located on the graph of figure 49, below torque values, show a trend toward stable changes with time. This is especially noticeable during the first year of operation--between commissioning of the ship and its first drydocking.

Fluctuations of ambient and scavenging-air temperatures correspond to the periodicity of the trip (the ship was operated on the Australia-Japan route) and were caused by differences in climatic conditions at the extreme

*The experimental data used in this chapter section were taken from work [39].

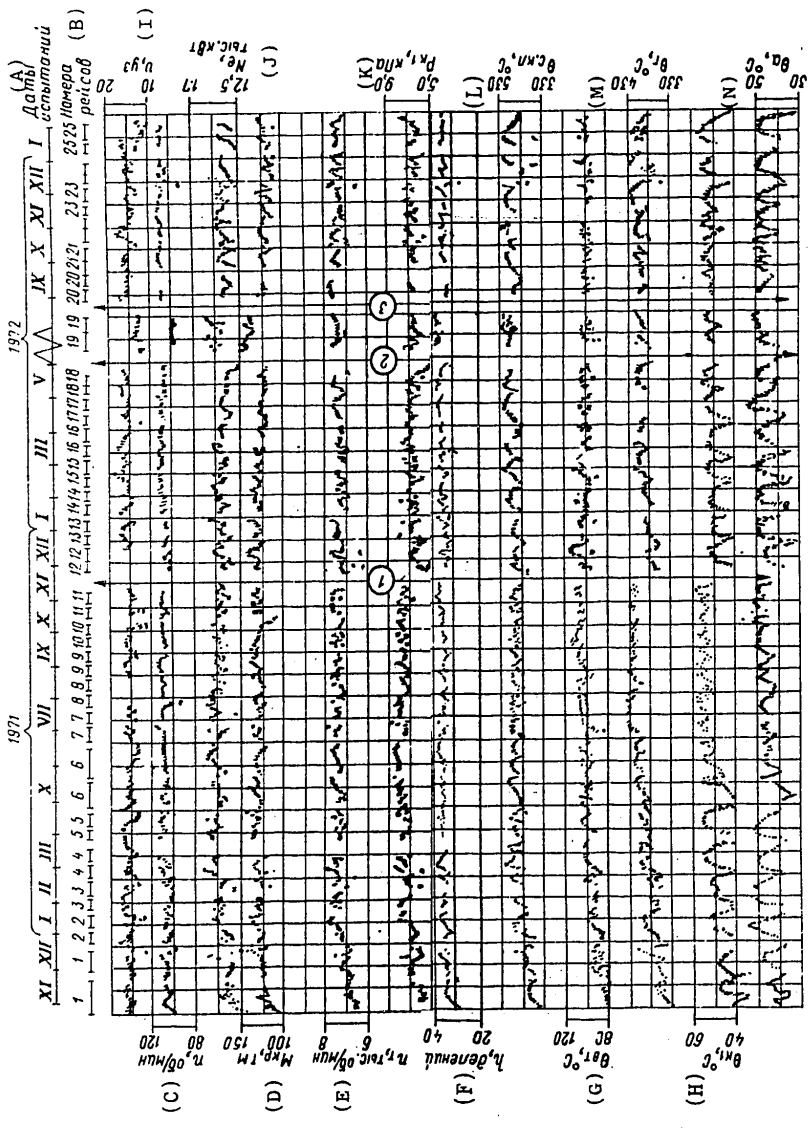

Figure 49. Dynamics of the Main Parameters of a 23,000-hp Diesel Power Plant in the First Two Years after Commissioning. [Key on next page]

[Key to figure 49]

Each point on the graph expresses the average daily value that was obtained by averaging all the measurements made during the day.

Withdrawals from operation [circled numerals]:

1. First drydocking.
2. Prolonged anchoring.
3. Second drydocking.

A. Dates of tests.
B. Trip number.
C. Propeller-shaft rotating frequency, rpm.
D. Moment on the propeller shaft, ton-meters.
E. Turbosupercharger rotating frequency, rpm.
F. Fuel rod graduations.
G. Cylinder-sleeve temperature, degrees C.
H. Scavenging air temperature, degrees C.
I. Ship's speed, knots.
J. Engine power, kilowatts.
K. Scavenging air pressure, kilopascals.
L. Exhaust valve seat temperature, degrees C.
M. Exhaust gas temperature, degrees C.
N. Temperature of air at the compressor intake, degrees C.

points of the itineraries. However, average temperature values rose gradually. Simultaneously, exhaust gas temperatures increased, as did the turbosupercharger rotating frequency and the exhaust valve seat temperature.

The most significant rise in air temperature was found at the compressor suction; this rise apparently should be viewed as the original cause of the other changes.

Figure 50 shows temperature changes that were obtained while processing figure 49 data. Figure 50 illustrates from the qualitative and quantitative viewpoints the considerable influence of air temperature and outside water on processes occurring within the machinery. In this case attention should be devoted to the total effect of the action of these temperatures. Thus, one-third of the pace of rise in temperature of exhaust gases (according to the graph in figure 50, it is about 25 degrees for each 10 degrees in rise of air temperature) is occasioned by a rise in air temperature, two-thirds of it by an increase in the temperature of the outside water, as a result of which air-cooler effectiveness was reduced.

The maximum rise in temperature during the first year of operation was: for exhaust gases 60-70 degrees, for the exhaust valve seat 50 degrees and for the cooled side of the cylinder sleeve $\theta_{ц.в.}$--about 30 degrees; in the latter case, the total effect on this indicator of scavenging-air and outside-water temperatures, as well as some increase in power of the machinery because of fouling of the ship's hull, must be considered.

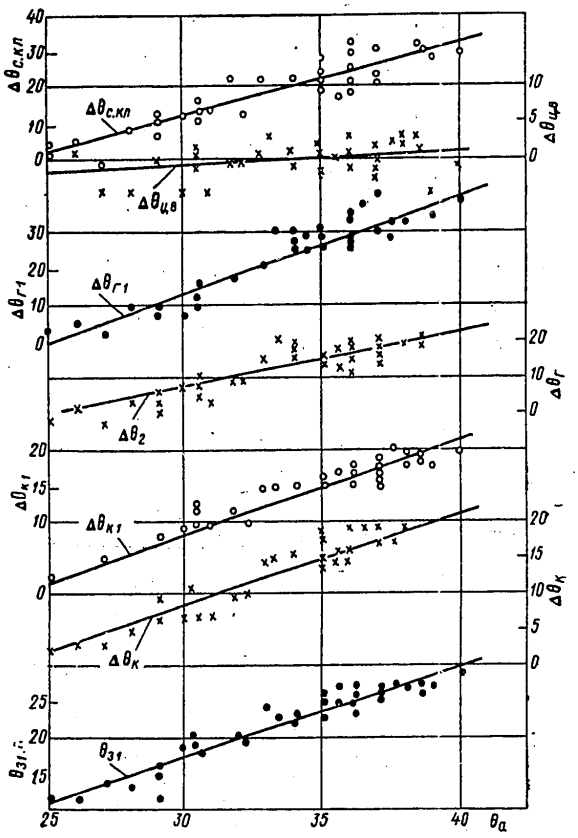

Figure 50. Dependence of Temperature Increments That Characterize the Diesel's Operating Regime Degrees C., on the Temperatures of Compressor Suction Air and Outside Water θ_{31}.

Notation is the same as for figure 49.

In November 1971, between the 11th and 12th voyages, the ship was drydocked for cleaning the underwater part of the hull. It should be noted that modern high-tonnage tankers and ore carriers with bulbous shape that have a substantial draft are little different laden and in ballast, and the share of the component of frictional drag reaches 60-70 percent of the hull's full resistance. The main part of the residual drag, which is caused by vortex generation behind the stern, also depends upon the drag components. The wave component of drag is not great (the Froude number does not exceed 0.17). All this leads to a substantial increase in the effect of roughness (fouling) of the hull on the propulsion performance of ships of this type in comparison with ships that have high relative speeds and, correspondingly, Froude numbers within the 0.2-0.25 range. In accordance with statistical data obtained during the operation of medium- and high-tonnage tankers of Japanese construction, speed losses of a tanker with a deadweight of 130,000 tons reach 1.1 knots within a year of operation. Therefore, in foreign practice the time between drydockings of high-tonnage tankers has become a matter of rigid regulation.

A comparison of the results of observations carried out prior to and after the first drydocking has enabled observation of change in the position of the fuel measuring rod: when the ship's hull is clean, the cyclic feed of fuel to support the same propeller-shaft rotating frequency and ship speed is lower than when the hull is fouled. Exhaust gas temperatures were reduced appreciably as a result of the reduction in fuel feed, and also because the machinery's working conditions were approaching the rated condition. The cylinder wall temperature underwent extremely small change. When the insignificant influence of air temperature on this parameter (see figure 50) is considered, the conclusion can be drawn that a gradual rise in sleeve temperature with time is governed mainly by inevitable and irreversible changes of its condition.

Between the 18th and 19th voyages, the ship was idle in port for about 60 days. In this case, the fouling of the hull and the screw strongly distorted the power plant's rated operating condition.

The torque on the propeller shaft (see figure 49) grew by about 15 percent (corresponding to a change in fuel-rod position and an increase in the cyclic feed of fuel), but the propeller-shaft rotating frequency turned out to be lower than normal and the ship's speed was reduced to 12 knots. Such a situation forced the shipowners to conduct an unscheduled drydocking between the 19th and 20th trips, as a result of which the rise in torque on the shaft was eliminated and the ship's speed also returned to the norm. However, a comparison of other parameters indicates that the second drydocking improved the work-regime indices to a lesser degree than the first one did. Thus, after the second drydocking a jump in the position of the fuel pump rod (in comparison with that at the end of the 18th trip) was practically absent. The rotating frequency of the turbocharging unit, the supercharging pressure, the exhaust gas temperature and other parameters changed but little. However, this apparent lessening in the effectiveness of drydocking actually was linked with a gradual deterioration in the status of the power plant's units, which is a continuous increasing function of time.

Operation of the Motorship's Power Plant Under Stormy Conditions. With respect to dynamics, a low-rpm marine diesel with direct drive to the screw is characterized, in comparison with a steam turbine, by the comparatively small inertial moment that is applied to the propeller shaft. As a consequence of this, the diesel power plant is quite sensitive to periodic changes in drag on the propeller screw while sailing in cold and stormy weather. Change in draft of the stern during encounter with an ordinary wave leads to change in shaft rotating frequency of almost the same phase and causes deviations in the whole set of power-plant parameters associated with the shaft rotating frequency.

Figure 51 shows recordings of certain parameters that cause disturbances of the normal machinery-operating regime (in this case these are the draft of the stern and the angle of helm) also characterize the dynamics of its loading.

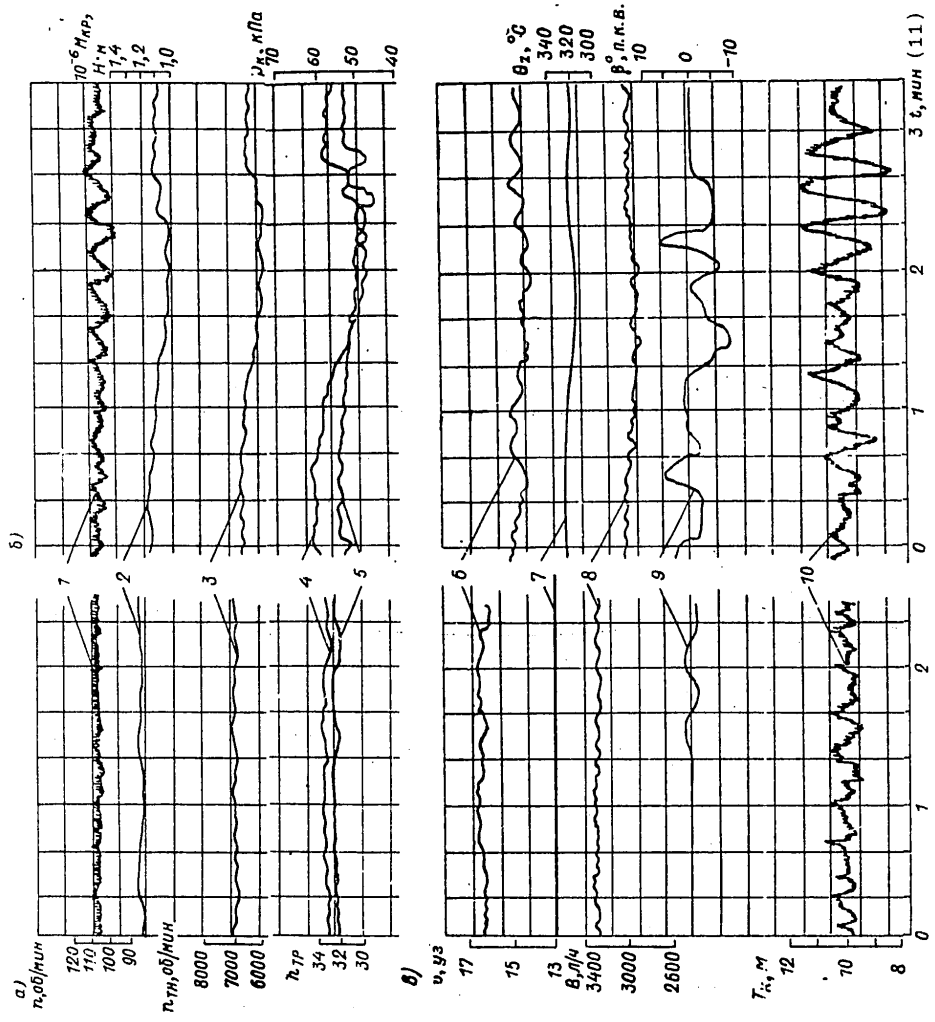

Figure 51. Synchronous Record of the Operating Characteristics of a Diesel Power Plant with Direct Drive to a Fixed-Pitch Screw. [Key on next page]

[Key to figure 51]

а. In normal conditions (force numbers 2-3).
б and в. During a storm.

1. Propeller-shaft rotating frequency n [rpm].
2. Moment on the propeller shaft M_{kp} [Newtons-meters].
3. Rotating frequency of the turbosupercharger n_{TH} [rpm].
4. Scavenging air pressure p_k [kilopascals].
5. Position of the fuel-pump measuring rod h_{TP}.
6. Ship's speed v [knots].
7. Exhaust gas temperature $\theta_г$ [degrees C].
8. Fuel consumption B [liters per hour].
9. Angle of helm, β^o, П.К.В.
10. Draft of the ship (stern) T_k [meters].
11. Time, minutes.

Maximum swings of the hull in the vertical plane do not under normal conditions (figure 51a) exceed 4 meters, which, for the given ship, has a weak effect on change in the moment of resistance on the screw and, consequently, does not lead to any considerable disturbance of the power plant's operating regime. The moment on the propeller shaft and the scavenging air pressure deviate appreciably only with the largest of changes in draft of the stern of those recorded in figure 51a.

In stormy weather, when the swings of the stern in the vertical plane reach 8 meters or more, practically all the parameters are changed with the frequency of the pitching oscillations (in this case about 3.5 periods per minute). In this case, the propeller-shaft rotating frequency is changed by 10-15 rpm, torque on the shaft by 10 ton-meters (about 10 percent of the normal value) and the ship's speed by up to 1 knot. The turbosupercharger, whose moment of inertia exceeds 10-fold to 20-fold the inertial moment of the main engine, reacts less sharply to external conditions. Nevertheless, the average turbosupercharger rotating frequency is reduced. The correspondence in the nature of scavenging air pressure oscillations to change in position of the fuel-pump rod is explained by the fact that the cyclic fuel feed in the given case is regulated with a restriction on scavenging air pressure. This limits considerably possible reductions in the air concentration ratio and prevents engine smoking.

Figure 52 shows an example of change in engine operating parameters during a strong storm. Fluctuations of the draft of the stern have a frequency here of about 6 periods per minute and are of higher amplitude than in the case shown in figure 51.

If swings of the stern do not exceed 8 meters, parameter changes are similar to these shown in figure 51. As swings of the stern increase, the drag sharply drops, and shaft rotating frequency rapidly rises. A regulator actuates a reduction in fuel feed, which leads to sharp dips in

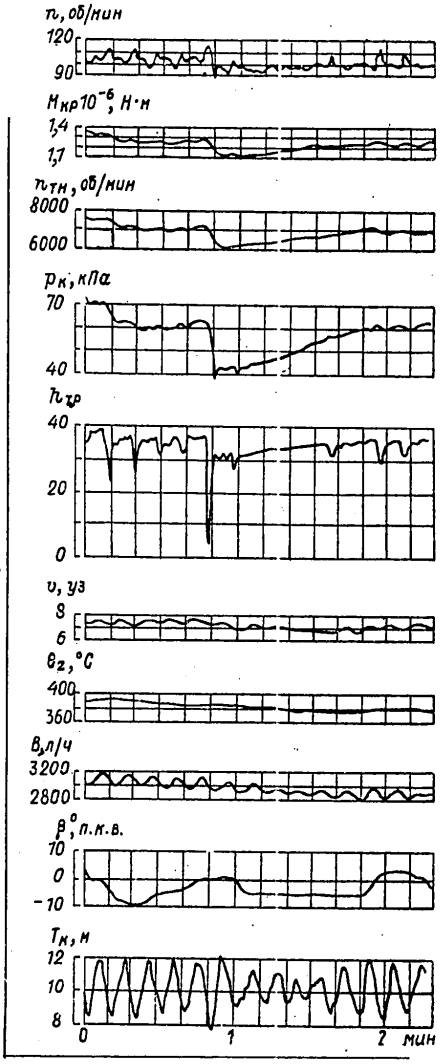

Figure 52. Dynamics of Change of Parameters of a Diesel Power Plant During a Strong Storm.

Notation is the same as for Figure 51.

rotating frequency of the turbocharger unit and a reduction of more than 20 kilopascals in supercharging pressure. The oscillogram of change in exhaust gas temperature apparently does not reflect the actual picture at the cylinder output because of the smoothing effect of the adjacent cylinders and the thermocouple's inertness. It should be expected that the cylinder's actual thermal loading, which is governed by increased fuel-feed portions at reduced supercharging pressure, is substantial.

Thus, changes in basic main-engine operating parameters are closely connected with navigational conditions of the voyage, the condition (age) of the units and external conditions. Statistical consistencies of the changes noted should, in the final analysis, help to establish standard values of parameters for diagnostics and for predicting the technical condition of a power plant.

CHAPTER 4. ELEMENTS OF SYSTEMS FOR DIAGNOSTICS AND PREDICTING THE TECHNICAL STATUS OF MARINE POWER PLANTS

18. The Level of Vibration and the Technical Condition of the Units

Statistics indicate that a high level of vibration precedes breakdowns and malfunctions of mechanisms 90 percent of the time. A mechanism's vibration level serves to that extent as a natural indicator of its condition, since its effectiveness, which is expressed by productivity, efficiency, or specific costs, reflects the degree of deviation of the processes that occur in a mechanism from the rated conditions.

Setting vibration norms for new equipment became long ago a mature problem, the solution of which is important both for evaluating the quality of

manufacture of a product and for establishing a base for reporting observations of changes in level of vibration as the product ages.

Shipbuilders' rating associations establish maximum vibration levels for marine electric drives. For example, USSR Registry Rules call for vibration-resistance norms and vibration strength for marine electrical equipment. Tests are conducted for smooth change of frequency in the interval shown in table 12, for a period of about 1 minute. Tests for vibration resistance and vibration strength are performed in accordance with Registry Rules on no less than two plane surfaces, one of which should be the plane of the normal operating position. Tests for vibration resistance are performed in that portion of the frequency spectrum (table 12) in which resonance phenomena arise, and, if they are absent, in any part of the subspectrum.

Table 12

USSR Registry Norms for Vibration Resistance and Vibration Strength for the Electrical Equipment of Domestic Ships

Frequency interval, Hz	Vibration resistance		Vibration strength			
			Prolonged test		Brief test	
	Amplitude, mm	Time, hours	Amplitude, mm	Time, hours	Amplitude, mm	Time, hours
5-8	1	The time necessary for	1.4	450	2.5	9
8-16	0.5	checking the effect and	0.7	220	1.3	4.5
16-31.5	0.95	the appearance of the	0.35	110	0.7	2.2
31.5-63	0.15	resonance phenomena	0.2	55	0.35	1.1

Some countries set norms for vibration levels for rotating motors and mechanisms. Vibration levels for piston engines and other marine equipment are specified in some cases by the suppliers.

It should be stressed that vibration tests of marine equipment under bench conditions cannot reproduce the peculiarities of the seating and the influence of other units; measurement of equipment vibration aboard ship in an operating installation should be considered effective.

The criterion for establishing permissible vibration levels is chosen in accordance with the data of strength calculations and statistical generalizations. In the ideal case a unit should be opened up for preventive maintenance or repair immediately prior to malfunctioning or onset of that degree of degradation of operating condition at which losses from interruption of operation will be less than the overexpenditure from the operation of worn equipment.

The setting of norms for the condition of units is usually done according to the rate of vibration that best characterizes its potential hazards. As an example, table 13 shows data developed by the USA's Maritime Administration [32]. These data also relate to rotating mechanisms; the level of vibration of a well-balanced multicylinder piston engine ordinarily does not exceed 7-8 mm/second.

Table 13

Vibrating Speeds of Marine Equipment

Maximum speed of vibration, mm/second	Characteristics of the vibrations	Characteristics of the equipment's condition
More than 15	Very strong	Sudden breakdown is possible, analysis of the causes is necessary. The vibration can disturb the oil film in bearings. The unit should be shut off.
10-15	Strong	Great risk. A detailed analysis of the causes is necessary to prevent breakdown or rapid wear. Prescribe the repair.
5-10	Increased	Malfunction is possible, special analysis is needed to establish the causes. Where necessary, prescribe the repair.
2.5-5	Minor	Unimportant malfunction is possible. Establish the cause during planned inspection.
0-2.5	Negligible	Quiet operation, typical for a well-balanced machine in good working order

As has already been noted, with increase in vibrating frequency, acceleration of a unit turns out to be a more characteristic index of its condition. It is natural to establish norms for vibration level as a function of frequency, as is done in figure 86, where the data of a diagram of conditions for rotating equipment of stationary power systems has been given.

As an example of the effect of frequency on vibration level, let us examine a vibratory motion of 0.1 mm in accordance with the diagram in figure 86. At frequencies below 100 Hz such movements correspond to a satisfactory operating condition, at frequencies of about 100 Hz they become dangerous, and, where the frequency is about 200 Hz, they are impermissibly high, since the acceleration exceeds gravitational acceleration 10-fold. Let us also note that measuring a motion of 0.1 mm at a low frequency is not a simple task as regards equipment support, whereas accelerations on the order of one or a few gravitational accelerations are observed by ordinary sensors.

In order to forecast the condition, a change in measured vibrating speeds from one interrogation to the next is an extremely important indicator. Where the interval between vibration-level measurements is one month, special measures to avert possible malfunction are superfluous; an increase in vibrating speed by a factor of no more than two is permitted.

A comparison of the vibration resistance norms shown in table 13 with the data of the diagram in figure 86 indicates their acceptable conformity (except for the first row in the table, which calls for more rigid demands

on equipment vibration levels. The vibration-resistance norms shown in table 12 coincide to a lesser extent with the data of figure 86: in the area of operating regimes that are permissible, only the regimes cited in the last line of the table prove to be acceptable, according to the data of the diagram. It should be kept in mind that amplitudes are cited in table 12, whereas in figure 86 swings in the vibration process are laid off along the axis of the ordinate. As a whole, domestic requirements for permissible vibration levels are more rigid than foreign requirements.

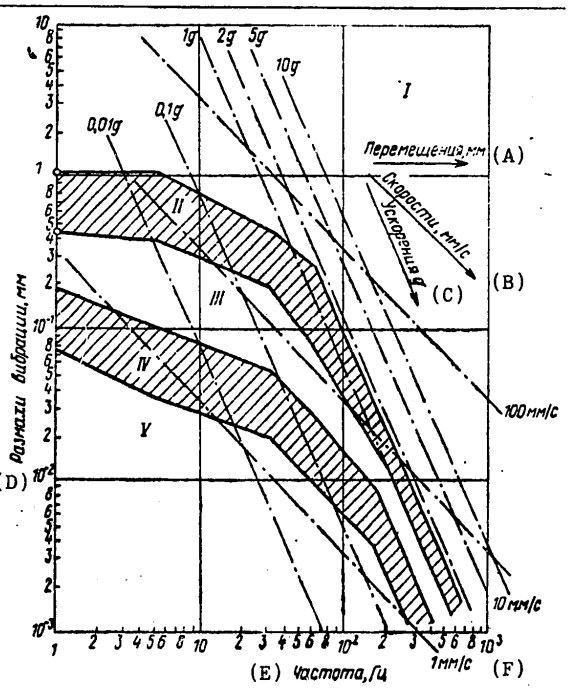

Figure 86. Diagram of Characteristics of the Vibration Status of Power Equipment [38].

Zones:

I. Dangerous condition; quick stoppage of the machine is necessary.
II. Threatening condition, breakdown is possible; must be inspected within 2 days.
III. Dangerous condition, inspection should be performed within 10 days.
IV. Satisfactory condition.
V. Good condition, typical for new equipment.

Key:
A. Motion, mm. B. Speed, mm/sec. C. Acceleration, g.
D. Vibration swings, mm. E. Frequency, Hz. F. 1 mm/sec.

The cause of an irregularity that arises is established by an analysis of the frequencies: a rise in one of the characteristic frequencies of a unit points to the presence of increased vibration. Characteristic sources of vibration in mechanisms and the frequencies that correspond to them are shown in table 14.

Based upon spectral analysis of the vibration diagrams, faults connected with dynamic imbalances, violations of coaxial alignment, bearing wear, shaft-line cant, wear or breakage of turbine or compressor blading, breakage of reduction gears, and so on are discerned quite accurately. Also revealed are lubrication system faults, cavitational phenomena in pumps,

Table 14

Sources of Vibration and the Frequencies That Correspond Thereto

Vibration source	Frequency	Direction of the vibration	Remarks
Faulty balancing	n	Radial, as a rule	
Misalignment of centers, faulty coupling	n 2n 3n	Both radial and axial	Axial vibration is the main indicator; it frequently exceeds the radial vibration.
Gearing, 1 tooth is damaged	n	Radial	The nonsinusoidal oscillations between peaks are smooth intervals.
Gearing, tooth surfaces damaged, or the pressure line is out of parallel	n_i	Radial	The most usual source of noise in toothed transmissions.
Motor, the electrical section	f	Radial, usually of low frequency	
Motor, the magnet section	2f	Radial, usually of low frequency	Oscillations of the magnetic field in the gap between rotor and stator.
Pump or impeller vane. Fan blade affected by aerodynamic forces	nk	Radial	
Damage to belting	Belt rpm: 60	Unstable, erratic oscillations	High-speed belt can create a stroboscopic effect.
Roller bearings	A wide band: from <n to very high	Radial, usually of low amplitude	For high frequencies, use indication of accelerations. (Computational methods are given in the book: "Handbook of Noise Control." London. McGrow-Hill [sic]. 1967)

Note: i is number of teeth; f is frequency of the current; and k is the number of pump vanes or impeller or fan blades.

and the initial stages of scoring of the diesel's cylinder-sleeve surfaces. It should be noted, however, that the identification of faults by vibration-diagram data requires some practice and experience on the part of the operator.

20. Organization of the Collection and Processing of Current Information.

As was noted above, the random nature of change in parameters and quantitative indices that govern the work of an installation gives rise to the need for a minimum amount of information in order to establish the average magnitude of the values being monitored with the prescribed precision. The system for collecting information is presented as a unified one for the whole installation, with periodic interrogation of the sensors. In organizing the collection of discrete information about continuous random processes, the task of minimizing this work is reduced to establishing the length of the interrogation period for each sensor and the number of interrogation cycles for each computation. The following fact testifies to the importance of such minimization. According to statistical data of the USA, about 90 percent of the total stream of information processed in the country by digital computers proves to be superfluous, unneeded for computation of the necessary average values, causing an enormous overexpenditure of funds.

It is known from V. A. Kotel'nikov's theorem [14], that, by replacing a continous random process with a latticed function, information will not be lost if the period of quantization Δt_{KB} is computed according to the expression

$$\Delta t_{\text{кв}} = \frac{1}{2\Delta\omega_{\text{пр}}},$$

where $\Delta\omega_{\text{пр}}$ is the effective belt pass-band width.

The period of quantization can be evaluated on the basis of an analysis of the magnitude of the random process being examined. Given the maximum speed of change in the value being monitored $(dy/dt)_{max}$, its magnitude during the period of quantization should be distinguished by no more than the prescribed error $\pm\varepsilon$, that is

$$\frac{2\varepsilon}{\Delta t_{\text{кв}}} \leqslant |(dy/dt)_{\max}|,$$

from which

$$\Delta t_{\text{кв}} \leqslant \frac{2\varepsilon}{|(dy/dt)_{\max}|}. \tag{181}$$

If the normal ergodic random processes are being examined, for which the probability density has the form

$$P(\Delta x) = \frac{1}{\sqrt{2\pi\sigma^2}} e^{-\frac{\Delta x^2}{2\sigma^2}},$$

then the number of intersections of the random function for a given interval x_n per unit of time is [16]

$$n'_{x_n} = \frac{1}{2\pi}\left(\frac{\partial^2 A_{kk}(\tau)}{\partial\tau^2}\right)^{1/2}_{\tau_{1,2}} e^{-\frac{\Delta x^2}{2\sigma^2}}, \tag{182}$$

so that the average time between deviations from the parameter on both sides will be

$$t_{cp} = \pi \left(\frac{\partial^2 A_{kk}(\tau)}{\partial \tau^2} \right)^{-1/2}_{|\tau=0} e^{\frac{\Delta x^2}{2\sigma^2}}.$$

The probability of observation of the deviation of a parameter beyond one of the given limits is

$$P(x > x_n) = 2 \int_{\Delta x_n}^{\infty} P(\Delta x)\, d(\Delta x).$$

If x_n is a prescribed limiting value of a parameter, x_0 is its average value and

$$\frac{x_n - x_0}{\sigma} = y_n,$$

$$\frac{x - x_0}{\sigma} = y,$$

then

$$\Delta t_{\text{кв}} = \pi \left(\frac{\partial^2 A_{kk}(\tau)}{\partial \tau^2} \right)^{-1/2}_{|\tau=0} e^{\frac{y_n^2}{2}} [1 - \Phi(y_n)], \tag{183}$$

where $\Phi(y_n) = \frac{2}{\sqrt{2\pi}} \int_0^{y_n} e^{-\frac{t^2}{2}} dt$ is the integral of probability.

As was indicated in the preceding chapter, the values of the partial derivative $\frac{\partial^2 A_{kk}}{\partial \tau^2}$ at the initial point can be established for a given installation in accordance with expressions that approximate the autocorrelational function on the basis of (174) by means of the data of table 11.

Strictly speaking, because of changing operating conditions, even for one and the same marine installation, the quantitative characteristics of the random processes that accompany established operating regimes can change. This is well apparent, for example, from an analysis of the processes of change in propeller-shaft rotating frequency that were examined above (see table 10). A computation for current characteristics of correlational functions can be included in the program of a computer mechanism that can, during the period that immediately precedes the measurements for the computation of generalized indicators, record and conduct the required analysis of the prescribed number of realizations of the random process. In so doing, naturally, machine operating volume and time are sharply increased. However, after studying typical processes for characteristic

operating conditions, a processing program based upon more unfavorable forms (surges at maximum speed) can be made up. Apparently, it is more desirable to have one program for an interrogation of sensors with prescribed cycles that is adopted from a calculation of the maximum running speed than to change the length of the cycles in accordance with the results of current analysis.

The running cycle time $T_{ц.о.} = k\Delta t_{ср}$ is established as a function of the requirements for precision and other characteristics of the interrogation system. The values of $\Delta t_{КВ}$ for the typical random processes of a marine steam-turbine installation that are being examined are computed by means of expression (183) in table 11.

It can be concluded that all the values that are being monitored in the system for generalized monitoring of the power-plant installation, based upon the analysis of random processes that was made in Chapter III, should, because of important differences in the nature of these processes, be broken up into several groups, for each of which their own periods of quantization should be established. For the system as a whole, these periods are multiples of each other. According to the data cited in Chapter III, such a parameter as propeller-shaft rotating frequency, should, for a system of generalized monitoring, have a quantization period that is measured in tenths of a second; the head of air that is fed to the steam-generator firebox should be measured every few seconds, indications of fuel-consumption and the ship's log every few minutes, and so on.

The overwhelming portion of the transformations and computations performed above are based upon assumptions about the normality of the law of distribution of errors in measurements of the parameters being studied. During probability analysis, this rule can be applied with extremely satisfactory approximation also for complicated objects and nonlinearities [19]. As is known, in this case it is sufficient to evaluate the mathematical expectation and the correlational function that determine the law of probability distribution. The latter can be taken as normal, since, as a consequence of inertness, all the installation's elements possess the generalized characteristics of a filter, by virtue of which

$$|W_n(jk\omega)| \ll |W_n(j\omega)|, \quad k = 2, 3\ldots, \tag{184}$$

where $W_n(j\omega)$ is the transfer function for the transformation of a linear part of a nonlinear system.

We shall illustrate the procedure for collecting initial information in concrete examples.

The Condition of Boiler Blower Bearings, Which Is Evaluated in Accordance with the General Level of Vibration of the Unit. For purposes of monitoring the vibration status of the blower, vibration-speed measurers have been installed on the bearings of the unit at the points designated in figure 94 by Latin letters.

Figure 94. Chart of Calculation of Vibration Level on Fan Bearings after a Year.

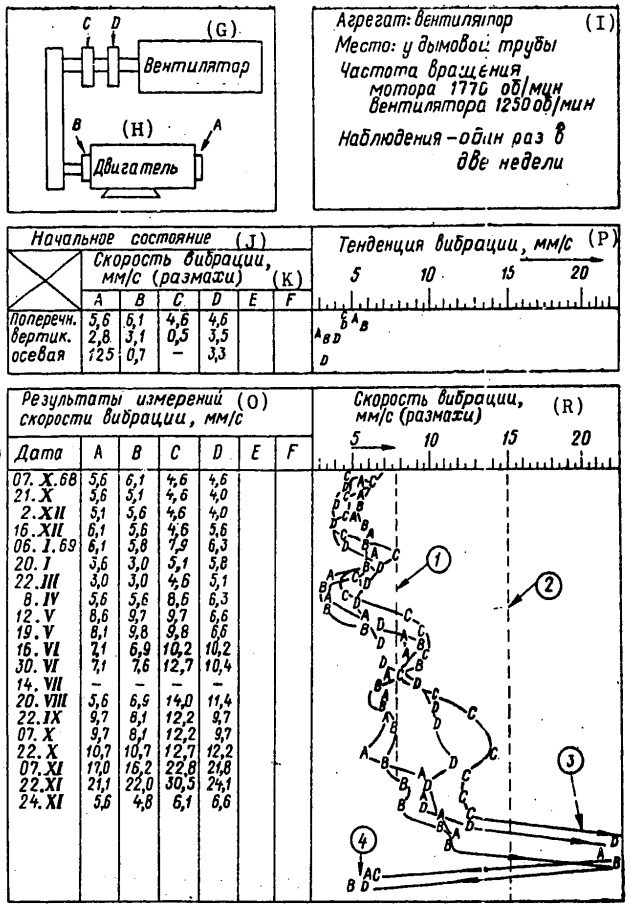

Key:

G. Blower.
H. Motor.
I. Unit: Blower. Location: at the flue. Rotating frequency (rpm's): Motor: 1,770. Blower: 1,250. Observations: once each 2 weeks.
J. Initial condition.
K. Speed of vibrations, mm/sec (swings).
L. Lateral.
M. Vertical.
N. Axial.
O. Results of vibrating-speed measurements, mm/second.
P. Tendency of the vibration, mm/second.
Q. Date.
R. Speed of vibrations, mm/second (swings).

Measurements are made either continuously or periodically, depending upon the unit's size and its importance in the installation. Where there is continuous collection of information, signals from the output of the measurers' block usually are sent to the digital computing installation, where they are subjected to treatment as a random process. Here also the data is averaged for each of the loading levels at which these data were obtained. The values obtained after exclusion of rejections (for example, based upon the criterion for statistical compatibility of the deviations)

are sent to the immediate-access memory of the EVU [electronic computing installation]. At a definite time, twice each month, for example, data about the average daily vibration levels are averaged, after which only the results of the deviations for the measurements for a period of many days remain in the EVU memory. The tendencies for change in condition are computed on the basis of these deviations, usually by the least squares method.

In extrapolating the time function thus obtained to the maximum permissible level of vibration, optimal data for preventive inspection of the unit is obtained. Warning and recording are performed in addition to long-term forecasting.

With periodic monitoring of the condition, the measuring apparatus is installed only for the period of measurements. Each condition is determined as an average from a series of consecutive measurements and is recorded in the report form for the unit's vibration status in the form of a numeral for each of the measuring places. In order to establish the rate and trend of the deviations, these same data are plotted on a chart (see figure 94), where the prescribed levels of vibration values at which the unit should be inspected (straight line 1) have been laid out, or, in order to establish special observation over its operation, in view of the hazard of a high level of vibration (straight line 2). Data that is being systematized in the form being examined will enable gradual changes in the unit's overall condition to be observed.

Information about the level of vibration does not contain indications about the causes and places of its appearance. If a rise in the general level of vibration is recorded, it is recommended that a frequency analysis of the vibration oscillogram be made. During such an analysis, the amplitude and frequency of the main cycles are measured, and these measurements are then compared with the appropriate standard values and with previously conducted measurements. The location of a source of a vibration that has arisen can be determined by the frequency at which the increased amplitudes have been recorded.

CHAPTER 5. FORECASTING THE TECHNICAL CONDITION OF MARINE STEAM-TURBINE INSTALLATIONS.

25. Auxiliary Mechanisms and Equipment

The status of a generator's turbodrive is characterized rather completely by specific steam consumption per kw/hr of energy generated. Since the steam parameters for the main steam generator are regulated automatically, the need to introduce corrections for initial pressures and temperature of the steam prior to its entry into the turbine's regulating valve is done away with; only a correction for deviation of the current vacuum from the rated vacuum is introduced.

Specific steam consumption is a function of the turbogenerator's power, so the standard values for specific consumption are a function of the power.

Heat-Exchange Units. The operating effectiveness of the feedwater preheaters, which are heated by saturated steam, is determined unambiguously by a comparison of the saturation temperature θ_s that corresponds to the pressure p_s in the regenerative bleed from which the preheater being examined is fed with the feedwater temperature θ_{2B}, measured at the output of the preheater. The difference $\Delta\theta = \theta_s - \theta_{2B}$ permits establishment of the presence of sediments on the heating surfaces, the choking of heating steam in the pipeline, and faultiness of the system for withdrawing heating-steam condensate from the preheater.

The normal course of the process in the thermal deaerator is monitored in similar fashion: the difference $\Delta\theta$ between the temperature of the water at the output of the deaerator to the feed pump $\theta_д$ and the saturation temperature of the heating steam $\theta_{т.д.}$, computed according to the pressure in the deaerator volume, is established

$$\Delta\theta = \theta_{т.д} - \theta_д. \qquad (224)$$

As was indicated above, this difference is standardized fairly rigidly and is measured in tenths of a degree.

The condition of the high-pressure preheater can be monitored automatically in accordance with change of the thermodynamic parameters of the working fluids--pressure and temperature of the condensate, the heating steam and the feedwater, as well as the preheater condensate levels. Diagnosis of faults is reduced to monitoring and comparison of current parameters with the standard and, in accordance with the buildup in the results of such a comparison, to prediction of the dates for conducting preventive maintenance and repair work.

Figure 117 presents a modern scheme for a high-pressure regenerative section that consists of sectional preheaters and has been adopted for high-tonnage tankers. Its important peculiarities are: a developed tube system of heat-exchange surfaces made from steel spiral tubing; precisely delineated sections (steam cooler, preheater and condensation cooler) with different operating conditions; regulation of the heating-steam condensate level; and protection from a rise in pressure and overflow by the bypassing of condensate excesses.

Steel pipes under pressure are subject to quite intensive corrosion, which is explained by breakdown of the cuprammonium complexes that form in the low-pressure regenerative portion. Corrosion of the low-pressure section's copper tubing promotes suction of air in the vacuum part of the tract, where fluctuations in the hydrogen indicator of the feedwater occur. Copper oxides are partially deposited under high pressure on the steel pipe surfaces, forming electrolytic steam and promoting corrosion of the pipe.

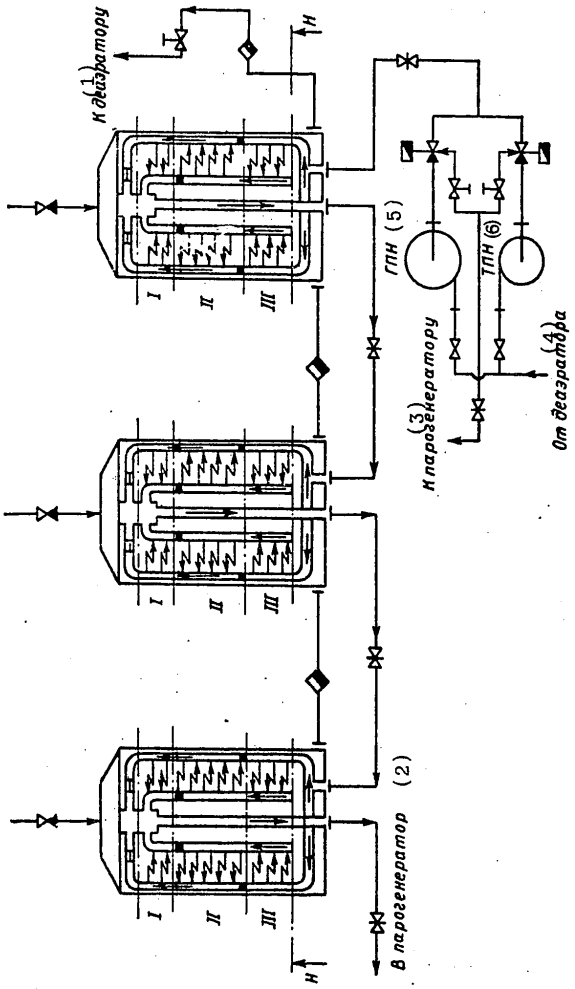

Figure 117. Diagrams of a Group of Regenerative High-Pressure Feedwater Preheaters

Key:
I, II and III. Sections for cooling steam, preheating feedwater and cooling condensate.
H. The level of heating-steam condensate that is being regulated.

1. To the deaerator.
2. Into the steam generator.
3. To the steam generator.
4. From the deaerator.
5. Main feed pump.
6. Turbodrive feed pump.

The condition of each of the high-pressure preheaters is evaluated in accordance with the overall heat-transfer coefficient. In so doing, formulas similar in structure to the formulas in the algorithm for diagnostics of the main condensational installation (section 23) are used:

$$K_{cp} = A_к \frac{K_q}{\Delta\theta_i} \ln\left(1 - \frac{\Delta\theta_i}{\Delta\theta_{si}}\right), \qquad (225)$$

where $A_к = \left(\frac{\Delta\theta_i K_{cp}}{\ln\left(1 - \frac{\Delta\theta_i}{\Delta\theta_{si}}\right)}\right)_0$ is a constant obtained for the nominal regime at the rated temperature of the water at the intake; $\Delta\theta_i = \theta_{2i} - \theta_{1i}$ is the difference in feedwater temperatures at, respectively, the output from the preheater and the intake; $\Delta\theta_{si} = \theta_{si} - \theta_{1i}$ is the difference in saturation temperature θ_s (at the pressure of the heating steam in the superheater) and feedwater temperature at the output θ_2; $K_q = Q/Q_0$ is the relative change in the superheater's heat loading, which is defined as a function of the steam pressure at the corresponding point of the regenerative bleed.

The dependencies $K_{cp} = K_{cp}(\theta_{1i}, Q)$ and K_q are represented in the function of the loading in a comparatively narrow (90-100 percent) range of main turbine powers.

Verification of the normal position of the condensate levels in the preheaters and of an absence of other faults in their operation precede engagement of the diagnostics algorithms.

The general status of the evaporator installation is most fully characterized by its specific productivity--the ratio of the amount of distillate obtained to the consumption of heating steam. This index is extremely sensitive to any faultiness of the evaporator. Most often a worsening of the operation of the evaporator results from the appearance of scale sediments on its coils; this is discerned by change in the difference in temperatures between heating steam and secondary steam

$$\Delta\theta = \theta_{гр} - \theta_{вт}. \qquad (226)$$

It is recommended that these expressions be used for evaporator loadings that are close to nominal; standard values of the difference being monitored should be presented as a function of the temperature of boiling in the evaporator.

The condition of the centrifugal electric-drive pumps--the main circulation and the condensate pumps--is evaluated according to their effectiveness, which is computed as the ratio of the hydraulic capacity, which is computed in accordance with expression (218), to the capacity of the electric-drive pump.

Monitoring the Status of the Auxiliary Equipment under the VIDEC System of Diagnostics [37]. The state of the turbogenerator is monitored in accordancew with the specific consumption of steam per kw of energy generated. The data are compared with the standard characteristics for the function of the volume; this enables degradation in the turbine drive to be established. Measured changes are corrected according to the current values of the vacuum in the main condenser and the loading of the main turbine.

High-pressure feedwater preheaters (sectional, similar to those shown in figure 117) are monitored according to the three following indices.

The weighted mean coefficient for heat transfer $\overline{K}$ is determined through the average logarithmic difference of the temperature $\Delta\theta_{cp}$ and the amount of heat Q transmitted into each section of the preheater

$$\overline{K}=\frac{\sum_{i=1}^{n}K_iF_i}{\sum_{i=1}^{n}F_i};\quad K_i=\frac{Q_i}{F_i\,\Delta\theta_{cp\,i}}, \tag{227}$$

where F_i is the surface of the i-th section.

The effectiveness $\eta_{п.в.}$ of a high-pressure preheater is determined as the ratio of the measured rise in feedwater temperature to the maximum possible corresponding case where the feedwater output temperature $\theta_{п.в.}$ has reached the saturation temperature θ_s, which corresponds to the pressure of the heating steam in the preheater:

$$\eta_{п.в}=\frac{\theta_{п.в2}-\theta_{п.в1}}{\theta_s-\theta_{п.в1}}. \tag{228}$$

The third indicator of the condition of a high-pressure feedwater preheater is defined as the ratio of the heating-steam consumption and of feedwater and corresponds to the correlation (101) in Chapter I.

The magnitude of the temperature at the preheater output is used as supplementary information. The first two indicators express the degree of perfection of the heat-exchange processes that are occurring in them, and the third facilitates evaluation of the degree of degradation of the overall technical condition. In order to evaluate the condition of the low-pressure feedwater preheater, only the second and third indicators are used, since computation of the heat-transfer coefficient in the area of moist steam is rather complicated.

The deaerator's condition is evaluated on the basis of two indicators (figure 118). Effectiveness in cooling the steam-and-water mix that leaves the deaerator, $\eta_{д1}$, is determined by the ratio

$$\eta_{д1} = \frac{\theta_2 - \theta_1}{\theta_3 - \theta_1}. \qquad (229)$$

Figure 118. Diagram of Measurements for Monitoring the Quality of Operation and the Condition of the Deaerator in the VIDEC Diagnostic System.

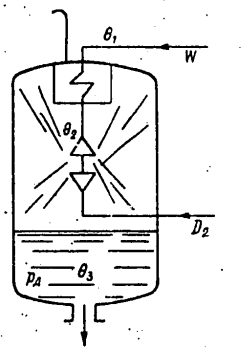

Underheating of water in the deaerator volume below the saturation temperature, which corresponds to the pressure in the deaerator

$$\Delta\theta_н = \theta_{д.т} - \theta_2,$$

indicates the degree of perfection of the deaerating process (see explanation to figure 26, Chapter I).

The condition of centrifugal pumps--the main-circulation and the condensate pumps--is evaluated according to overall efficiency; this is computed as the ratio of the fluid power developed by the pump (see formula 218) to the power required for its electric drive.

The evaporator installation is monitored for the amount of steam that is spent on the output of 1 kg of condensate and the value of the heat transfer coefficient in the outside-water preheater. The first indicator characterizes the overall condition of the evaporator, the second the fouling of the preheater by the outside water; in addition, the second indicator characterizes the effect of outside-water temperature deviations on the computed values.

The VIDEC system is called upon to monitor irreversible leakage from the cycle, in addition to monitoring the objects listed.

Diagnostics of Auxiliary Mechanisms in the "Data Trend" System (30). The condition of the turbogenerator is established in accordance with changes in the parameters of the steam that passes through the turbine, which characterize the thermodynamic effectiveness of the process, as was described for the feed pump's turbine. This effectiveness indicator is compared with the standard as a function of the generator's electrical load.

The condition of the heat-exchange apparatus for the condensate-feed system is found in accordance with the coefficients for heat transfer and distribution of the heat load among items of the apparatus (figure 119). A rise in feedwater enthalpy is computed according to temperature and heat-balance measurements.

The pressure and hydraulic losses in the bleed lines between the turbine and the preheater are monitored. In computing the average logarithmic difference of the temperatures that are included in the expression for

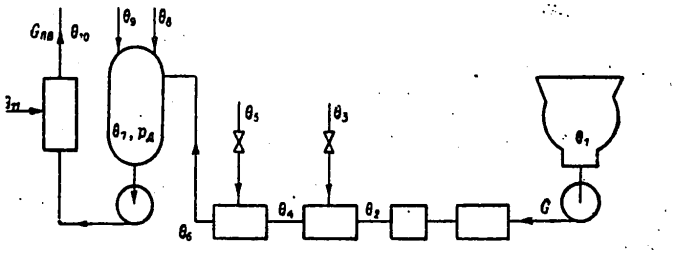

Figure 119. Diagram of Measurements for Monitoring the Condition of Apparatus on the Condensate-Feed Mainline in the "Data Trend Turbine" System.

Key:
θ. Temperature. p. Pressure. G. Consumption.

determining the heat-transfer coefficient, the temperature of the medium being heated (the steam) is taken as the saturation temperature that corresponds to the pressure in the preheater.

An accumulation of air in the preheater degrades heat exchange and changes the heat-transfer coefficient and the distribution of temperatures among the units along the condensate mainline and the feed system; these changes also are symptoms of abnormalities that arise. The condition of the deaerator is monitored in accordance with the degree of underheating of the temperature of the water at the output below the temperature of saturation that corresponds to the pressure in the deaerator, similar to correlation (224).

The condition of the centrifugal condensate pump is established in accordance with the effective efficiency factor, which is computed as the ratio of the hydraulic power to the electrical power of the pump drive. Since asynchronous drives operate at an unchanged rotating frequency, revision of the measured productivity and pressure for this frequency proves to be unnecessary.

Establishment of the condition of the ship's hull (the degree of its fouling) in operational conditions is the basis for forecasting the optimal date for the next drydocking. Usually the propeller screw's propulsive efficiency is changed very little,* as a consequence of which the main cause for gradual increase in resistance of the ship's hull is fouling that changes the main component--frictional drag.

The hull's friction factor is computed periodically, and the values obtained are accumulated for forecasting. Power is measured automatically, and results of the observations are processed under the rules given in Chapter III and are introduced into the program for computing this factor.

*The causes of screw fouling in the period between the 18th and 19th cruises in the example of figure 45, naturally, are not examined here.

Other data (ship speed, forward and stern draft, force and direction of the wind and waves) are usually fed into the digital computer manually.

CHAPTER 6. DIAGNOSTICS AND FORECASTING OF THE TECHNICAL CONDITION OF DIESEL POWER PLANTS

33. Monitoring the Fouling of the Ship's Hull.

An increase in plating roughness because of destruction of the paint, corrosion and, especially, fouling by marine plant and animal life influences loss in ship speed. According to the data of Japanese researchers, the formation alone of slimy film on plating, which is the first stage of fouling, can increase the overall drag of a 300-meter tanker by 9-10 percent. Because of this, the time between drydockings of high-tonnage tankers has become the subject of strict regulation in foreign practice, since speed losses even in a year of operation can reach 1 knot or more (figure 147).

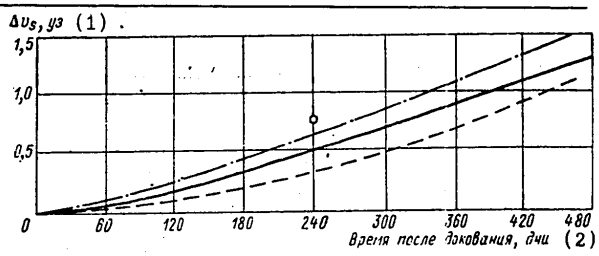

Figure 147. Losses of Speed Because of Fouling of the Ship's Hull.

Deadweight:
- - - - - 33,000 tons
——— 75,000 tons
—·—·—·— 130,000 tons
o 150,000 tons

Key:
1. Loss of ship speed, knots. 2. Time after drydocking, days.

Especially substantial are speed losses for modern high-tonnage tankers, for which the share of frictional drag reaches 60-70 percent of the hull's overall resistance. The main part of the residual drag is occasioned by vortex generation in the environment outside the hull, and, consequently, this also depends upon drag.

In the general case, fouling that degrades propulsive performance is divided into three groups: fouling of the underwater part of the ship's hull, the internal and external surfaces of the shrouding, and the propeller screw.

Fouling of the underwater part of the hull is observed most often of all. Its effect on under-way characteristics is displayed in an increase in the hull's resistance and an increase in the frictional wake. Both these factors, depending upon the degree of fouling, affect running characteristics: the ship's speed is reduced for the same power, propeller-shaft rotating frequency, sea state, wind and average draft.

Similar phenomena are observed, although to a lesser extent, in fouling of the shrouding. Fouling of the propeller screw also leads to an increase in the moment on the propeller shaft and loss of speed, the speed loss being maximum for this type of fouling.

The degree of degradation can be established by comparing the running characteristics of the encrusted hull, shrouding and screw with the characteristics of a clean hull. By analogy with what was presented above, it is necessary, for this purpose, to have at one's disposal the running characteristics of the ship with a clean and an encrusted hull.

As an example of the effect of hull fouling, figure 148 presents the running characteristics of a high-tonnage tanker that were obtained during tests of ships with a clean and an encrusted hull. For the very same ship speeds, the power and torque curves are much higher than calculated. Thus, at a speed of 16 knots, the power and torque exceed those computed by 30 percent: at a power of 220,000 kw, the speed loss Δv_s as a result of fouling is 1.2 knots.

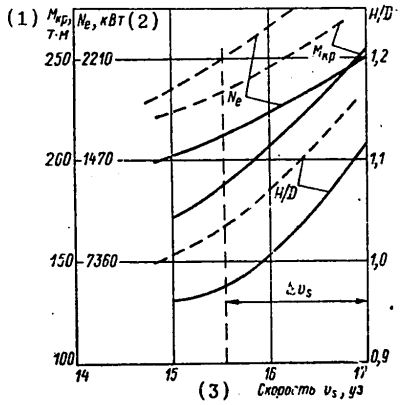

Figure 148. Under-Way Characteristics of a High-Tonnage Tanker with Adjustable-Pitch Screw (VPSh) in a Shrouding, Obtained During Tests over a Nautical Mile, with a Clean (continuous lines) and an Encrusted (broken lines) Hull.

N_e and M_{kp} are power and torque on the propeller shaft; H/D is the propeller pitch ratio.

Key:
1. Torque, ton-meters.
2. Engine power, kw.
3. Speed v_s, knots.

Fouling of the shrouding leads to further degradation of a ship's running characteristics. Roughness of the shrouding's inner surface exerts a considerable influence, while outer-surface roughness has an insignificant effect.

The hydrodynamic complex of screw and shrouding, where the shrouding is rough, has less shrouding resistance and greater propeller-screw thrust than a complex with a smooth shrouding. The torque for a complex with a rough shrouding is greater, but the efficiency is 2-4 percent lower. Where the complex operates behind an encrusted hull, the drop in efficiency will be still greater, since, because of an increase in the frictional wake, the loading coefficient is increased. The additional drop in speed from fouling of the shrouding (when it is installed on a VRSh) ship, does not exceed 0.1-0.2 knot.

The fouling of propeller screw blades exerts the greatest effect on running qualities. Propeller screw thrust is reduced and torque is sharply increased, leading to a great drop in efficiency. In practice, cases of propeller screw fouling are known that have led to great speed losses. Thus, the blade surfaces of a turbine ship, after a tropical voyage, were found to be covered with pipe-shaped mollusks 1-2 mm thick along the driving surface, from the hub to a relative radius of $\bar{r} = 0.7$, and along the suction surface to $\bar{r} = 0.6$. Measurements and calculations indicated that, of a total speed loss of 2.8 knots, the share for the propeller screw was 1.3-1.5 knots.

Blade fouling is usually observed only at radii close to the hub ($\bar{r} \leqslant 0.6$). But even that blade fouling changes considerably the propeller screw's hydrodynamic characteristics in free water. Figure 149 compares the hydrodynamic characteristics of a clean propeller screw with one with artificial roughness that involves the blade completely or partially. The torque coefficient curves of the encrusted screw K_2 with identical advance are located higher than those for a clean screw, and the thrust coefficient curves are lower. A substantial drop in efficiency also is observed for an encrusted screw.

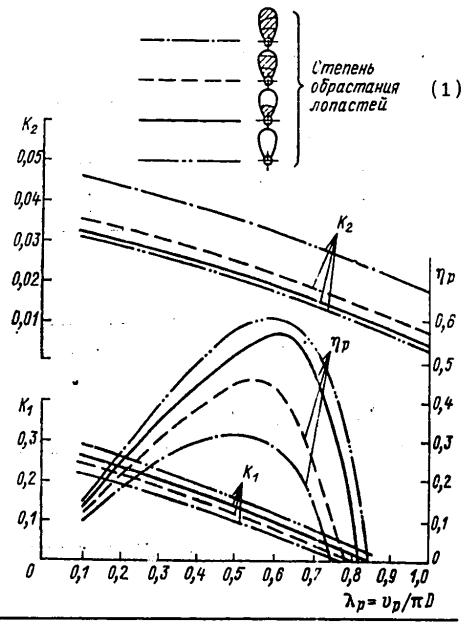

Figure 149. Effect of Propeller Screw Fouling on the Magnitudes of Its Coefficients: thrust K_1, torque K_2 and useful effect η_p.

Key:
1. Degree of blade fouling.

The Standard Running Characteristics of a Ship. The standard running characteristics of a ship with a clean hull, screw and shrouding are obtained after acceptance and turnover tests or drydocking. Tests should be conducted over a nautical mile with a depth under the keel of

$$H \geqslant 2{,}75 \frac{v_s}{g}, \qquad (231)$$

where v_s is the ship's speed in knots, and g is the acceleration of the force of gravity.

During the tests, average ship depth T_{cp}, screw pitch, torque on the shaft M_{kp}, propeller-shaft rotating frequency n and the ship's speed are measured. As a result, an average arithmetic value is adopted, which is obtained in accordance with measurements on no less than three tacks over a nautical mile, with the force of waves and wind no greater than force 3. Running characteristics similar to those shown in figure 148 are set up as a result of the measurements.

For a quantitative evaluation of fouling and for forecasting an optimal date for drydocking the ship, calculations are made in accordance with the form in table 25. The coefficients of torque K_2 and wake ψ, as well as hull resistance R, are determined as a result of the calculations. The value of the thrust-reduction fraction coefficient, which is necessary for determining R, is found as a function of K_{de} in accordance with the formula

$$v_s = aK_{de} - b. \tag{232}$$

The values of the coefficients a and b are determined by approximation of the trials graph $v_s = v_s(K_{de})$ that is usually plotted as a result of special tests of the ship or of a model of it.

The method of diagnostics set forth below [25] assumes rather precise measurements of ship speed. Measurements over a nautical mile or measures made by means of radio-pulse systems, whose errors are about 1 percent, usually provide such precision. Existing dynamic pressure logs do not give such precision. Logs that are based on other principles for measuring speed should be installed on ships for prediction systems. Let us examine the sequence of diagnostic operations.

1. Several measurements of the values named above are made. The number of regimes at which these measurements are made is at least three, power at these regimes corresponding to average, full and emergency speed.

2. Computations are made for each regime in the sequence presented in table 25.

3. The function $H/D = f(v_s)$ is plotted (a parabola is established through three points) in accordance with the data of lines 1 and 2 of table 25.

4. The function $M_{kp} = M_{kp}(v_s)$ is plotted in accordance with line 6 data, which also produces a parabola.

5. The function $N_e = N_e(v_s)$, which represents a cubic parabola, is plotted in accordance with the data of line 7.

6. The relative advance of the screw λ_p (line 9) is found in accordance with the curves for operation of the screw in free water. For purposes of

Table 25

Determination of the Resistance of a Clean and an Encrusted Hull of a Ship in Accordance with Test Results

(T_{cp} [average draft] = 7.5 m; D = 7.5; η_e [engine efficiency] = 0.99; and ρ = 104 kg·force/cm^2)

Item No	Parameters	Clean hull			Fouled hull
1	Pitch ratio of VRSh [adjustable pitch propeller], H/D	0.96	1.06	1.17	1.0
2	Ship speed v_s, knots.....	15.0	16.0	17.0	14.84
	Ship speed v_s, meters/second...	7.718	8.232	8.764	7.64
3	Propeller-shaft rotating frequency n': rpm.....	85.0	85.0	85.0	84.8
	rps.....	1.416	1.416	1.416	1.414
4	Moment M_{BP}, kg·meters.....	171,000	207,800	250,300	221,700
5	Power on the shaft, $N_e = \frac{M_{BP}n}{974}$, kw.....	14,927	18,123	22,060	19,203
6	$K_2 = \frac{16{,}225N_e\eta_B}{\rho D^5 n^3}$	0.0340	0.0413	0.0503	0.0442
7	$\lambda_p = f_1(H/D, K_2)$	0.68	0.73	0.775	0.588
8	Trailing wake $\psi = 1 - \frac{\lambda_p nD}{v_s}$ ...	0.072	0.059	0.060	0.184
9	$K_1 = f_2(H/D, \lambda_p)$.....	0.200	0.228	0.266	0.264
10	Screw thrust $P = K_1\rho D^4 n^2$, kg·force.....	132,700	151,200	176,500	174,300
11	$K_{de} = Dv_s \Big/ \sqrt{\frac{P}{\rho}}$	1,623	1,625	1,500	1,405
12	Thrust-reduction fraction, $v = 0.1285\ K_{de} - 0.283$	-0.0743	-0.0741	-0.0774	-0.1025
13	Hull resistance R = P(1 - v), kg·force	142,500	162,400	190,000	192,200

computation on a digital computer, it is more convenient to present the function $K_2 = K_2(\lambda_p)$ for each pitch ratio in accordance with the parabolic-interpretation formulas

$$K_2 = K_{2ш.в} + A'\lambda_p^2 - B'\lambda_p, \tag{233}$$

where

$$\left.\begin{aligned} A' &= \frac{K_{2ш.в}}{\lambda_{p\,ср}\lambda_2} + \frac{K_2}{\lambda_{p\,ср}(\lambda_{p\,ср} - \lambda_2)}, \\ B' &= \frac{K_{2ш.в}}{\lambda_{p\,ср}} + \frac{K_{2ш.в}}{\lambda_2} + \frac{\lambda_2 K_{2ср}}{\lambda_{p\,ср}(\lambda_{p\,ср} - \lambda_2)}. \end{aligned}\right\} \tag{234}$$

In these formulas K_2 values are adopted as the base values for the following regimes: docking, where $\lambda_p = 0$; and rated, where there is $\lambda_{p\ ср}$ and where there are advances of zero moment $\lambda_2 (K_2 = 0)$.

The coefficients A and B can be computed in advance for the prescribed H/D pitch ratios. The value $\lambda_{p\ ср}$ for each pitch ratio can be taken as equal to about half of λ_2, with rounding off to the whole number after the decimal point. The value λ_p for a known K_2 is obtained from solving the quadratic equation of the two pitch ratios, between the values of which lie the desired H_1/D. Then λ_p and the corresponding H_1/D are determined by linear interpolation.

7. In accordance with the λ_p and H_1/D that have been found, the coefficient of propeller screw thrust K_1 is computed. Formulas for computing it are obtained similarly, by the use of parabolic interpolation

$$K_1 = K_{1ш.в} + A\lambda_p^2 - B\lambda_p, \tag{235}$$

where

$$\left.\begin{aligned} A &= \frac{K_{1ш.в}}{\lambda_{p\,ср}\lambda_1} + \frac{K_{1ср}}{\lambda_{p\,ср}(\lambda_{p\,ср} - \lambda_1)}, \\ B &= \frac{K_{1ш.в}}{\lambda_{p\,ср}} + \frac{K_{1ш.в}}{\lambda_1} + \frac{\lambda_1 K_{1ср}}{\lambda_{p\,ср}(\lambda_{p\,ср} - \lambda_1)}. \end{aligned}\right\} \tag{236}$$

Here, just as in formulas (233) and (234), $K_{1ш.в}$ is the thrust coefficient for the docking regime, $K_{1\ ср}$ is the same for the rated regime where there is $\lambda_{p\ ср}$ and λ_1 is the advance for zero thrust.

The value K_1 for the two pitch ratios is computed, and then it is found for the desired H/D by linear interpolation.

8. In lines 12-13, table 25, the hull resistance $R = R(v_s)$ is computed. In this case the coefficient of the thrust-reduction fraction should be adopted for the test data as a function of the load coefficient K_{de}.

For convenience in computing on a digital computer, the graph $v_s = v_s(K_{de})$ is replaced by the approximating function

$$v_s = 0{,}128\,5K_{de} - 0{,}283. \quad (237)$$

This function, which is obtained in tests of models with a smooth surface, can be used for cases of fouling, since the coefficient of the thrust-reduction fraction is a function of hull roughness.

The curve $R = R(v_s)$ is plotted in accordance with the measurements data; speed losses Δv_s for one and the same main turbogear assembly are determined by means of the characteristics $N_e = N_e(v_s)$ for a clean and an encrusted hull.

Indirect signs of hull fouling are as follows.

1. An increase in the trailing wake ψ. Thus, during tests of a high-tonnage tanker, the value ψ proved to be twice as large for a fouled hull as the rated value. In case of fouling of the inner surface of the shrouding and blades of the propeller screw, ψ also increases, especially for a VRSh [variable-pitch ratio] screw, since, at a constant rotating rate, torque increases and, consequently, so does K_2.

2. An increase in hull resistance R (line 13, table 25). Calculation of the resistance $R = R(v_s)$ is necessary for comparison of the resistance of clean and encrusted hulls. Rough calculations indicate that where hull resistance from fouling increases by about 30 percent, the speed loss at a turbine power of 22,000 kw is about 1 knot. If, as a result of comparison, the actual speed loss obtained by power measurements and by log indications is substantially different from the losses obtained by the indirect method (through increase of resistance), this indicates either errors of measurement or of primary data or a worsening of the propulsive coefficient (fouling or damage of the propulsion and steering complex).

Frequently a check of the condition (the degree of fouling) of the ship's hull is made where the draft is different from that for which the standard values that correspond to a clean hull were obtained. Differences within the bounds of no more than 10 percent are permitted, if the meteorological conditions match. Differences in a ship's draft are compensated for by introducing a correction to the value of measured power in accordance with the formula

$$N_{e2} = \left(\frac{D_2}{D_1}\right)^{2/3} N_{e1}, \quad (238)$$

where N_e and D are the ship's power and weight displacement; the subscripts 1 and 2 correspond to ship drafts T_1 and T_2.

Observations concerning the intensity of fouling, measurements of the ship's speed and the main engine's operating regime are started from the

moment the ship leaves the drydock. The data are used to forecast degradation of running qualities for the purposes of establishing a rational date for drydocking.

Running qualities are checked systematically.

It is recommended that tests start no earlier than 16 hours after leaving port. The date of the observations, the ship's draft and course, the sea state and speed and direction of the wind are indicated. A graph of the ship's speed losses from fouling, similar to the graph in figure 147, is plotted in accordance with the results of the tests.

As follows from this graph, the function that is plotted according to the data for 1 year and 2 months of operation is almost linear. In such a case, prediction of the expected losses in speed from fouling do not present difficulty. However, it should be kept in mind that where fouling density is more than 50 percent, the drag coefficient is practically unchanged, so the linear function (proportional to the time between drydockings) for losses in speed converts in this case to a constant. Because of this, the form of the function by means of which the prediction is made should be adopted to take into account the concrete data of the regime being analyzed.

BIBLIOGRAPHY

1. Viner, N., "Integral Fur'ye i nekotoryye yego prilozheniya" [The Fourier Integral and Some of Its Applications]. Moscow. Fizmatgiz, 1963.

2. Gokhshteyn, D. P. "Sovremennyye metody termodinamicheskogo analiza energeticheskikh ustanovok" [Modern Methods of Thermodynamic Analysis for Power Plants]. Moscow, Energiya, 1969.

3. "Dvigateli vnutrennego sgoraniya. Sistema porshnevykh i kombinirovannykh dvigateley" [Internal Combustion Engines. A System of Piston and Combined Engines]. Under the editorship of A. S. Orlina/V. P. Alekseyev, D. N. Vyrubov, N. I. Kostygov and others. Moscow, Mashinostroyeniye, 1973.

4. Dudnikov, Ye. G., "Osnovy avtomaticheskogo regulirovaniya teplovykh protsessov" [Fundamentals of the Automatic Regulation of Heat Processes]. Moscow, Gosenergoizdat, 1956.

5. Yenin, V. I., "Sudovyye parogeneratory" [Marine Steam Generators]. Leningrad, Sudostroyeniye, 1975.

6. Ivanov, L. A., "Teplonapryazhennost' i ekspluatatsionnaya nadezhnost' tsilindroporshnevoy gruppy sudogo dizelya" [Thermal Stress and Operating Reliability of the Cylinder and Piston Group of a Marine Diesel]. Murmanskoye Knizhnoye izdatel'stvo, 1974.

7. Ivakhnenko, A. G. "Samoobychayushchiyesya sistemy raspoznavaniya i avtomaticheskogo upravleniya" [Self-Teaching Systems for Recognition and Automatic Control]. Kiev, Tekhnika, 1969.

8. Iliyes, K., "Sudovyye kotli" [Marine Boilers]. Leningrad, Sudostroyeniye, 1964.

9. Kirillov, I. I.,, "Avtomaticheskoye regulirovaniye parovykh i gazovykh turbina" [Automatic Regulation of Steam and Gas Turbines]. Moscow-Leningrad, Mashgiz, 1961.

10. Kornilov, Yu. G. and Piven', V. D., "Osnovy teorii avtomaticheskogo regulirovaniya" [Fundamentals of the Theory of Automatic Regulation]. Moscow, Mashgiz, 1947.

11. Kotel'nikov, V. A., "Teoriya potentsial'noy pomekhoustoychivosti" [Theory of Steady-State Noise Immunity]. Moscow, Gosenergoizdat, 1956.

12. Koetin, L. and Fritts, V., "Sravneniye metodov opredeleniya k.p.d. sudovykh kotlov po ikh teplopotrebleniyu i nagruzke libo po teplovym poteryam" [A Comparison of Methods for Determining the Efficiency of Marine Boilers According to their Heat Consumption and Loading or by Heat Losses]. ENERGETICHESKOYE MASHINOSTROYENIYE [Power-Engineering Machine Building]. Series A, No 1, 1962, pp 34-36.

13. Kuz'min, I. V., "Otsenka effektivnoisti i optimizatsii avtomaticheskikh sistem kontrolya i upravleniya" [Evaluation of the Effectiveness and Optimization of Automatic Systems for Monitoring and Control]. Moscow, Sovetskoye Radio, 1971.

14. Levin, B. P., "Teoriya sluchaynykh protsessov i yeye primeneniye v radiotekhnike" [Theory of Random Processes and Its Application in Radio Engineering]. Moscow, Sovetskoye Radio, 1957.

15. Lubochkin, B. I., "Morskiye parovykh kotli" [Marine Steam Boilers]. Moscow-Leningrad, Transport, 1970.

16. Ovsyannikov, M. K. and Davydov, G. A., "Teplovaya napryazhennost' sudovykh dizeley" [Heat Stress of Marine Diesels]. Leningrad, Sudostroyeniye, 1975.

17. Piven', V. D., Bayasnov, D. B. and Med, G. A., "Avtomatizatsiya gazoturbinnykh ustanovok" [Automation of Gas-Turbine Installations]. Moscow-Leningrad, Mashinostroyeniye, 1967.

18. Profos, P., "Regulirovaniye parosilovykh ustanovok" [Regulation of Steam Power Plant Installations]. Moscow, Energiya, 1967.

19. Pugachev, V. S., "Teoriya sluchaynykh funktsiy" [Theory of Random Functions]. Moscow, Fizmatgiz, 1962.

20. Serov, Ye. P. and Korol'kov, B. P., "Dinamika protsessov v teplo i massoobmennykh apparatakh" [The Dynamics of the Processes in Heat and Mass Exchange Apparatus]. Moscow, Energiya, 1967.

21. Solsberi, K., "Detal'nyy kontrol' ekonomichnosti elektrostantsii." [Detailed Monitoring of the Economic Effectiveness of Electric Power Stations]. ENERGETICHESKOYE MASHINOSTROYENIYE, No 4, 1961, pp 103-121.

22. Syromyatnikov, V. F., "Avtomaticheskoye regulirovaniye sudovykh paroturbinnykh ustanovok" [Automatic Regulation of Marine Gas-Turbine Installations]. Leningrad, Sudostroyeniye, 1965.

23. Syromyatnikov, V. F., "Avtomatizirovannyy kontrol' ekspluatatsionnoy ekonomichnosti raboti sudovoy paroturbinnoy ustanovki" [Automatic Monitoring of the Operational Economic Effectiveness of Marine Steam-Turbine Installation Work]. TRUDY TsNIIMF [Transactions of the Central Scientific-Research Institute of the Maritime Fleet], No 96, Moscow-Leningrad, Transport, 1968, pp 3-12.

24. Syromyatnikov, V. F., "Differentsirovannyy kontrol' kachestva raboty i rasstoyaniya oborudovaniya paroturbinnoy ustanovki" [Differentiated Monitoring of the Quality of Operation and Spacing of the Equipment of Gas-Turbine Installation]. TRUDY TsNIIMF, No 123. Moscow-Leningrad, Transport, 1970, pp 3-14.

25. Fomenko, Yu. I., "Primeneniye garmonicheskogo analiza pri raschete kolebaniy periodicheskikh sil na grebnom vinte" [The Use of Harmonics Analysis in Calculating Periodic Forces on a Propeller Screw]. TRUDY TsNIIMF, No 119. Moscow-Leningrad, Transport, 1969, pp 58-72.

26. Enis, M., "Sravneniye dinamicheskikh modeley paroperegrevatelya" [A Comparison of Dynamic Models of a Steam Superheater]. TRUDY ASME Series C, 1962, No 4, pp 120-123.

27. Aue, G. K., "On the Mechanism of a Piston-Ring Seal." SCHIFF EN WERF, 1974, No 15, pp 305-317.

28. Blake, M. P., "New Vibration Standards for Maintenance," HYDROCARBON PROCESSING AND PETROLEUM REFINER, January 1964, pp 32-40.

29. Bohnstedt, H. J., "Die Grenzen der Korperschallmessung bei der Uberwachtung von Dampfturbinen." Maschinenschaden, 1970, No 3.

30. "Data Chief/Turbine, General Specification." Norcontrol, 1972.

31. Decker, S., "Ceramic Aspects of the Bosch Lambda Sensor," SEA Prep., Series A., No 750223.

32. Ellis, A., "Shipboard Trial of Vibration Analysis Equipment." SNAME, IX, 1970.

33. Endo, J., "Some Problems in the Measurement of Cylinder Pressure and the Diagnosis of Some Engineering Components for a Diesel Engine." The International Symposium on Marine Engineering, Tokyo, 1973, pp 127-135.

34. Hansen, A., "Diesel Engine-Condition Monitoring and Preventive Maintenance, Using a Shipboard Computer." The Ship Research Institute of Norway, Arbeidsnotat, ant. 22 May 1974.

35. Hirt, D., "Fruhenkennung verhindert Kolbenfresser." VDI NACHRICHTEN, No 9, 1975.

36. Hutchison, T. V., "30,000-bhp Unitized Reheat Steam-Turbine Propulsion." THE INSTITUTE OF MARINE ENG. TRANSACTIONS, 1966, Vol 78, No 4.

37. Kramer, A. R. and etc., "The Deviation Concept: a Tool for Preventive Maintenance of Marine Power Plants." MARINE TECHNOLOGY, X, 1972, pp 405-418.

38. Lundgaard, B., "The Relationship Between Machinery Vibration Levels and Machinery Deterioration and Failures." MARINE TECHNOLOGY, No 1, 1973, pp 22-28.

39. Mizushima, K., and etc. "Analysis of Operating Conditions of the Main Diesel Engine of a Ship under Service Conditions." The International Symposium of Marine Engineers, Tokyo, 1973, pp 105-132.

40. Myers, G. E., Mitchell, J. W. and Norman, R. F., "The Transient Response of Crossflow Heat Exchangers, Evaporators and Condensers." TRANSACTIONS ASME, 1967, No 1, 75-80.

41. Peters, G., "Schwingungs und Dehnungsmessungen an Turbomaschinen." VCB KRAFTWERKTECHNIK, No 4, 1973, pp 224-233.

42. Ranson, I. B., "Real-time Oxygen Measurement for Combustion Control." CONTROL AND INSTRUMENT, 1972, No 8.

43. ROUBINET, P. A., "Operation and Control of Surface Condensers." COMBUSTION, 1969, July, pp 39-43.

44. Rydland, K., Öyvag, K. and Glöersen, T. C., "A Mathematical Model for Dynamic Analysis of a Boiler." IMAE, 1973, Group 1.

45. Sandtory, H. and etc. Datatrend. "A Computerized System for Engine Condition Monitoring and Performance Maintenance of Large Bore Diesel Engines." CIMAC, Stockholm, 1971.

46. Solisbury, K. A., "A New Performance Criterion for Steam-Turbine Regenerative Cycle." TRANSACTIONS OF THE ASME, Series A, 1959, Vol 81, pp 389-397.

47. Upmalis, A., "Die thermische Entgasung von Kesselspeisewasser in Warmekraftwerken." WARME, 1974, 80, No 3, pp 41-45.

48. Wefonder, E. and Hasenkapf, O., "Vergleich determinicher und statistischen verlagen zur Systemandise gestorter industrieller Regelstrecken." BWK, 1970, No 6, pp 288-297.

49. Woodward, I. B., "Experiments in Ship Motion Effects on Boiler Tube Circulation and Heat Transfers." The Society of N. A. and M. E., 1966, paper No 15, pp 1-11.

11409
CSO: 8144/0016

END